EUROPEAN DEFENCE AGENCY

OPTRONICS WORKSHOP PROCEEDINGS

QUANTUM TECHNOLOGIES IN OPTRONICS

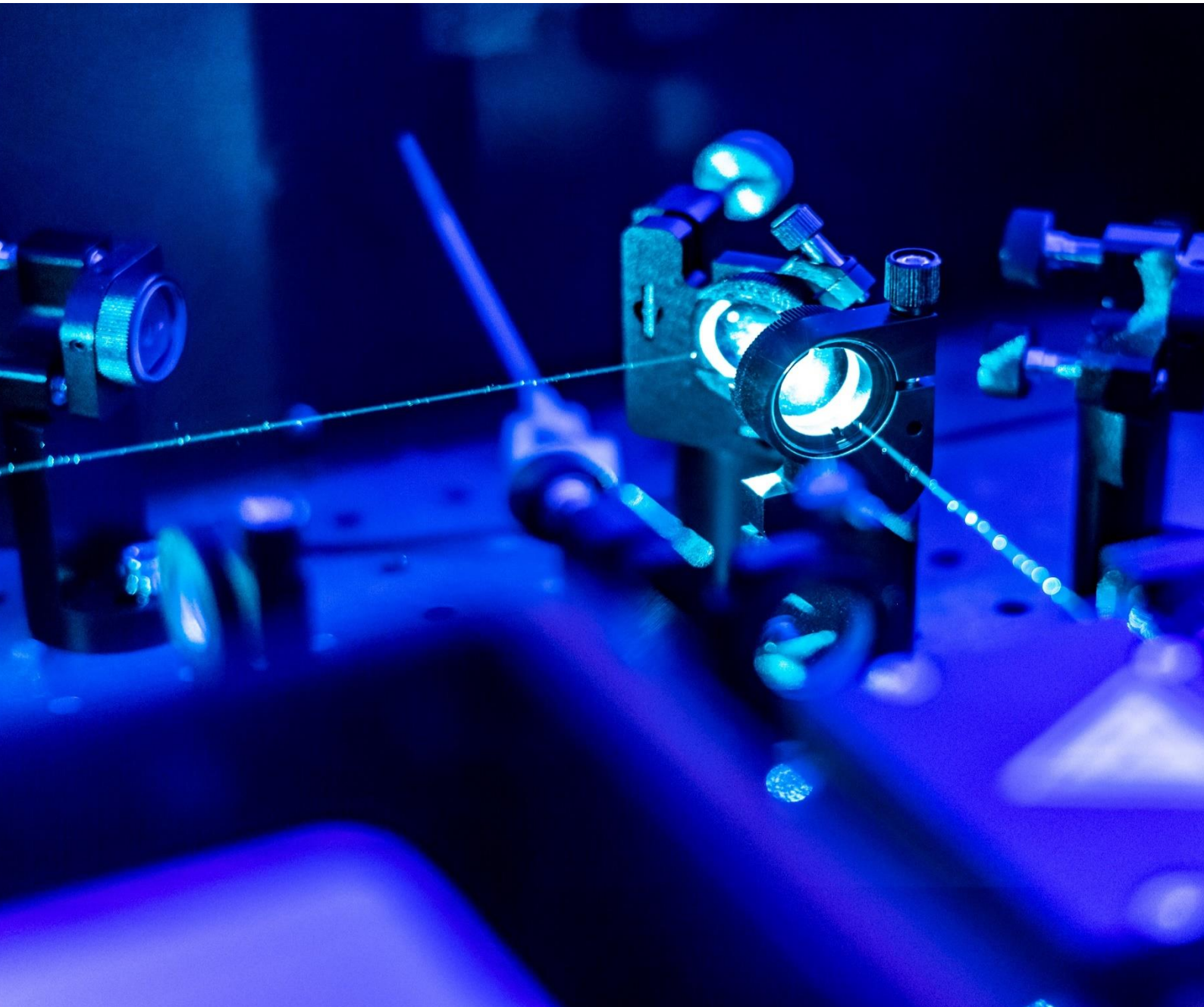

EUROPEAN DEFENCE AGENCY

CONTENTS

PREFACE

Quantum technology is an emerging field related to physics and engineering, which enables quantum physics to achieve performances which otherwise would be impossible. The different functions of quantum technologies are derived from science that cannot be explained by classical physics, such as Newton's Laws of motion, thermodynamics, or Maxwell's equations of electromagnetism.

Many of existing technologies, including microprocessors, solid state imaging devices or lasers are derived from quantum physics. These technologies paved the way for the emergence of today's 'Information Age' in the same manner that technologies based on classical physics underpinned the industrial revolution of the 18th and 19th centuries.

Quantum technologies are mainly based on properties of quantum mechanics, especially quantum entanglement, quantum superposition and quantum tunnelling.

Several applications are based on quantum technologies like quantum cryptography, quantum computing, quantum communication, optical metrology, imaging and sensing, quantum simulation, quantum metrology, gravitational wave detection, quantum radar, clock and network synchronization.

In the field of OPTRONICS, quantum technologies can be applied for designing cameras and devices for ghost imaging, beyond the wall and around the corner target detection, single photo counting and devices quantum illumination, or new detectors.

The main advantages of using quantum technologies are related to improved sensitivity, reduction of noise and background, hidden target detection, system compactness enabling technologies for miniature or chip-scale deploying sensing technologies including solid-state laser-free detectors, miniature pump-free vacuum chambers and grating magneto-optical traps.

In order to gain a better understanding of the current and potential future usage of quantum technology in defence applications related to Electro-Optical (EO) sensors & systems, the European Defence Agency's (EDA) Capability Technology Group (CapTech) on Electro Optical Sensors technologies (EOST) organised and run a workshop on "Quantum technologies in Optronics" on 12 March 2019 at the *Office national d'études et de recherches aérospatiales* (ONERA) in Toulouse (France).

The workshop was attended by representatives from seven EU Member States as well as from industry (one major company and four SMEs), the research world (five scientific centres) as well as academia (five universities). In total, 18 presentations were made to the audience.

This present publication, edited by Fabrizio Berizzi, EDA Project Officer of Electro-Optical Sensors Technologies CapTech, contains a collection of all papers presented during the workshop. It is structured in two main sections. The first section is related to scientific contributions strictly related to Electro Optical quantum technologies. The second section is mainly linked to communications and sensor quantum technologies that have direct or indirect impact on EOST applications.

The final part of the publication contains a set of conclusions and lessons learnt, as well as some recommendations related to research developments for defense.

CONTRIBUTORS

No	First name	Family name	Nationality	Organisation
1	LUDOVIC	ABALLEA	BELGIUM	OIP SENSOR SYSTEMS
2	HALIMA	AHMAD	ITALY	UNIVERSITA' DI NAPOLI FEDERICO II
3	GIOVANNI	AUSIANO	ITALY	UNIVERSITA' DI NAPOLI FEDERICO II
4	S.	AVINO	ITALY	CNR-INO
5	G.	BAILI	FRANCE	THALES RESEARCH AND TECHNOLOGY
6	SAVERIO	BARTALINI	ITALY	CNR-INO
7	MARCO	BELLINI	ITALY	CNR-INO
8	ANTONELLA	BOGONI	ITALY	SCUOLA SANT'ANNA DEGLI STUDI AVANZATI
9	P.	BRIGNON	FRANCE	THALES RESEARCH AND TECHNOLOGY
10	ANGELA SARA	CACCIAPUOTI	ITALY	UNIVERSITA' DI NAPOLI FEDERICO II
11	MARCELLO	CALEFFI	ITALY	UNIVERSITA' DI NAPOLI FEDERICO II
12	ROBERTA	CARUSO	ITALY	UNVERSITA' DI NAPOLI FEDERICO II
13	F.S.	CATALIOTTI	ITALY	UNIVERSITA DI FIRENZE & LENS
14	GIACOMO	CORRIELLO	ITALYK	ISTITUTO FOTONICA E NANO TECNOLOGIE -CNR-MILANO
15	ERIC	COSTARD	FRANCE	IRNOVA AB
16	ANDREA	CRESPI	ITALY	POLITECNICO DI MILANO
17	ROBERTO	CRISTIANO	ITALY	CNR SPIN
18	PAOLO	DE NATALE	ITALY	CNR-INO
19	MAURIZIO	DE ROSA	ITALY	CNR-INO
20	T.	DEBUISSCHERT	FRANCE	THALES RESEARCH AND TECHNOLOGY
21	MATTHIEU	DUPONT-NIVET	FRANCE	THALES RESEARCH AND TECHNOLOGY
22	MIKKEL	EJRNAES	ITALY	CNR SPIN
23	NICOLE	FABBRI	ITALY	CNR-INO
24	G.	FEUGNET	FRANCE	THALES RESEARCH AND TECHNOLOGY
25	F.	GUTTY	ITALY	CNR-INO
26	MARIA	JOKELA	FINLAND	VTT TECHNICAL RESEARCH CENTRE OF FINLAND LTD.
27	PENTTI	KARIOJA	FINLAND	VTT TECHNICAL RESEARCH CENTRE OF FINLAND LTD.
28	KARI	KAUTIO	FINLAND	VTT TECHNICAL RESEARCH CENTRE OF FINLAND LTD.
29	MATTI	KUTLA	FINLAND	VTT TECHNICAL RESEARCH CENTRE OF FINLAND LTD.

30	MARKKU	LAHTI	FINLAND	VTT TECHNICAL RESEARCH CENTRE OF FINLAND LTD.
31	C.	LARAT	ITALY	CNR-INO
32	ANDREA	MASINI	ITALY	FLYBY S.R.L
33	DAVIDE	MASSAROTTI	ITALY	UNIVERSITA' DI NAPOLI FEDERICO II
34	ALESSANDRO	MIANO	ITALY	UNIVERSITA' DI NAPOLI FEDERICO II
35	ALESSIO	MONTORI	ITALY	pppSense S.r.L.
36	DMITRY	MORITS	FINLAND	VTT TECHNICAL RESEARCH CENTRE OF FINLAND LTD
37	SIMONA	MOSCA	ITALY	CNR-INO
38	OLEG	MUKHANOV	ITALY	SeeQC-EU
39	ROBERTO	OSELLLAME	ITALY	ISTITUTO DI FOTONONCA E NANO TECNOLOGIE – CNR – MILANO
40	RALF	OSTENDORF	GERMANY	Fraunhofer Institute for Applied Solid State Physics
41	LOREDANA	PARLATO	ITALY	University of Napoli Federico II and CNR SPIN
42	GIOVANNI PIERO	PEPE	ITALY	University of Napoli Federico II
43	EMANUELE	POLINO	ITALY	UNIV. SAPIENZA DI ROMA
44	MIKA	PRUNILLA	FINLAND	VTT TECHNICAL RESEARCH CENTRE OF FINLAND LTD.
45	I.	Ricciardi	ITALY	CNR-INO
46	DANIELA	SALVONI	ITALY	UNVERSITA' DI NAPOLI FEDERICO II
47	ROBERTA	SATARIANO	ITALY	UNVERSITA' DI NAPOLI FEDERICO II
48	FABIO	SCIARRINO	ITALY	IFN-CNR
49	GIOVANNI	SERAFINO	ITALY	CNIT
50	TEEMU	SIPOLA	FINLAND	VTT TECHNICAL RESEARCH CENTRE OF FINLAND LTD.
51	S.	SMUK	SWEDEN	IRNOVA
52	NICOLO'	SPAGNOLO	ITALY	UNIVERSITA' LA SAPIENZA DI ROMA
53	D.	STORNAIUOLO	ITALY	UNIVERSITA' DI NAPOLI FEDERICO II
54	FRANCESCO	TAFURI	ITALY	UNIVERSITA' DI NAPOLI FEDERICO II
55	HANS DIETER	THOLL	GERMANY	DIEHL DEFENCE
56	COSTANZA	TONINELLI	ITALY	CNR-INO
57	SANNA	UUSITALO	FINLAND	VTT TECHNICAL RESEARCH CENTRE OF FINLAND LTD.
58	MAURO	VALERI	ITALY	UNVERSITA LA SAPEINXZA DI ROMA
59	I.	VERNIK	ITALY	SeeQC-eu
60	TESSA	VERSTRYNGE	BELGIUM	OIP SENSOR SYSTEMS
61	MIRIAM SERENA	VITIELLO	ITALY	CNR - NEST
62	ALESSANDRO	ZAVATTA	ITALY	CNR-INO

EUROPEAN DEFENCE AGENCY

PART I

ELECTRO OPTICAL QUANTUM TECHNOLOGY

OPTOELECTRONIC QUANTUM DEVICES FOR SENSING, PROTECTION AND RECONAISSANCE

Dr. Ralf Ostendorf
Business Unit Semiconductor Lasers
Fraunhofer Insitute for Applied Solid State Physics
79108 Freiburg, Germany
ralf.ostendorf@iaf.fraunhofer.de

***Abstract*— This article gives a brief overview of the military application spectrum of quantum devices. These include infrared emitters such as quantum cascade lasers as well as infrared detectors based Type 2 superlattice structures. Both technologies are based on quantum effects in solids such as tunneling electrons through potential barriers or the formation of discrete energy levels in quantum wells. By exploiting these quantum effects, lasers and detectors can be specifically optimized for military applications like missile warning and optical countermeasures for protection of airborne, naval or ground based vehicles.**

Further quantum devices considered in this overview include highly sensitive magnetic field sensors based on nitrogen vacancy centres ("NV centres"). This technology shows high potential for the detection of submarines and for GPS-free navigation using the Earth's magnetic field.

Keywords—Quantum technology, Quantum Cascade Laser, Type II Superlattice Detector, NV centres, Quantum Magnometry

Introduction

The term "quantum technology" refers to technical application of quantum mechanical effects such as wave particle dualism, tunnel effect but also state superposition or quantum entanglement. Even if the rules of the microscopic quantum world are difficult to reconcile with our macroscopic perception, they have been determining our everyday life for a long time. Groundbreaking inventions such as transistors or lasers are based on the technical application of quantum mechanics.

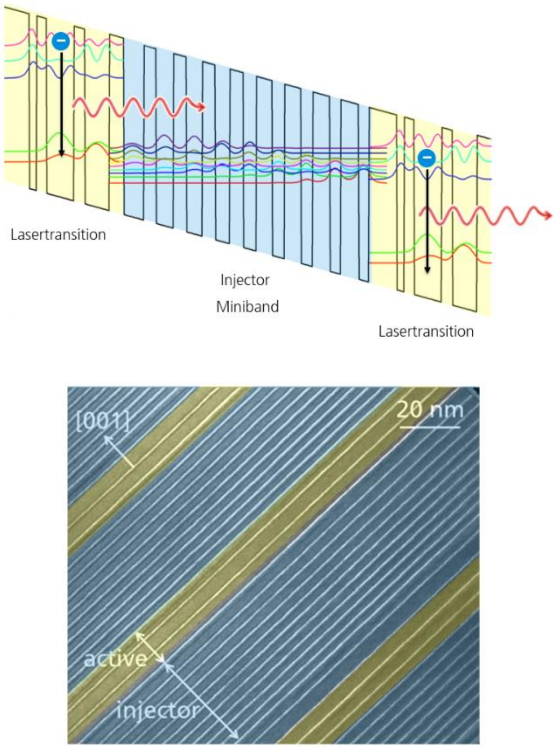

Fig. 1: Top: Schematic electronic bandstructure of a quantum cascade laser. Bottom: Electronic microscope picture of the semiconductor layer structure.

The technical exploitation of quantum mechanics was enabled by the development of capabilities to specifically influence and control processes at atomic and subatomic levels. Already in the nineties, Gerard J. Milburn outlined in his book "Schrödinger's Machines" how this technical progress enables the development of extremely sensitive sensors, the production of new, exotic materials or powerful computers based on quantum effects [1]. Thus quantum technology plays a central role in the development of future key technologies in the field of civil and military security research.

This article is intended to give a brief insight into the areas in which quantum technology is already being used today for security and protection in the military

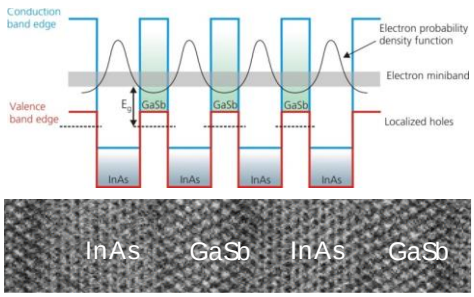

Fig. 2: Electronic bandstructure and layer structure of a InAs/GaSb based Type II superlattice detector.

environment and what perspectives future technical developments offer in this area.

Quantum components of the first generation

The "first quantum revolution" is usually associated with devices that use quantum mechanical effects to specifically influence and utilize a large number of particles or quantum states. Typical examples of quantum devices of the first generation, which are already used today in civil and military environments, are quantum cascade lasers and Type II superlattice detectors. Both technologies are based on complex sequences of semiconductor heterostructures. The realization of these has only become possible with decisive technical advances in molecular beam and gas phase epitaxy [2]. In both cases, the complex semiconductor structure consisting of several hundred only a few nanometre thick atomic layers shapes the electronic potential landscape in the solid in such a way that defined optical transitions of charge carriers can take place.

In the quantum cascade laser (QCL), two-dimensional quantum wells in the conduction band are realized by a sequence of semiconductor layers with different bandgaps, in which discrete energy levels are formed [Fig. 1]. By applying a voltage, optical intersubband transitions of electrons occur, in which photons are emitted in the mid-infrared wavelength range (4-12 µm). The emission wavelength of QCLs can thus be specifically adjusted during crystal growth by varying the layer thicknesses and thus the change in the quantum well width. The quantum mechanical tunnel effect allows the electrons in the QCL to move from one quantum well to the next, so that cascading of several optical transitions in succession - even of different emission wavelengths - is possible.

In superlattice detectors, the complex layer structure in the semiconductor achieves a superposition of numerous discrete energy levels, which leads to the formation of so-called electronic minibands [Fig. 2]. This results in a potential landscape for charge carriers with a flexibly adjustable artificial energy gap in the wavelength range of 3-20 µm.

By exploiting quantum effects, quantum cascade lasers and Type II superlattice detectors thus offer a high degree of flexibility with regard to the adaptation of their spectral range and optimization for applications of decisive parameters such as quantum efficiency, laser threshold or dark current. Due to well-known advantages of semiconductor technologies, such as compact and lightweight design and scalability of quantities, both technologies are highly interesting for use in military technologies, e.g. for protection of air- and seaborne plattforms against heat-seeking missiles.

The optical output power of QCLs at wavelengths of the atmospheric transmission windows is in the multi watt range [3], [4]. This is sufficient to disturb and deflect approaching missiles at a sufficient safety distance from the target by means of a coherent laser beam. In Europe as well as in the USA several companies are developing and offering QCL-based DIRCM (Directed Infrared Counter Measure) systems [5], [6].

Superlattice detectors can be used as a warning system to detect the CO2 emission of the exhaust plume already in the launch phase of missiles. EADS, for example, uses a detector based on Type II superlattice detectors for the "MIRAS" missile warning system in the A 400M military transporter [7]. This is the world's first military equipment programme to rely on Type II superlattice detectors.

Second generation quantum devices

The term "second quantum revolution" is generally used for components and devices that make use of single quantum states like electron spins by exploiting quantum effects such as superposition or entanglement of states. The best known example is the quantum computer, where spin states of single ions or electrons are used as "Qbits". The preparation and read out of such defined quantum states is still

very a complex technological task. In many cases, this can only be achieved by using large laboratory equipment and at cryogenic temperatures. In particular, keeping the quantum state stable over a long period of time, the so-called coherence time, poses a major challenge.

These great technical efforts are one reason why second-generation quantum devices are not yet widely used and are mainly the subject of academic research today. However, the new approaches enabled by second generation quantum devices especially in the fields of sensor technology and tap-proof communication promise a high application benefit for the civil and military market,.

Promising systems, which have a high potential to boost quantum sensor technology to room temperature operation and thus to open a wide field of new applications, are defect centers in semiconductors, in particular the so-called nitrogen vacancy centers (NV centers) in diamond. NV centers are generated by substituting a carbon atom by a nitrogen atom in the diamond crystal and removing another carbon atom in the direct vicinity of the nitrogen atom. The electric potential of this void captures an electron of the nitrogen atom whose spin can be oriented and used as the smallest possible "tactile magnet" [Fig. 3].

Due to the high Debye temperature of 1860 K, the crystal structure of the diamond is almost “frozen” at room temperature, so that hardly any interference of magnetic signals by phonons occur. Therefore, in contrast to established superconducting sensors (SQUIDS), magnetometers based on NV centres do not require cryogenic cooling and can achieve sufficient long coherence times for the preparation and read out of the electron spin even at room temperature. As NV centres in diamond absorb and emit light in the visible range, the preparation and read out of the quantum state can be realized by established optoelectronic methods using diode lasers and photodetectors.

So far, the achieved sensitivity record in magnetic field measurements with NV ensembles is 1pT/√Hz [8]. Thus, magnetometry with NV centers has the potential to achieve higher sensitivities at room temperature than the SQUID sensors with cryogenic cooling used today. This opens up the possibility of realizing compact, highly integrated and extremely sensitive magnetometers that e.g. can be used in networks of autonomous unmanned underwater vehicles (UUV) for submarine detection. Further, this approach can also be utilized in navigation systems that are oriented to the earth's magnetic field and thus work independently of a satellite connection.

Another approach of the "second quantum revolution" is the use of entangled photons, for example for tap-proof communication or sensor technology. This quantum effect, which Einstein referred to as the "spooky action at a distance", connects two particles in such a way that a change in one particle has measurable effects on the other particle.

This makes it possible to establish a physically secure connection between participants to exchange quantum keys. In fact, this technology is already in use on a larger scale for some time. China established a secure connection based on quantum communication over a distance of more than 2000 km between Beijing and Shanghai [9]. Recently the encrypted communication by entangled photons between satellites over a distance of more than 1200 km could also be shown [10].

The so-called "Ghost Imaging" is a sensing technique based on entangled photons [11]. One photon interacts with the object to be measured, while the actual detection takes place with the second photon that never came into contact with the object. Since the photons do not necessarily have to have the same wavelength, it is possible to scan objects in the mid-infrared spectral range using ghost imaging, while the actual detection can be realized with low-cost CCD cameras in the visible wavelength spectrum.

Summary

Various types of quantum devices are already being used today in both civilian and military security and protection technologies. Lasers, such as QCLs, but also optical infrared detectors, are the most important of these. These components are essentially based on the application of quantum effects of the "first quantum revolution".

The "second quantum revolution" currently taking place holds great potential for establishing novel measuring principles, especially in the fields of quantum sensor technology and quantum

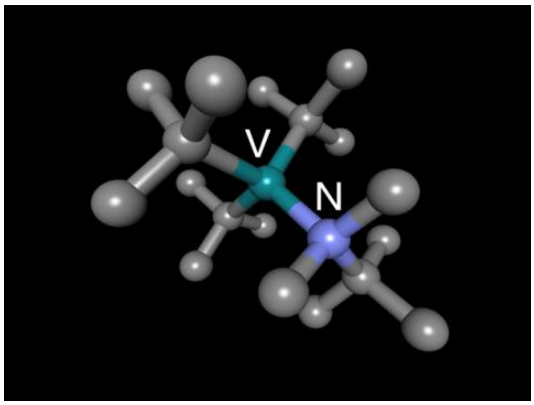

Fig. 3: Schematically structure of a Nitrogen Vacancy centre.

communication, which surpass existing technologies in terms of sensitivity and can be used in numerous applications for protection and reconnaissance.

References

[1] Gerard J. Milburn, Schrödinger's machines : The quantum technology reshaping everyday life. W.H. Freeman, 1997.

[2] J. Faist, F. Capasso, D. L. Sivco, C. Sirtori, A. L. Hutchinson, and A. Y. Cho, "Quantum Cascade Laser," Science (80-.)., vol. 264, pp. 553–556, 1994.

[3] A. Lyakh et al., "3 W continuous-wave room temperature single-facet emission from quantum cascade lasers based on nonresonant extraction design approach," Appl. Phys. Lett., vol. 95, no. 14, p. 141113, 2009.

[4] R. Maulini, A. Lyakh, A. Tsekoun, R. Go, and C. K. N. Patel, "High average power uncooled mid-wave infrared quantum cascade lasers," Electron. Lett., vol. 47, no. 6, p. 395, 2011.

[5] "Elettronica Group and Indra work towards first European Quantum Cascade Laser based Infrared Counter Measure System dubbed EuroDIRQM | indra." [Online]. Available: https://www.indracompany.com/en/noticia/elettronica-group-indra-work-towards-first-european-quantum-cascade-laser-based-infrared. [Accessed: 17-May-2019].

[6] "Northrop Grumman Announces Quantum Cascade Laser-Based Solution for Its Common Infrared Countermeasures (CIRCM) Offering | Northrop Grumman." [Online]. Available: https://news.northropgrumman.com/news/releases/photo-release-northrop-grumman-announces-quantum-cascade-laser-based-solution-for-its-common-infrared-countermeasures-circm-offering. [Accessed: 17-May-2019].

[7] "EADS and Thales to Supply Latest-Technology Missile Warner to A400M." [Online]. Available: http://www.defense-aerospace.com/article-view/release/63242/eads-win-rwr-contract-for-a400m-(sep-29).html. [Accessed: 17-May-2019].

[8] T. Wolf et al., "Subpicotesla Diamond Magnetometry," Phys. Rev. X, vol. 5, no. 4, p. 041001, Oct. 2015.

[9] "China eröffnet 2.000 Kilometer lange Leitung für Quantenkommunikation_China.org.cn." [Online]. Available: http://german.china.org.cn/txt/2017-09/30/content_50029834.htm. [Accessed: 17-May-2019].

[10] J. Yin et al., "Satellite-based entanglement distribution over 1200 kilometers.," Science, vol. 356, no. 6343, pp. 1140–1144, Jun. 2017.

[11] G. B. Lemos, V. Borish, G. D. Cole, S. Ramelow, R. Lapkiewicz, and A. Zeilinger, "Quantum imaging with undetected photons," Nature, vol. 512, no. 7515, pp. 409–412, 2014.

IRNOVA'S NOVEL T2SL AND QWIP: THE LONG-AWAITED INFRARED GAME CHANGERS

L. Höglund, S. Smuk, E. Costard
IRnova AB,
Electrum 236, Kista, Sweden, SE-164 40
Contact author:eric.costard@ir-nova.se
www.irnova.se

***Abstract*— IRnova is an independent Swedish company serving the OEM high-end infrared detector market and related services. IRnova's leading researchers and state of the art production assets combine to serve both challenging military requirements and emerging infrared applications. Recent breakthroughs in both QWIP and HOT MWIR T2SL focal plane arrays strengthened IRnova's position as the European pioneer in IR sensors. During this presentation we will introduce our recent T2SL technology development and demonstrate our HOT MWIR detectors for compact, lightweight and battery life time friendly infrared systems.**

We will also introduce the key advantages of T2SL and QWIP technologies for LWIR applications. While the high resolution QWIP is an affordable solution for terrestrial applications with its excellent imaging properties and long-term stability, T2SL is designed for high QE space applications in the VLWIR region. Finally, we will introduce the unique capability of QWIP to reveal the unseen polarimetric infrared information, which enables enhanced face recognition as well as detection of man-made objects hidden in vegetation.
Keywords—Quantum technology, Quantum Cascade Laser, Type II Superlattice Detector, NV centres, Quantum Magnometry.

Keywords : QWIP, T2SL, IR detector, LWIR, MWIR, Polarimetric

Introduction

The In a first chapter "T2SL Technoloy"we will present the key advantages of T2SL especially for HOT MWIR and we will introduce our first SWaP_C detector (reduced Size, Weight and Power, without forgetting reduced Cost).

In the second chapter "QWIP technology" we will show that high resolution QWIP is an affordable solution for LWIR applications with its excellent imaging properties and long-term stability, and we will introduce the unique capability of QWIP to reveal the unseen polarimetric infrared information, which enables enhanced face recognition as well as detection of man-made objects hidden in vegetation.

T2SL Technology

Type-II superlattices have proven to be a mature technology for production of infrared focal plane arrays (FPAs), with well-established products in several companies [1]. Major breakthroughs for high operating temperature operation (HOT) and large format FPAs have been demonstrated which proves the important role of this technology [1,2,3,4]. High operating temperatures enables smaller coolers and overall smaller camera systems with reduced Size, Weight and Power (SWaP), which open up for entirely new fields of applications for this technology, such as high-performance infrared payloads for drones, light-weight / high-performance handheld and battery powered cameras . IRnova has been manufacturing midwave infrared (MWIR) FPAs since 2012 and has since then demonstrated excellent manufacturability of these FPAs with good stability over time, high operability, and narrow noise distribution [1,2,3]. In the initial studies, the FPAs were operated at 85 K, however, during the past years improvement of the design and fabrication techniques have enabled operating temperatures up to 120 K with great imaging quality which makes these FPAs ready for low-SWaP applications.

a) Material

The photodiode designs have been modelled using a complete set of simulation tools developed by IRnova [1]. The designs of the MWIR structures used in this study are schematically illustrated in Figure 1a. These designs are similar to the MWIR epitaxial design reported in ref. [1], but with the InAs, GaSb and AlSb layer thicknesses of the SLs slightly modified to

change the bandgaps to the desired cut-off wavelengths. Standard III/V processing techniques were used to fabricate the FPAs. The pixels were formed by a combination of dry and wet etching, with fully reticulated pixels (Figure 1b). After passivation and metallization, the arrays were hybridized to VGA format read out circuits, underfill was deposited, the GaSb substrate was fully removed and finally an antireflection (AR) coating was applied.

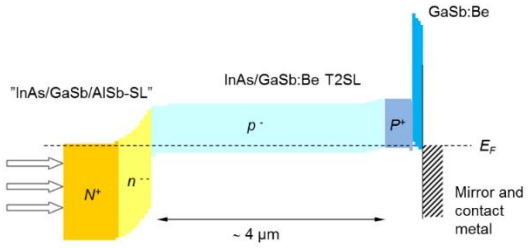

(a)

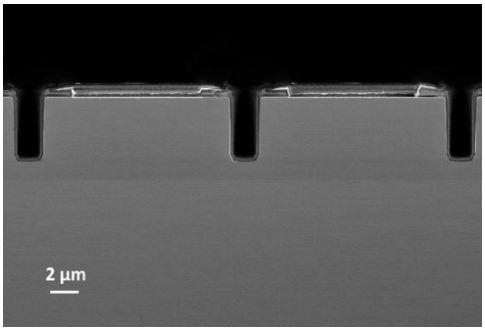

(b)

Figure 1. (a) Double heterostructure (DH) detector design used in IRnova's detectors
(b) SEM image of etched pixels in a 640 × 512 array with 15 µm pitch.

b) Modeling

Two different detector structures have been modelled with respect to external quantum efficiencies, photocurrent density and dark current density and are referred to as the RED HOT (5.3µm cut-off wavelength) and the DEEP BLUE (4.2µm cut-off wavelength) designs. The RED HOT design is already in production at IRnova and is used as a reference point for the detector design and the modelling. For the DEEP BLUE design the absorber SLs have been slightly modified to the cut-off wavelengths of 4.2 µm and the barrier layers have been designed in order to avoid barriers in the conduction band layer which could result in a high turn-on bias.

The external quantum efficiencies of the different designs were calculated using a model that takes both the absorption and the diffusion transport of photogenerated carriers to the contacts into account [9]. For the absorption modelling, the measured absorption coefficient as well as thicknesses and refractive indices of the layers in the detector structure are used as input. The transport is affected both by the minority carrier lifetime as well as the mobility in the material. For the RED HOT design (Figure 2a) a minority carrier lifetime of 80 ns and a mobility of 1000 cm2/V were assumed, which resulted in very good agreement between measured and simulated quantum efficiencies. The diffusion length corresponding to this mobility and minority carrier lifetime is 7.3 µm, which is long enough to enable collection of most of the photogenerated carriers in the ~4 µm thick absorber. This diffusion length is also in good agreement with what other groups have reported for MW InAs/GaSb p-type material [1]. From the calculated QE spectra, the photocurrent was also extracted for different irradiances and geometries of the optics. For the RED HOT design, a photocurrent density of ~40 µA/cm2 was calculated for F/4 optics and 303 K illumination (Figure 3). This calculated photocurrent density correlates well with measured integrated photocurrent densities for these devices.

The same model was used to predict the performance of the DEEP BLUE design. The absorption coefficient was set to be the same as for the RED HOT design, but with the spectrum shifted to the designed cut-off wavelength. A modest increase of the minority carrier lifetimes to 100 ns for the DEEP BLUE design was assumed due to the shorter cut-off wavelength. The resulting QE spectra and corresponding photocurrent densities are shown in Figure 2 nd in Figure 3, respectively.

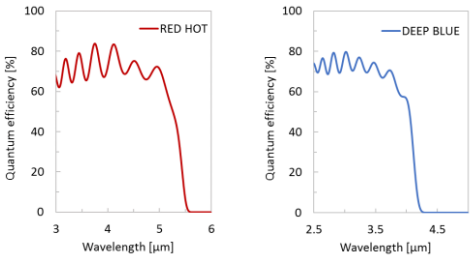

(a) *(b)*

Figure 2. Opticalsimulation of quantum efficiencies for different IRnova designs for HOT application, with cut-off wavelengths at: 5.3µm: RED HOT and (b) 4.2 µm: DEEP BLUE

By comparing photocurrent densities to dark current densities, the maximum operating temperatures with these designs with F/4 optics are deduced to:

RED HOT: ~130 K
DEEP BLUE: ~150 K

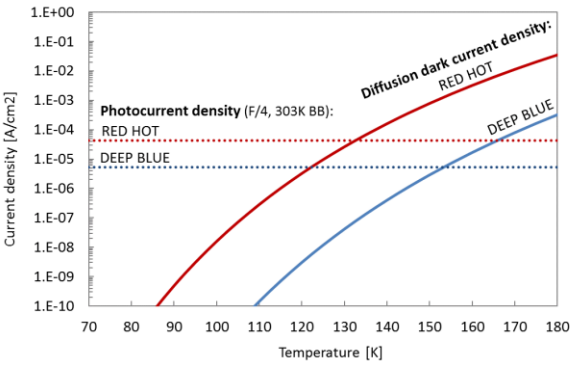

Figure 3. Comparison between calculated photocurrent densities (dotted lines) at F/4 (303K blackbody) and diffusion dark current densities (solid lines) for different IRnova designs : λ_{off} =5.3µm@RED HOT and λ_{off} =4.2 µm@DEEP BLUE.

c) FPA performance

In a second step, the external QE and dark current density were studied on FPA level to see the effect of the FPA fabrication on the device performance. The individual quantum efficiency of each pixel in the FPA was estimated by 1) calculating the number of photons from the known light source (black body) that is absorbed by a pixel, and 2) converting the pixel's signal to the number of electrons in the respective ROIC capacitor. The external quantum efficiency is then calculated from the slope of the relation between *absorbed photons* and *generated and collected electrons*. The average QE on FPA level was deduced to ~80% at 110 K, which is comparable to the simulated value of QE (Figure 2) and in good agreement with the measurements on single pixel photodiodes from which an external QE higher than 75% was estimated (with AR coating and double pass). The dark current densities of the reference pixels in the frame of the FPA were measured and compared to the calculated diffusion dark current density (Figure 4b). The measured dark current density in the 13×13 µm^2 sized pixels deviates slightly from the diffusion limited behavior, however the dark current density stays lower than the photocurrent density up to 126 K (with F/4 optics, 303 K black body) enabling high operating temperatures of these FPAs.

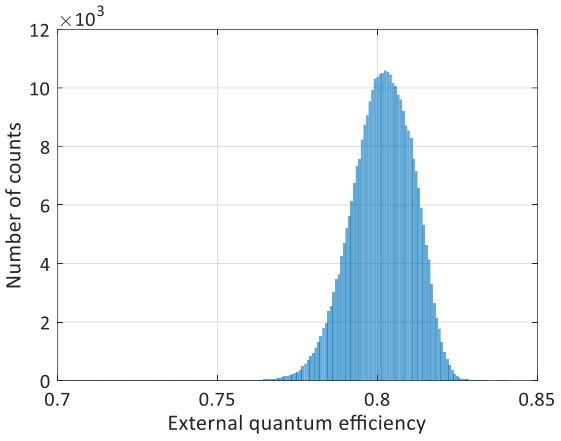

(a)

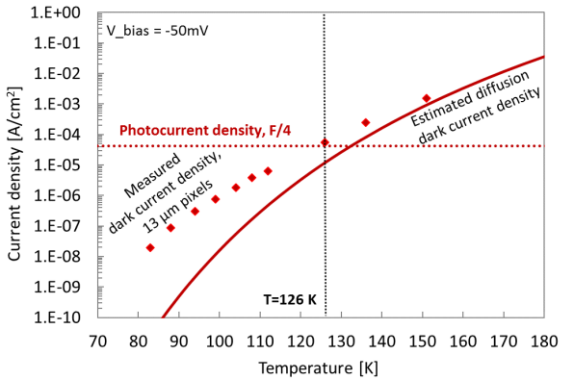

(b)

Figure 4. (a) External QE histogram deduced from the FPA pixels in a 640×512 FPA with 15µm pitch and the RED HOT design. (b) Measured temperature dependence of the dark current density of 13µm sized reference pixels in the frame of an FPA (squares) compared to calculated bulk diffusion dark current (solid line).

To study the evolution of the FPA performance with increasing temperature of the RED HOT FPAs, the temporal and spatial NETD values are measured and compared (Figure 5a). As observed in Figure 5a, both the temporal and spatial NETD are almost unaffected by the temperature increase up to 110 K, with temporal NETD of ~20 mK and spatial NETD of ~5 mK. At 120 K a minor increase of the NETD values is observed (up to 23 mK and 7 mK, respetively) and

above 125 K the NETD values start to increase more rapidly. This behavior is correlating well with the evolution of the ratio between photocurrent and dark current shown in Figure 4b, which equals 1 at ~126 K (at F/4) and crosses at slightly higher temperature (~140 K) for F/2. The low temporal noise and uniformity across the array is also observed in the narrow distribution of the temporal NETD, shown in Figure 5b.

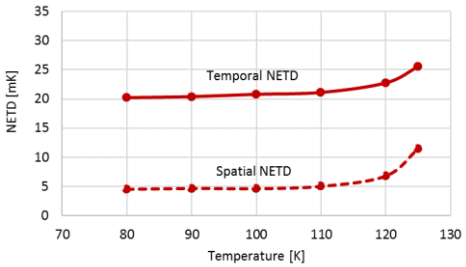

(a)

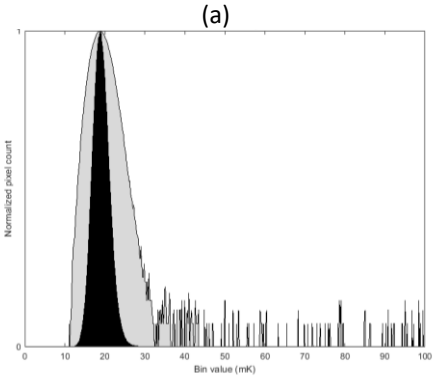

(b)

Figure 5. (a) Temperature dependence of the temporal and spatial NETD from 80 K up to 125 K for VGA FPA with RED HOT design, F/4. (b) NETD histogram of 640 x 512 FPA with 15 µm pitch (VGA) at 80 K, RED HOT design.

d) HOT SWaP IDDCA performance

The excellent performance observed for the RED HOT FPAs at operating temperatures above 110 K, enables the use of a small cooler (RMs1, see Figure 6) and a small dewar designed for F/4 optics, with a total size of 10 cm x 5 cm and a weight of 230 g. This brings the IRnova T2SL FPAs in to the HOT SWaP regime and excellent performance has been demonstrated with this IDDCA, as summarized in Table 1 and in Figure 7 .

Figure 6. RED HOT FPA integrated in SWaP IDDCA with RMs1 cooler from Thales Cryogenics.

Measurement: HOT SWaP IDDCA	
Cut-off wavelength [µm]	5.3
Operating temperature [K]	110
Temporal NETD [mK]	21
Spatial NETD [mK]	7
Integration time [ms]	10
Operability [%]	99.8
Optics	F/4

Table 1. Performance of RED HOT FPA integrated in SWaP IDDCA with a RMs1 cooler.

Figure 7. Imaging with RED HOT FPA (640x512 pixels, 15µm pitch), operated at 110 K. Temporal NETD = 21mK, spatial NETD = 7 mK, F/4, and 10 ms integration time.

With further optimization, the operating temperature with the RED HOT design will be increased to 130K, as estimated in Figure 3. The next step is to also implement the DEEP BLUE design to further increase the operating temperature and reduce the restriction for cooling power.

QWIP Technology

Quantum Well Infrared Photodetectors (QWIP) is a well-known III-V technology employing band-gap engineering through confinement of electrons in thin layers of semiconductor material with different compositions. These detectors are rather well studied, and their shortcomings are widely discussed [13]. Low overall conversion efficiency is what the QWIPs are most often blamed for and what had caused the infrared experts to claim the short life expectancy for the technology some 15 years ago. However, thanks to numerous benefits offered by the technology, the QWIPs have found their way to many applications where they remain the first-choice technology. Uniformity and stability are the features firmly associated with QWIPs. Also, manufacturability and low cost, which come together with the reliable and well-developed III-V semiconductor process, are undeniable benefits of QWIPs as compared with some other technologies. Extensive expansion of QWIPs in modern applications has been hindered by widely-shared scepticism about their performance in detectors on smaller pitch. The referring was most often given to the fundamental limitations with the employment of diffraction grating on small pixels in combination with low conversion efficiency. The recent progress in the QWIP development at IRnova showed that the fears are somewhat overdriven and QWIP detectors offer excellent performance for VGA format arrays on 15 µm pitch[14, 15].

One of the key benefits of the QWIP technology is the possibility for easy adjustment of the wavelength range of the detector's response. IRnova make use of this feature to move the peak absorption wavelength to around 10.5 µm for gas detection, primarily aiming at SF6 gas.

Selective sensitivity of QWIPs to polarization of the incident light and the consequent necessity of using diffraction mirror *for increasing the light coupling* has always been pointed out as a negative feature. This, however, opens for a natural expansion of QWIP's application domain to polarimetric imagers by employing wire grid grating instead of the isotropic 2D grating. This possibility was discussed for many years and some attempts were made earlier, as well [16,17]. IRnova have reported the development of QWIP-based polarimetric detectors earlier [18] and launched a product based on it. In this article we will present further development of this field of QWIP applications.

The QWIP part of IRnova's product portfolio today includes detectors of VGA format on 15 µm pitch with the peak absorption wavelength at 8.5 µm for general purpose applications and at 10.5 µm for civilian applications (SF6 gas detection), as well as a quarter VGA format on 30 µm pitch for polarimetric applications, further on referred to as 640-LW, 640-SF6 and polQWIP, respectively. Some other formats based on 30 and 25 µm pitch are also available but not addressed in this paper.

Typical responsivity curves for all three detector types are presented on the same plot in Figure 8 together with absorption lines for various gases (not specified).

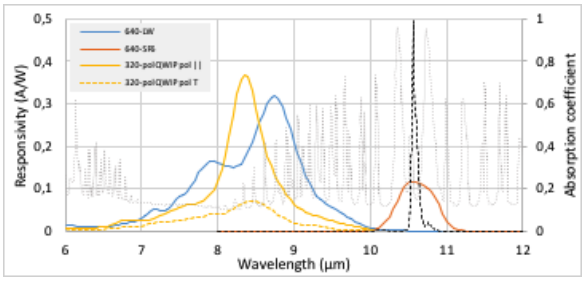

Figure 8. Responsivity of 640-LW, 640-SF6, and polQWIPs by IRnova (at –1.5 V bias with 70 K, 57 K, and 70 K operation temperatures, respectively). Absorption lines for various gases are given for reference: for SF6 – in black, and ammonia – in gray.

Manufactured detectors are integrated in IDDCA according to the procedure described in [15]. It should be noted that 320-SF6 has been available on the market for several years and delivered in significant volumes to the customers. 640-SF6 is a new product released late 2018, and it is interesting to compare its performance with the 320- format. Both IDDCA share basically the same envelope and the same model of 0.5 W cooler.

Figure 9. General view of IRnova's IDDCA for SF6 gas detection in quarter VGA and VGA resolution with F/numbers of 2.0 and 1.2, respectively. The IDDCA share most of the envelope parts and the 0.5 W cooler. The operating temperature is 57 K.

Detector type	F/number	Operating temperature, K	Frame rate, Hz	Integration time, ms	Temporal NETD, mK	Spatial NETD at 35 °C BB, mK	Responsivity, mV/K	Operability, %	Cooler power consumption, W
320-SF6	2.0	57	30	15*	23	6	18	99.95	7.8
640-SF6	1.2	57	30	32	26	10	18	99.90	8.2

Table 1. Comparison of typical performance of 320-SF6 and 640-SF6 IDDCA at 30 and 40 °C correction temperatures and max scene temperature of 50 °C

In the wavelength region above 10 µm QWIP maintains all its benefits and shows very robust and stable performance. Excellent image quality remains the QWIP's characteristic feature for these detectors, as well (Figure 10 a). The distribution of NETD values is very narrow and symmetrical, showing only very little tail seen only in log scale (Figure 10 b). The operability remains at the levels above 99.9 % typical for QWIPs.

It can be concluded that overall performance of high-resolution SF6 gas sensing detector is well in line with the expectations and accurately follows the model's predictions.

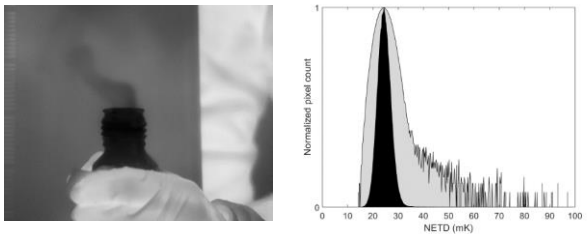

(a) (b)

Figure 10 (a) Imaging of ammonia vapour obtained by IRnova's 640-SF6 QWIP DDCA with F/1.2 optics at 15 Hz frame rate. The background is black-coloured metal plate at room temperature.
(b) Histogram of NETD distribution on 640-SF6 QWIP FPA when imaging an extended black body source with 30 C. Black colour shows data in linear scale, and grey – in logarithmic scale.

a) Polarimetric QWIP FPA

The necessity of using a diffraction grating for improving the light coupling in QWIP detectors has always been considered as a conceptual drawback. This very feature, however, introduces additional degree of freedom for manipulating the light detection. By breaking isotropy of the diffraction element we get access to otherwise hidden information about polarization state of the incident light. IRnova consider this feature of QWIP as rather a benefit than a drawback and made use of it to design a polarization-sensitive detector. IRnova's high performance LWIR QWIP detector [14] was used as the starting point for designing a polarization-sensitive IR detector (pol-QWIP). The 2D grating was replaced by 1D wire grids with the four orientations (0°, +45°, 90°, or -45° with respect to the pixel edge) in a checkerboard pattern (Figure 11 b). A 2×2 block of neighbouring pixels forms a functional unit, which is further referred to as microgrid superpixel (Figure 11 b). Two different pitch sizes were investigated: 30 µm for 320×256 (QVGA) and 15 µm for 640×512 (VGA) FPA formats. The corresponding pixel sizes were 26 and 13 µm, respectively.

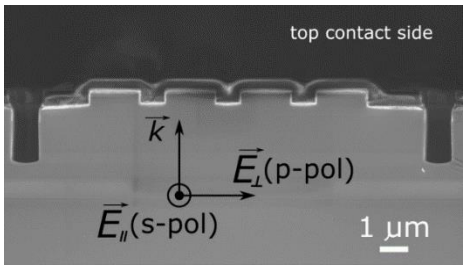

(a)

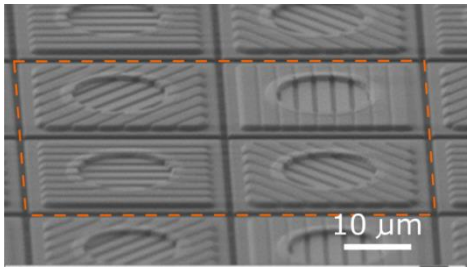

(b)

Figure 11 (a) SEM image of a single pixel (13 µm)2 with indication of the illumination path in the real geometry.(b) SEM image of a pixel array with 30 µm pitch size, showing different lamellar gratings fabricated on top of the pixels. Microgrid superpixel is denoted by dashed orange line.

For efficient optimization of the 1D grating structure, a 3D finite-difference time-domain (FDTD) model of detector pixel has been built using Meep simulation toolbox [20]. The wire grid grating has been optimized for maximum coupling efficiency at 8.5 µm (Figure 12). The optimal values for the grating period, etch depth and duty cycle were obtained from the simulation and used for fabrication of pixel arrays. Spectral response of the pixels with optimized grating design was measured on the single-pixel samples, the results of the measurements are given in Figure 12 (a). For 30 µm pitch arrays, the measured spectral response of the pol-QWIP with grating orientations 0° and 90° are comparable to that of regular QWIPs, as shown in Figure 12 (b).

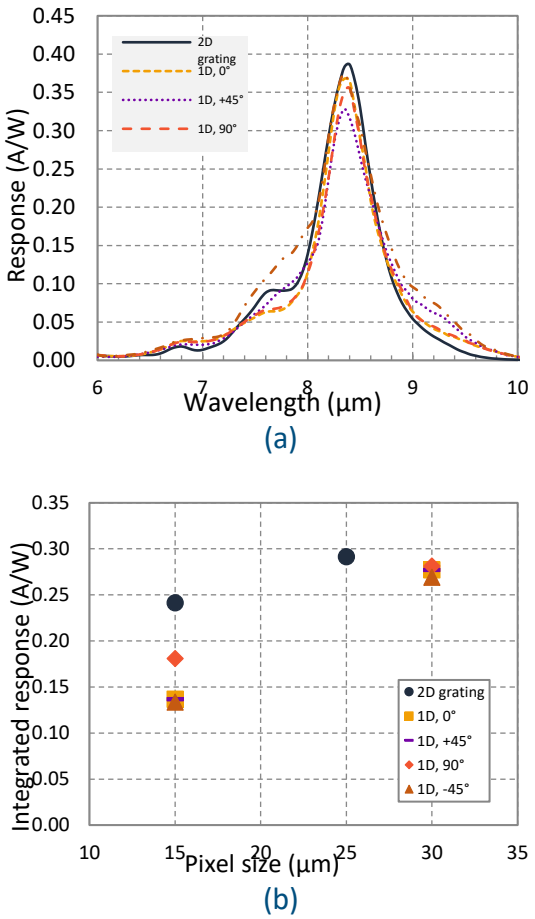

Figure 11. (a) Spectral response of the pixels with optimized 1D grating in relation to that of pixels with regular 2D grating.
(b) The inset to part (b) summarizes spectrally integrated responses.

Typical spectral response of a single pixel to illumination with linearly polarized light is presented in Figure 13 (a) along with the simulation results from our model. Good agreement is observed between the experimental and simulation data, which verifies the credibility of the employed FDTD model. Large extinction ratio of the optical response for orthogonal polarizations indicates good grating quality. To assess the ability of a pixel to resolve the state of linear polarization we used polarization contrast, $C_R=(R_\perp-R_\parallel)/(R_\perp+R_\parallel)$, where $R_\perp$ and $R_\parallel$ are the pixel response to illumination by light polarized perpendicularly (p- polarization) and parallelly (s-polarization) to the grating lamellae, respectively. The achieved CR values of ~0.6 for 26 μm pixels are on the state-of-the art level [16].

Summary

In this article, modelling and performance of high operating temperature type-II superlattices FPAs have been demonstrated. The temperature dependence of the performance deduced from modelling corresponds well to the demonstrated performance, both at single pixel level, FPA level and IDDCA level. Excellent imaging has been demonstrated at 110 K with the HOT FPA integrated in an F#4 IDDCA, which with the small RMs1 cooler shows that this technology is ready for low SWaP applications.

In this article we also demonstrated that QWIPs remain the first-choice technology for a number of applications in the long-wave infrared range. It has been proven that QWIPs can show excellent performance at VGA and 15 µm pitch format. Being properly tuned, the area of applications can be extended to a rather demanding cases, such as gas detection on handheld devices. IRnova proposes a polarimetric LW detector that is already implemented in a camera of Noxant Figure 14.

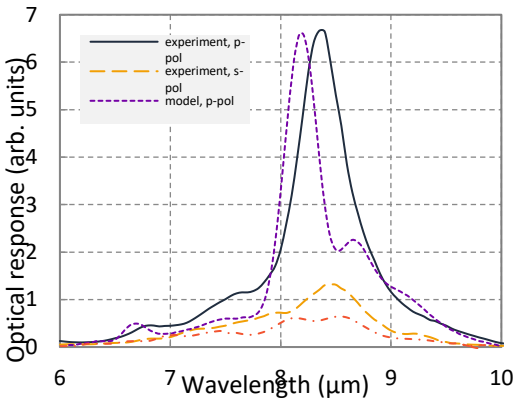

Figure 12.Measured (experiment) and simulated (model) spectral response of a (26 µm)² size pixel with 0° grating to illumination by p- and s-polarized light

Figure 13. Commercial camera by Noxant, https://www.noxant.com, based on IRnova's polQWIP detector with quarter VGA resolution on 30 µm pitch.

References

[1] Gerard J. Milburn, Schrödinger's machines : The quantum technology reshaping everyday life. W.H. Freeman, 1997.

[2] J. Faist, F. Capasso, D. L. Sivco, C. Sirtori, A. L. Hutchinson, and A. Y. Cho, "Quantum Cascade Laser," Science (80-.)., vol. 264, pp. 553–556, 1994.

[3] A. Lyakh et al., "3 W continuous-wave room temperature single-facet emission from quantum cascade lasers based on nonresonant extraction design approach," Appl. Phys. Lett., vol. 95, no. 14, p. 141113, 2009.

[4] R. Maulini, A. Lyakh, A. Tsekoun, R. Go, and C. K. N. Patel, "High average power uncooled mid-wave infrared quantum cascade lasers," Electron. Lett., vol. 47, no. 6, p. 395, 2011.

[5] "Elettronica Group and Indra work towards first European Quantum Cascade Laser based Infrared Counter Measure System dubbed EuroDIRQM | indra." [Online]. Available: https://www.indracompany.com/en/noticia/elettronica-group-indra-work-towards-first-european-quantum-cascade-laser-based-infrared. [Accessed: 17-May-2019].

[6] "Northrop Grumman Announces Quantum Cascade Laser-Based Solution for Its Common Infrared Countermeasures (CIRCM) Offering | Northrop Grumman." [Online]. Available: https://news.northropgrumman.com/news/releases/photo-release-northrop-grumman-announces-quantum-cascade-laser-based-solution-for-its-common-infrared-countermeasures-circm-offering. [Accessed: 17-May-2019].

[7] "EADS and Thales to Supply Latest-Technology Missile Warner to A400M." [Online]. Available: http://www.defense-aerospace.com/article-view/release/63242/eads-win-rwr-contract-for-a400m-(sep-29).html. [Accessed: 17-May-2019].

[8] T. Wolf et al., "Subpicotesla Diamond Magnetometry," Phys. Rev. X, vol. 5, no. 4, p. 041001, Oct. 2015.

[9] "China eröffnet 2.000 Kilometer lange Leitung für Quantenkommunikation_China.org.cn." [Online]. Available: http://german.china.org.cn/txt/2017-09/30/content_50029834.htm. [Accessed: 17-May-2019].

[10] J. Yin et al., "Satellite-based entanglement distribution over 1200 kilometers.," Science, vol. 356, no. 6343, pp. 1140–1144, Jun. 2017.

[11] G. B. Lemos, V. Borish, G. D. Cole, S. Ramelow, R. Lapkiewicz, and A. Zeilinger, "Quantum imaging with undetected photons," Nature, vol. 512, no. 7515, pp. 409–412, 2014.

QUANTUM-ENHANCED SENSORS WITH SPINS AND PHOTONS

N. Fabbri
CNR-INO, and LENS
Sesto Fiorentino (FI), Italy
fabbri@lens.unifi.it

S. Avino
CNR-INO
Pozzuoli (NA), Italy
saverio.avino@ino.cnr.it

F.S. Cataliotti
Univ. Firenze, and LENS
Sesto Fiorentino (FI), Italy
fsc@lens.unifi.it

M. De Rosa
CNR-INO
Pozzuoli (NA), Italy
maurizio.derosa@ino.cnr.it

G. Gagliardi
CNR-INO
Pozzuoli (NA), Italy
gianluca.gagliardi@ino.it

A. Masini
FlyBy s.r.l.
Livorno (LI), Italy
andrea.masini@flyby.it

I. Ricciardi
CNR-INO
Pozzuoli (NA), Italy
iolanda.ricciardi@ino.it

P. De Natale
CNR-INO, and LENS
Sesto Fiorentino (FI), Italy
paolo.denatale@ino.cnr.it

***Abstract* — Quantum-enhanced technologies tailored for imaging and sensing can make possible nowadays to realize advanced measurement systems surpassing the capabilities of their classical counterpart for applications in the defence domain. CNR-INO deploys different research activities focused on the development of novel optical and solid-state technologies, based on NV centers in diamond and optical interferometry, and targeting the key areas of Quantum spectroscopy and Quantum-enhanced imaging and sensing systems.**

Keywords — NV centers, sensors of magnetic fields and rotation, interferometry, Quantum spectroscopy, Quantum-enhanced imaging and sensing systems

Introduction

Can real-world practical devices based on quantum resources strikingly outperform the capabilities of the classical devices currently adopted in the defence domain?

Interestingly, a class of applications has emerged in recent years, employing quantum-mechanical objects as ultraprecise *quantum sensors* for physical quantities, ranging from magnetic and electric fields, to time, frequency, and rotations.

Quantum sensors can offer two major breakthroughs for applications in the defence domain, that are, the superior *sensitivity and compactness*. The *sensitivity* advantage is guaranteed by the use of quantum resources, that is, quantum superposition and entanglement. Quantum superposition states can usefully encode information in their phase – a feature that can be exploited for computation and communication, but this phase is actually very susceptible to tiny external disturbances: quantum sensors use this pronounced sensitivity to extract precise information about the physical quantity to be measured. Entangled states, and more generally non-classical states as *e.g.* squeezed states, can be used to surpass the classical limit in sensitivity (which improves rather slowly with the number of resources, as $1/\sqrt{N}$), and to achieve the quantum metrology limit, where precision improves linearly with the number of resources. *Compactness* stems from the use of nanoscale-sized sensing modules. This leads to higher spatial resolution thanks to miniaturization of the devices and makes quantum sensors suitable for integrated solutions in small and flexible systems.

Quantum sensors are accessible technologies in today's laboratories and have shown to be the most promising to be turned in the short term in systems operating in relevant environments. This trend in quantum technology is reminiscent of the history of semiconductors, where photodetectors have reached commercial distribution decades before computers [1].

The Italian National Institute of Optics (Istituto Nazionale di Ottica - Consiglio Nazionale delle Ricerche, CNR-INO) has a widely-recognized experience in the development of quantum sensors for a diverse range of applications. CNR-INO focuses on the following areas.

- *Optically-addressable spin-qubits sensors.* We develop nanoscale sensors based on the spin of optically-active Nitrogen-vacancy (NV) centers in diamond, for ultraprecise measurement of magnetic and electric fields, and rotation. The NV sensors enable an unprecedented combination of sensitivity, enhanced by the application of quantum control methods [2], [3], solid-state-enabled spatial resolution, and suitability for on-chip integration.

- *Quantum-enhanced optical interferometry.* We investigate quantum-enhanced optical interferometry schemes, based on squeezed light and single-photon interference. Nonlinear interferometers, where linear beam-splitters are replaced with parametric amplifiers, are expected to surpass classical interferometers and lead to a significant improvement of phase-shift measurement uncertainty, towards the quantum metrology limit. We develop a nonlinear interferometer based on quadratically nonlinear parametric amplifiers injected by squeezed light in one of the interferometer ports. In a second configuration, a single-photon interferometer realizes interaction-free measurement (IFM) experiments [4], crucial in all cases where the measurement perturbation is critical. Optical fiber sensors (OFS) are powerful tools for several applications thanks to their unique feature [5]: low-cost, light-weight, miniaturization, immunity to EM-interference, remote operation and in diverse environments. We combine IFM with OFS through evanescent-wave fiber-optic interferometers interrogated with single photons.

Spin-based sensors with diamond NV centers.

We develop robust, tunable, compact, and non-invasive quantum sensors based on NV centers in diamond, which are operable at room temperature, in unshielded environments. NV centers are optically-addressable atom-like impurities trapped in the diamond lattice. The NV-based sensors offer state-of-the-art combination of spatial resolution and sensitivity to DC and AC magnetic fields and are also promising sensors of rotation.

The NV-based sensors benefit from the advantages of solid-state platforms in terms of miniaturization, enabling compact and flexible solutions. The core of the sensing module is the ground-state electronic spin associated to the NV center. This spin is manipulated with microwave radiation (around 3 GHz) and optically addressed by collecting the emitted fluorescence (in the band 638-850 nm) under 532-nm optical illumination (see Fig.1). A Ramsey interferometer scheme (obtained by applying two Hadamard gates, at the beginning and at the end of the interrogation time) can be used to monitor the phase accumulated by a quantum superposition state due to the coupling with a tiny external field to be measured.

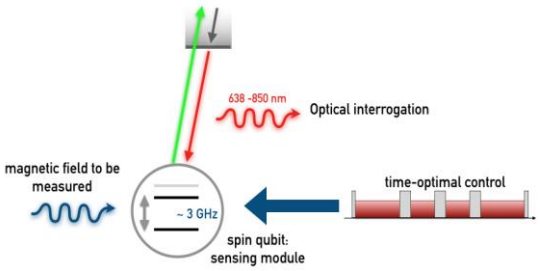

Fig.1 Basic scheme of operating principle of an optimized NV sensor.

Ensembles of NV centers can be collectively addressed in densely doped diamond crystals. In this kind of settings, the predicted sensitivity is competitive with atomic sensors, reaching around 250 aT/(√Hz/cm$^{-3/2}$) for NV magnetic field sensors [6], and 10^{-5} (rad/s)/(√Hz/mm$^{3/2}$) for NV gyroscopes [7]. Complementary, single NVs can serve to push the spatial resolution of the sensor down to the nanoscale. The integration of high-resolution scanning probe microscopy has enabled for example imaging of magnetic fields with sub-100 nm resolution [8].

For any physical platform, sensitivity is limited by the decoherence affecting the qubit sensor. The minimum measurable field scales indeed with the coherence time τ of the qubit as $\eta \sim 1/\sqrt{\tau}$. Decoherence implies loss of information and limits the available interrogation time. Note that also the bandwidth of the sensor depends on the interrogation time. This especially constitutes a severe constraint for solid-state based sensors, where decoherence stems from the coupling of the qubit sensor to crystal impurities and to the phonon bath. Compared to other solid-state platforms, the NV center has orders-of-magnitude better coherence time – microseconds at room temperature, and up to almost a second at cryogenic temperature. Crucial to further improve sensitivity is to devise appropriate control methods to prolong the sensor coherence time.

We develop fast and high-fidelity control techniques inspired by quantum information to improve the performances of sensing devices. The focus is to obtain strong coupling of the sensor with the field to be measured, while protecting the sensor from the deleterious effects of decoherence. To this purpose, we explore a broad range of strategies, in particular strong resonant driving to achieve time-optimal solutions. We use advanced schemes based on pulsed resonant control fields, which are used to manipulate the spin by implementing sets of quantum gates [9],

including the Hadamard gate and the Pauli X and Y gates. Recently, we have experimentally demonstrated the superior performance of a NV sensor based on optimal control, showing quantum-enhanced sensitivity to measure ultra-weak time-varying magnetic fields in noisy environments [2], [3]. The considered sensing task consists in measuring the amplitude of an ultra-weak spectrally characterized magnetic field with multiple frequency components. Usual pulsed dynamical decoupling composed by the application of equispaced Pauli gates sequences show high frequency selectivity that can be exploited to measure monochromatic ac magnetic fields [6], but this same feature leads to suboptimal performances when probing a multitone target field due to attenuation of some frequency components. We have thus designed a direct and fast search method that looks for the optimal pulse sequence minimizing the cost function η, that is, sensitivity. This approach can be extended also to gyroscopes. These optimized sensors are suitable for integration in small, portable, and low power consumption configurations, in view of the on-field applications in the defence domain.

Nonlinear interferometry at the Heisenberg limit

Optical interferometry lies at the heart of a myriad of sensing techniques. Quantum-enhanced interferometry provides a step ahead towards non-classical measurements with unprecedented capabilities and sensitivities. In the last decades, the quest for the fundamental limit of interferometric measurements has been mainly promoted by the international effort aimed at detecting gravitational waves by means of long-arm interferometers.

A paradigmatic model of interferometer is represented by the Mach-Zehnder interferometer (MZI). Here, a first beam splitter is employed to divide the input laser beam into two parts: these two beams travel along distinct paths, experiencing different phase shifts, and finally recombine by means of a second beam splitter (Fig 2a). The resulting light intensity pattern can be used to measure the accrued phase difference with great accuracy. While classical physics sets no limit to the smallest detectable phase shift, according to quantum mechanics a limit exists on the sensitivity of the phase measurement. For coherent states of light (laser) and linear optics, Heisenberg Uncertainty Principle leads to a phase

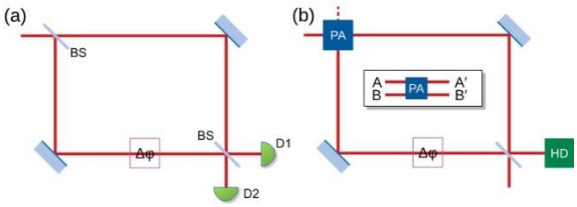

Fig. 2 a) Linear Mach-Zehnder interferometer with conventional beam splitters (BSs). b) Nonlinear interferometer, where a beam splitter is replaced with a parametric amplifier (PA). HD indicates homodyne detection of the interferometer output.

sensitivity limit $\Delta\varphi = 1/\sqrt{N}$, where N is the average photon number entering the interferometer. This Standard Quantum Limit (SQL) is a consequence of the Poissonian statistics of photons in a coherent beam. Actually, the sensitivity of interferometers can be improved beyond the SQL by using quantum states of light instead of, or in addition to, coherent states. Such improvements have been demonstrated by injecting squeezed light, Fock states, or other non-classical states of light, into an interferometer. A different approach would consist in working still with classical light but changing the structure of the interferometer itself, by replacing beam splitters with parametric amplifiers [10], four-port devices (inset of Fig. 2b) where two input states, signal A and idler B, transform in two output states, A' and B', according to

$$A' = GA + gB$$
$$B' = GB + gA\,,$$

where G and g are the amplitude parametric gains, with $|G|^2 - |g|^2 = 1$. A practical implementation of nonlinear interferometry has been realized, for instance, using parametric amplifiers based on four-wave mixing in Rubidium atom vapors [11].

We propose to achieve parametric amplification by using second-order nonlinearities in crystals, which have several advantages over four-wave mixing in atom vapour: a larger nonlinear efficiency; a higher flexibility in the choice of the operating wavelengths, not related to a particular set of atomic transitions; and the possibility to be engineered in small-footprint, integrated photonic devices. The particular configuration we are interested in is an MZI with a first nonlinear beam splitter and a second conventional one for recombination (Fig 2b). In this scheme, the correlation of the beams coming from the nonlinear beam splitter, after recombination on

the second beam splitter, leads to a reduction of the final noise below the quantum vacuum level, resulting in a net improvement of the signal-to-noise ratio. The optical parametric amplifier (OPA) is implemented in the form of an optical parametric oscillator operated below threshold. The OPA is based on a crystal with second-order nonlinearity, placed in an optical cavity and pumped by the second harmonic of a pump laser. The input signal beam is provided by the same laser used for second harmonic generation, while a vacuum state enters the second port (idler) of the OPA. Then, the output signal and idler follow two different paths, accumulating a relative phase difference which is the observable to be detected. The signal and idler are recombined by a conventional beam splitter. The output of the interferometer is monitored by balanced homodyne detection. Quantum noise performance of the interferometer and hence phase sensitivity can be monitored through homodyne detection, by placing another balanced (R/T=50/50) beam splitter on the path of one of the interferometer outputs, which is mixed with a "local oscillator" field, provided by the laser. The two output beams are finally detected by two identical photodetectors, and the signal obtained by subtracting the two photocurrents bears the information of the phase shift. By a proper choice of the local oscillator phase the SNR can be optimized. The interferometer will work on the dark fringes. This scheme is expected to provide an enhancement by a factor of about $2G$ in the phase sensitivity, compared to the SQL of a linear interferometer.

To further improve the phase sensitivity, a squeezed vacuum state can be injected into the second input port of the OPA. In this case, if r is the squeezing parameter ($r > 1$), it is possible to show that the minimum measurable phase shift becomes [12]

$$\Delta\varphi = \frac{1}{2G\, e^{r}\sqrt{N}},$$

which approaches the Heisenberg limit for large values of the squeezing parameters.

Quantum interaction-free sensing via evanescent-wave optics

One of the best-known contrasts between classical physics and quantum mechanics is that while in classical systems it is, in principle, possible to arbitrarily reduce any measurement perturbation, in quantum systems there is always a minimum, non-null disturbance introduced by the measurement itself. However, as proposed by Renninger [13] and Dicke [14], it is possible to design quantum systems where the *non-observance* of a result may give an *interaction-free* measurement (IFM). Successively, these concepts where extended by Elitzur and Vaidman to the case of single-photon optical interferometers [4].

Let us consider the Mach-Zehnder interferometer of Fig. 3a, illuminated with single photons one at a time. We can adjust the arm-length difference in order to have each photon (that has interfered with itself) in detector D1. If we introduce an obstacle in the upper

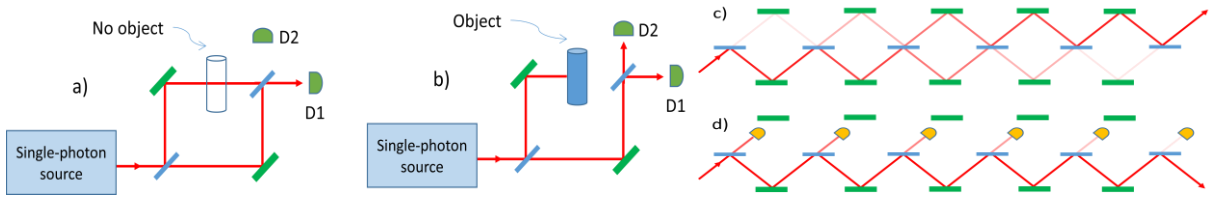

Fig. 3 a) No object in the upper arm, the photon interferes with itself and D2 does not count any photon. b) An object is inserted in the upper arm; the interference is destroyed and D2 counts photons with probability 1/4 (for 50-50 beam splitters) [4]. c) A single photon enters a sequence of interferometers, where the reflectivity of the beam splitters depends on N. If N is large enough, the photon will exit via the up-port of the last beam splitter. d) Introduction of detectors/absorbers prevents the interference. At each beam splitter there is a low probability that the photon takes the upper part and interact with the detector. After all the stages the photon will exit the down-port of the last beam splitter with large probability (2/3 in this case), thus indicating the presence of the detector/absorber. By increasing the number of stages N, the system can in principle reach efficiencies close to 100% with an arbitrarily small number of photons interacting with the object.

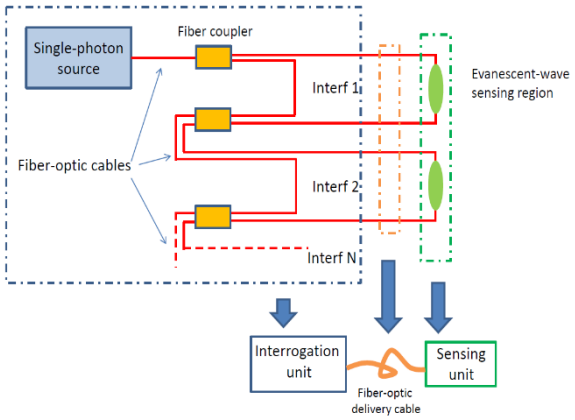

Fig. 4 OFSs lend themselves to the realization of sequential structures and interferometers via fiber-optic multi-interferometers. IFM may be of great advantage in sensing apparatuses where the measurement perturbation is one of the main limits, for example in chemical/biological sensing, microscopy or delicate quantum systems.

arm (Fig. 3b), the photon interference is destroyed and we can have the following possibilities: the photon takes the upper path and interact with the obstacle (50% probability); the photon takes the lower path and goes in D1 (25%), no information on the presence of the object can be extrapolated; the photon takes the lower path and goes in D2 (25%), we certainly know that there is an object in the upper path but the photon has not interacted with it. The efficiency of this setup is low (25%) and half of photons do interact with the object. More complex configurations have been designed and realized, mostly using arrays of coupled interferometers and optical cavities, or exploiting an optical version of the quantum Zeno effect [15] - [17]. These systems can in principle reach efficiencies close to 100% with an arbitrarily small number of photons interacting with the object (see Fig 3 c, d).

Although the optical scheme of a single stage is simple, an increase of *N* requires the use of a large number of optical mirrors and splitters, which present several drawbacks: large costs, complexity to align all optical components, difficulty to keep the whole system stable, large space and difficulty to interrogate small targets with all stages working together. Optical fiber sensors (OFSs) may be a possible alternative as they show a wealth of advantages: cheap, small, compact, high quality and lightweight, operation in delicate, harsh and hard-accessible environments, operation at high and low temperature and pressure, under stress and in presence of electromagnetic fields. OFSs may be equipped with evanescent-wave (EW) elements which show an intrinsically-weak light-matter interaction [5], [17]. Indeed, it is possible to realize cheap, compact and transportable systems which can also be efficiently integrated in more complex architectures (Fig. 4). In addition, very stable multi-interferometers for repeated measurements can be devised, as well as tailored EW interaction/sensing regions. IFM may be of great advantage in sensing apparatuses where the measurement perturbation is one of the main limits, for example in biological imaging and microscopy or delicate quantum systems such as Bose-Einstein condensates, trapped atoms etc. [15].

Conclusions

Quantum sensing devices, exploiting quantum resources to measure physical quantities, are able to surpass their classical counterparts in sensitivity and spatial resolution, and are very promising to realize integrated systems to be operated in relevant environment.

We develop optimized sensors of magnetic fields and rotation based on NV centers in diamond, a platform that offers an unprecedented combination of sensitivity and spatial resolution. The construction of integrated NV-based sensors of rotation and magnetic fields in small, portable, and low power-consumption configurations is particularly promising for applications in the defence domain, ranging from systems for stabilization and flight control feasible for aerospace and naval applications, to systems for remote detection and imaging of AC and DC fields useful for detection of hidden magnetic components on field.

Nonlinear interferometry is instead the most promising path towards practical implementation of a genuinely quantum sensing technique as far as distance measurement, angle measurement, velocimetry and vibrometry are concerned. Quantum interferometry offers significantly faster scaling of phase sensitivity with light intensity and can also impact on quantum imaging techniques that overcome the limit of classical imaging. On the other hand, IFM via single-photon interference represents a

powerful sensing technique which can be valuable in all cases where the measurement perturbation is a limiting factor, both for sensitivity/stability of the interrogation system and for the interaction with the object/sample observed. The combination with OFSs easily increases its performance via sequential interferometers and extends its capabilities to off-laboratory environments.

References

[1] C. L. Degen, F. Reinhard, and P. Cappellaro, "Quantum sensing" Rev. Mod. Phys. **89**, 3141 (2017).

[2] S. Hernández-Gómez, F. Poggiali, P. Cappellaro, N. Fabbri, "Noise spectroscopy of a quantum-classical environment with a diamond qubit" Phys. Rev. B **98**, 214307 (2018).

[3] F. Poggiali, P. Cappellaro, N. Fabbri, "Optimal control for one-qubit quantum sensing" Phys. Rev. X, **8** (3), 021059 (2018).

[4] A. Elitzur and L. Vaidman, Found. Phys. 23, 987 (1993).

[5] S. Avino, A. Giorgini, M. Salza, M. Fabian, G. Gagliardi, and P. De Natale, Appl. Phys. Lett. 102, 201116 (2013).

[6] J. M. Taylor et al., "High-sensitivity diamond magnetometer with nanoscale resolution", Nat. Phys. 4, 810 (2008).

[7] A. Ajoy and P. Cappellaro, "Stable three-axis nuclear-spin gyroscope in diamond", Phys. Rev. A 86, 062104 (2012).

[8] G. Balasubramanian et al., "Nanoscale imaging magnetometry with diamond spins under ambient conditions" Nature 455, 648 (2008).

[9] M. A. Nielsen and I. L. Chuang, Quantum Computation and Quantum Information. Cambridge University Press, Cambridge, 2000.

[10] B. Yurke, S. McCall, and J. Klauder, "SU(2) and SU(1,1) interferometers" Phys. Rev. A **33**, 4033 (1986).

[11] F. Hudelist, J. Kong, C. Liu, J. Jing, Z. Y. Ou, and W. Zhang, "Quantum metrology with parametric amplifier- based photon correlation interferometers" Nature Commun. **5**, 3049 (2014).

[12] J. Kong, Z. Y. Ou, and W. Zhang, "Phase-measurement sensitivity beyond the standard quantum limit in an interferometer consisting of a parametric amplifier and a beam splitter" Phys. Rev. A **87**, 023825 (2013).

[13] M. Renninger, Z. Phys. 158, 417 (1960).

[14] R. H. Dicke, Am. J. Phys. **49**, 925 (1981).

[15] A. G. White, J. R. Mitchell, O. Nairz, and P. G. Kwiat, Phys. Rev. A 58, 605 (1998).

[16] P. G. Kwiat, A. G. White, J. R. Mitchell, O. Nairz, G. Weihs, H.Weinfurter, and A. Zeilinger, Phys.Rev. Lett. 83, 4725 (1999).

[17] A. C. R. Pipino, Phys. Rev. Lett. **83**, 3093 (1999).

EUROPEAN DEFENCE AGENCY

INTEGRATED PHOTONIC PLATFORM FOR MULTIPHASE ESTIMATION

Emanuele Polino
Dipartimento di Fisica
Sapienza Università di Roma
Rome, Italy
emanuele.polino@uniroma1.it

Mauro Valeri
Dipartimento di Fisica
Sapienza Università di Roma
Rome, Italy
emanuele.polino@uniroma

Giacomo Corrielli
Istituto di Fotonica e Nanotecnologie
Consiglio Nazionale delle Ricerche
Milano, Italy
giacomo.corrielli@polimi.it

Andrea Crespi
Diparimento di Fisica
Politecnico di Milano
Milano, Italy
andrea.crespi@polimi.it 1.it

Nicolò Spagnolo
Dipartimento di Fisica
Sapienza Università di Roma
Rome, Italy
nicolo.spagnolo@uniroma1.it

Roberto Osellame
Istituto di Fotonica e Nanotecnologie
Consiglio Nazionale delle Ricerche
Milano, Italy
roberto.osellame@polimi.it

Fabio Sciarrino
Dipartimento di Fisica
Sapienza Università di Roma
Rome, Italy
fabio.sciarrino@uniroma1.it

***Abstract*—Integrated quantum photonics has recently enabled the implementation of several quantum information protocols, leading to experiments of progressively increasing size with respect to a bulk optics approach. Among these applications, quantum metrology aims at measuring unknown physical parameters reaching improved precision with respect to any classical approach. When moving to the multiparameter regime, several open problems on the definition of optimal probes and measurements still have to be addressed. Multiphase estimation, namely the simultaneous measurement of more than one optical phase, represents a benchmark problem to develop appropriate methodologies for multiparameter estimation, and at the same time a relevant scenario for quantum imaging applications. Here, we discuss an integrated photonic platform implemented via the femtosecond laser writing technology designed for multiphase estimation experiments. The obtained results show that such platform represents a viable approach towards development of quantum sensors capable of improving performances with respect to their classical counterpart.**

Keywords—integrated photonics, multiphase estimation, quantum metrology, single photons

This work is supported by the European Research Council (ERC) Advanced Grant CAPABLE (Composite integrated photonic platform by femtosecond laser micromachining, grant agreement no. 742745), by the QuantERA ERA-NET Cofund in Quantum Technologies 2017 project HiPhoP (High dimensional quantum Photonic Platform, project ID 731473), and by the Amaldi ResearchCenter funded by the MIUR program "Dipartimento diEccellenza" (CUP:B81I18001170001).

Introduction

Quantum sensors hold the promise to provide improved capabilities in the estimation of physical quantities with respect to what can be achieved with any classical approach. The framework behind this class of systems is provided by quantum metrology [1], namely the application of quantum theory to obtain improved performances in the measurement of unknown physical parameters. This field represents one of the most promising application of quantum theory towards a practical task. Indeed, it has been shown that the adoption of quantum probes in such a problem can lead to a sub-standard quantum limit precision in parameter estimation, the latter representing the classical lower bound of $N^{-1/2}$ in the measurement error, where N is the amount of resources employed in the process (i.e., the number of particles). Indeed, by using quantum states as probes, such as entangled or squeezed states, it is possible to achieve the fundamental Heisenberg limit [2], which states that the optimal precision scales as N^{-1}.

Given the general framework above, phase estimation represents a paradigmatic problem to study and develop appropriate methods to reach the Heisenberg limit, including the identification of useful quantum states and the definition of suitable measurement schemes to optimally extract the information encoded in the probe state. Several studies [1-6] have investigated the adoption of quantum states in this context, as well as different measurement schemes including adaptive protocols. However, up to now most of the analysis has been devoted to the single parameter scenario, namely when the unknown

quantity to be estimated is a single optical phase embedded in an interferometric setup.

Conversely, only few investigations have been reported in the multiparameter regime [7-14], where more than a single parameter have to be estimated simultaneously. This general scenario represents a relevant benchmark, since several tasks such as quantum imaging are inherently a multiparameter one. Furthermore, several open problems remain both from a theoretical and an experimental point view, mostly related to the identification of appropriate measurement schemes and protocols to efficiently extract the information on multiple parameters simultaneously. Hence, it is necessary to identify suitable experimental platforms which can provide a test bench for this task. A possible approach is provided by integrated quantum photonics, that has recently enabled the experimental demonstration of several quantum information protocols, including applications in quantum computing [15-17], and quantum simulation [18-25]. Different platforms have been employed, leading to the integration of several passive and active optical elements. Given the capability of implementing optical systems with a significant number of modes, and the intrinsic stability of integrated devices, such platform can be employed as a benchmark system for multiphase estimation.

In this paper we discuss an integrated platform realized with the femtosecond laser-writing technology [26] for multiphase estimation experiments. More specifically, we discuss an integrated source [27] of entangled photons at telecom wavelength, which is designed with a modular approach capable of generating different classes of quantum states. Then, we discuss an integrated reconfigurable multiarm interferometer [28] that can be employed as a platform to develop and test suitable protocols for the estimation of multiple phases. The implemented interferometer includes additional reconfigurable phase elements that can be employed as control parameters for adaptive protocols [29]. These two systems can be then combined to integrate photon sources and manipulation in the same device, leading to improved performances due to reduced injection losses.

Multiarm Interferometer for Multiphase Estimation

Multiphase estimation corresponds to measuring a set of d unknown optical phases $\boldsymbol{\phi}=(\Delta\phi_1,\ldots,\Delta\phi_d)$ embedded within an interferometric setup. The general scheme of such process is shown in Fig. 1 (a). An input probe state ⍰ is prepared, which can be either a classical laser field or a multiphoton quantum state, and injected into the interferometer. The state than evolves according to a unitary transformation $U_{\boldsymbol{\phi}}$ that depends on the unknown phases $\boldsymbol{\phi}$.. Finally, the state at the output of the interferometer is detected according to the set of operators that describe the measurement scheme, and the value of the unknown phases is retrieved by a suitable function called estimator.

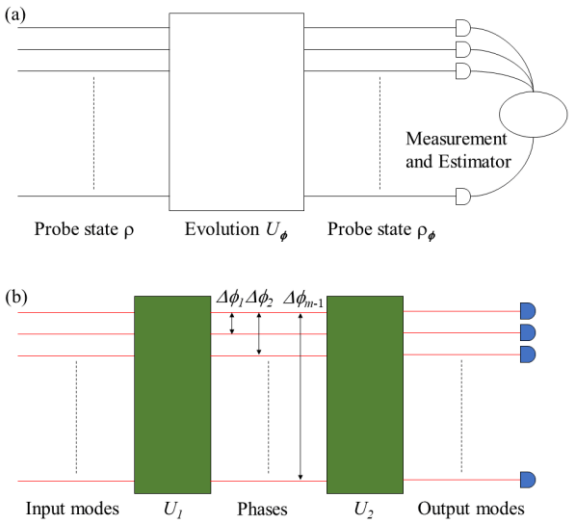

Fig.1
(a) General framework for multiparameter estimation. (b) Layout of linear interferometers for simultaneous estimation of multiple phases.

Multiarm interferometers [14] can be employed as a physical system [see Fig. 1 (b)] that allows to investigate multiphase estimation according to the framework described above. A m-mode multiarm interferometer acting on a n-photon input state can be built by inserting a first linear transformation U_1, that prepares the input n-photon state as the chosen probe to be employed for the estimation process. Then, the state acquires information on the d=m-1 relative phases between the interferometers arm and the first mode, which is chosen as a reference. Finally, the states undergoes a second linear evolution U_2 that, together with photo-detection state at the output of the system, acts as the measurement operators. The measured events are then processed through a suitable function, such as maximum likelihood or Bayesian ones, to provide an estimation of the unknown phases.

Recently, it has been suggested that quantum-enhanced performances can be reached in such a system [8,14], by injecting a single photon on each input port of the interferometer, and by appropriately choosing the input and output [14,30] transformations to be balanced multiport splitters. The latters represent the multimode counterpart of conventional two-mode beam-splitters, and have been recently demonstrated experimentally [31]. In general, the flexibility of this platform resides in the possibility of implementing arbitrary unitary transformation with an appropriate design [32,33], thus enabling the capability of generating a large variety of input states as well as tuning the measurement process.

Laser-written reconfigurable circuits for multiphase estimation

An integrated platform for multiphase estimation can be implemented with femtosecond laser micromachining [26]. This technique has been recently shown to be capable of implementing several optical elements, including directional couplers [34], waveplates for polarization manipulation [35,36], as well as the realization of complex interferometric structures able to support the polarization degree of freedom [18,24]. This has lead to the implementation of several demonstrations within the quantum simulation and quantum computation framework [16,18,24,31,34,35]. Recently [37], with this technique it has been also shown the possibility of integrating reconfigurable elements within the fabricated devices, that allowing to tune the system operation during the process.

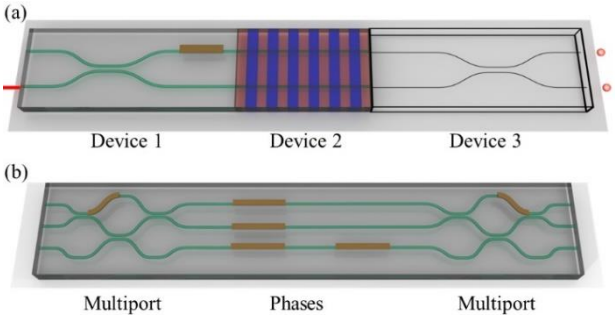

Fig.2
(a) Integrated source of entangled photons at telecom wavelength. The third device can be chosen to generate different classes of output state as described in the main text. (b) Multiarm interferometer for multiphase estimation, comprising two multiport splitters and six overall reconfigurable phase shifters.

The operating mechanism of femtosecond laser-writing is due to the permanent and localized index of refraction change that is induced in the focal region on a transparent material by focusing a femtosecond laser. Then, by translating the sample with respect the beam, optical waveguides can be written on the material. Complex structures can then be inscribed by writing several waveguides and directional couplers. A unique feature of this technique is the capability of designing optical circuits that exploit the possibility of moving the substrate in all three dimensions, thus enabling to obtain interferometers with properties and layouts otherwise not accessible with a technique capable of writing only on the plane [38].

a) Integrated tunable source of entangled states at telecom wavelength

A widely exploited class of materials to write integrated circuits with femtosecond laser micromaching is provided by glass substrates. Nevertheless, this technique can be employed to process other materials, including those presenting nonlinear properties. This feature has been exploited to implement an integrated source of entangled photons [27] at telecom wavelength, which has been completely fabricated with this techniques and that exploits a modular design to generate different classes of output states. The layout of the source is shown in Fig. 2 (a). A first device, comprising a balanced directional coupler and a reconfigurable phase shifter, is employed to inject the pump laser beam into the system, which is divided in two equal parts propagating through parallel waveguides. The pump beam at 780 nm is then injected in a second device, that is fabricated by writing two identical parallel waveguides on a periodically poled lithium niobate (PPLN) chip. In this second device, type-0 parametric down-conversion (PDC) process occurs to generate a pair of photons at 1550 nm. In the low pump power regime, the photon pair can be emitted coherently in one of the two parallel waveguides.

Finally, a third device is employed to generate different classes of output entangled states. For instance, a third device comprising a balanced directional coupler has been employed to generate path-entangled two photon states. More specifically, the output can be coherently tuned between states of the form $|1,1\rangle$ and $|2,0\rangle+|0,2\rangle$ by changing the phase ϕ inserted by the reconfigurable phase shifter in the first device. The measured interference pattern as a function of ϕ reached an average visibility of

V=0.975±0.004, by subtracting for accidental coincidences, thus showing the high quality of the generated state. A different choice for the third device corresponds to a layout comprising two integrated optical waveplates with optical axis at +22.5° and -22.5° respectively and a balanced polarization independent directional coupler. With this choice, polarization entangled two-photon states of the form $|+,+\rangle+e^{i\phi}|$can be generated, where |+> and |-> are linear polarization states at +45° and -45° respectively. The high quality of the generated state is quantified by the average visibility of polarization correlations on the output states, reaching values *V*=0.957±0.015 and *V*=0.929±0.017 for measurements in the |+,+> and |+,-> polarization bases. Finally, tomography of the output state lead to a high value of the concurrence in the measured state *C*=0.905±0.022.

b) Integrated reconfigurable multiarm interferometer

A reconfigurable three-mode multiarm interferometer working at 785 nm has been implemented [28] as a benchmark platform for multiparameter phase estimation, according to the design [14] discussed in Sec. II. The layout of the device is shown in Fig. 2 (b). A first three-mode interferometer realizes the tritter transformation by using the layout of [32] with suitable values of the directional couplers transmittivities. Furthermore, a reconfigurable phase has been inserted to improve control in the implemented transformation, as well as to tune its operation to generate different classes of input states. Then, 4 phase shifters are inserted in the three internal optical modes. Two of them are employed to tune the value of the two relative phases $\Delta\phi_1$ and $\Delta\phi_2$ with respect to the first arm, acting as a reference, and represent the two unknown parameters to be estimated. The other two phase shifters can be conversely employed as control parameters for adaptive protocols [29]. Finally, a second tritter transformation having the same layout of the first one acts as measurement operator, followed by photodetection on the output modes. A reconfigurable phase shifter is inserted in the output trasformation to change the measurement process, thus permitting to study the role of this stage to obtain an optimal estimation process [30].

The action of the implemented device has been experimentally characterized by injecting single photon states with an off-chip PDC source in the different input modes, and by measuring the outputs with single photon detectors. Single photons are coupled into the device by means of single-mode fiber arrays placed on a roto-translational mechanical positioner. More specifically, the reconstruction procedure is performed to completely characterize the action of the reconfigurable phase shifter, thus allowing to retrieve the coefficients of the functional relation between the applied voltage and the actual value of the phases inserted in the interferometer. The reconstruction process shows that a high value of the fidelity is achieved by the device with respect to the desired transformation, reaching a value of *F*=0.963±0.015, averaged over the full set of phase values.

Then, a multiphase estimation experiment on a chip has been performed by injecting a two-photon input state, showing that enhanced performances with respect to classical inputs (corresponding here to distinguishable single-photon states) can be achieved by using the same amount of resources, post-selected to the number of detected coincidences.

Conclusions

Quantum metrology promises to enable improved precision in the measurement of physical quantities, leading to the development of novel quantum sensors. Phase estimation represents one of the most representative example, with applications ranging from quantum imaging to fundamental measurements such as gravitational wave dection [6].

Here, we have discussed a laser-wrriten integrated photonic platform [27,28] that can be employed for multiphase estimation experiments. More specifically, we have presented an integrated source of entangled photons at telecom wavelength [27], generating quantum states that can be used as a probe for phase estimation tasks. Then, we have discussed a three-mode reconfigurable interferometer [28], whose design can be scaled up to larger number of modes, that can act as a benchmark platform to test and develop suitable methods for multiparameter estimation. Interfacing these two classes of devices (source and evolution) implemented with the same technology can lead to improved performances in this task.

References

[1] V. Giovannetti, S. Lloyd, and L. Maccone, “Quantum metrology,” Phys. Rev. Lett. vol. 96, pp. 010401, 2006.

[2] V. Giovannetti, S. Lloyd, and L. Maccone, “Advances in quantum met-rology,” Nat. Photonics vol. 5, pp. 222–229, 2011.

[3] S. L. Braunstein and C. M. Caves, “Statistical distance and the geometryof quantum states,” Phys. Rev. Lett. vol. 72, pp. 3439–3443, 1994.

[4] M. W. Mitchell, J. S. Lundeen, and A. M. Steinberg, “Super-resolving phase measurements with a multiphoton entangled state”, Nature vol. 429, pp. 161-164, 2004.

[5] S. Slussarenko, et al., “Unconditional violation of the shot-noise limit in photonic quantum metrology,” Nat. Photonics vol. 11, pp. 700–703, 2017.

[6] R. Schnabel, N. Mavalvala, D. E. McClelland, and P. K. Lam, “Quantum metrology for gravitational wave astronomy,” Nat. Commun. vol. 1, pp. 121, 2010.

[7] M. Szczykulska, T. Baumgratz, and A. Datta,“Multi-parameter quantummetrology,” Adv. Phys.:X vol. 1, pp. 621–639, 2016.

[8] P. C. Humphreys, M. Barbieri, A. Datta, and I. A. Walmsley, “Quantum enhanced multiple phase estimation,” Phys. Rev. Lett. vol. 111, pp. 070403, 2013.

[9] M. D. Vidrighin, et al., “Joint estimation of phase and phase diffusion for quantum metrology,” Nat. Commun. vol. 5, pp. 3532, 2014.

[10] E. Roccia, et al., “Entangling measurements for multiparameter estima-tion with two qubits,” Quantum Sci. Technol. vol. 3, pp. 01LT01, 2018.

[11] M. Altorio, M. G. Genoni, M. D. Vidrighin, F. Somma, and M. Barbieri, “Weak measurements and the joint estimation of phase and phase diffusion,” Phys. Rev. A vol. 92, pp. 032114, 2015.

[12] E. Roccia, et al., “Multiparameter approach toquantum phase estimation with limited visibility,” Optica vol. 5, pp. 001171, 2018.

[13] C. N. Gagatsos, D. Branford, and A. Datta, “Gaussian systems for quan-tum-enhanced multiple phase estimation,” Phys. Rev. A vol. 94, pp. 042342, 2016.

[14] M. A. Ciampini, et al., “Quantum-enhanced multiparameter estimation in multiarminterferometers,” Sci. Rep. vol. 6, pp. 28881, 2016.

[15] A. Politi, M. J. Cyan, J. G. Rarity, S. Yu, J. L. O’Brien, “Silica-on-Silicon Waveguide Quantum Circuits”, Science vol. 32, pp. 646-649, 2008.

[16] A. Crespi, et al., “Integrated photonic quantum gates for polarization qubits”, Nat. Commun. vol. 2, pp. 566, 2011.

[17] J. Wang, et al., “Multidimensional quantum entanglement with large-scale integrated optics”, Science vol. 360, pp. 285-291, 2018.

[18] A. Crespi, et al., “Anderson localization of entangled photons in an integrated quantum walk”, Nat. Photonics, vol. 7, pp. 322-328, 2013.

[19] N. Spagnolo, et al., “Experimental validation of photonic boson sampling”, Nat. Photonics vol. 8, pp. 615-620, 2014.

[20] J. Carolan, et al., “On the experimental verification of quantum complexity in linear optics”, Nat. Photonics vol. 8, pp. 621-626, 2014.

[21] J. Carolan, et al., “Universal linear optics”. Science vol. 349, pp. 711-716, 2015.

[22] F. Caruso, A. Crespi, A. G. Ciriolo, F. Sciarrino, and R. Osellame, “Fast escape of a quantum walker from an integrated photonic maze”, Nat. Commun. vol. 7, pp. 11682, 2016.

[23] L. J. Maczewsky, J. M. Zeuner, S. Nolte, and A. Szameit, “Observation of photonic anomalous Floquet topological insulators”, Nat. Commun. vol. 8, pp. 13756, 2017.

[24] I. Pitsios, et al., “Photonic simulation of entanglement growth and engineering after a spin chain quench”, Nat. Commun. vol. 8, pp. 1569, 2017.

[25] J. Carolan, et al., “Quantum transport simulations in a programmable nanophotonic process”, Nat. Photonics vol 11, pp. 447-452. 2017.

[26] R. Osellame, G. Cerullo, and R. Ramponi, “Femtosecond Laser Micromachining: Photonic and Microfluidic Devices in Transparent Materials”, Springer, 2012.

[27] S. Atzeni, et al., “Integrated sources of entangled photons at the telecom wavelength in femtosecond-laser-written circuits”, Optica vol. 5, pp. 311-314, 2018.

[28] E. Polino, et al., “Experimental multiphase estimation on a chip”, Optica vol. 6, pp. 288-295, 2019.

[29] A. Lumino, et al., “Experimental phase estimation enhanced by machine learning”, Phys. Rev. Appl. vol. 10, pp. 044033, 2018.

[30] L. Pezzè, et al., “Optimal measurements for simultaneous quantum estimation of multiple phases,” Phys.Rev. Lett. vol. 119, pp. 130504, 2017.

[31] N. Spagnolo, et al.,“Three-photon bosonic coalescence in anintegrated tritter,” Nat. Commun. vol. 4, pp. 1606, 2013.

[32] M. Reck, A. Zeilinger, H. J. Bernstein, and P. Bertani, “Experimental realization of any discrete unitary operation”, Phys. Rev. Lett. vol. 73, pp. 58-62, 1994.

[33] W. R. Clements, P. C. Humphreys, B. J. Metcalf, W. S. Kolthammer, and I. A. Walmsley, “Optimal design for universal multiport interferometers”, Optica vol. 3, pp. 1460-1465, 2016.

[34] L. Sansoni, et al. “Polarization entangled state measurement on a chip”, Phys. Rev. Lett. vol. 105, 200503, 2010.

[35] G. Corrielli, et al., “Rotated waveplates in integrated waveguide optics”, Nat. Commun. vol. 5, pp. 4249, 2014.

[36] R. Heilmann, M. Grafe, S. Nolte, and A. Szameit, “Arbitrary photonic waveplate operations on chip: Realizing Hadamard, Pauli-X, and rotation gates for polarisation qubits”, Sci. Rep. vol. 4, pp. 4118, 2014.

[37] F. Flamini, et al., “Thermally reconfigurable quantum photonic circuits at tele-com wavelength by femtosecond laser micromachining,” Light Sci. Appl. vol. 4, pp. e355, 2015.

[38] A. Crespi, et al., “Suppression law of quantum states in a 3D photonic fast Fourier transform chip”, Nat. Commun. vol 7, pp. 10469, 2016.

SUPERCONDUCTING DEVICES FOR QUANTUM PLATFORMS

Giovanni Piero Pepe
Università di Napoli Federico II
Department of Physics "E. Pancini"
Naples, Italy
gpepe@na.infn.it

Loredana Parlato
Università di Napoli Federico II
Department of Physics "E. Pancini"
Naples, Italy
lparlato@unina.it

Francesco Tafuri
Università di Napoli Federico II
Department of Physics "E. Pancini"
Naples, Italy
tafuri@na.infn.it

Davide Massarotti
Università di Napoli Federico II
Department of Electrical Engineering and Information Technologies
Naples, Italy
davide.massarotti@unina.it

Roberto Cristiano
Consiglio Nazionale delle Ricerche
CNR SPIN
Pozzuoli, Italy
roberto.cristiano@cnr.it

Mikkel Ejrnaes
Consiglio Nazionale delle Ricerche
CNR SPIN
Pozzuoli, Italy
mikkel.ejrnaes@cnr.it

Roberta Caruso
Università di Napoli Federico II
Department of Physics "E. Pancini"
Naples, Italy
caruso@fisica.unina.it

Daniela Salvoni
Università di Napoli Federico II
Department of Physics "E. Pancini"
Naples, Italy
salvoni@unina.it

Roberta Satariano
Università di Napoli Federico II
Department of Physics "E. Pancini"
Naples, Italy
rosata@

Oleg Mukhanov
SeeQC-eu
via dei Due Macelli 66, I-00187
Rome, Italy
olegm@seeqc.eu

I. Vernik
SeeQC-eu
via dei Due Macelli 66, I-00187
Rome, Italy
ivernik@seeqc.com

D. Stornaiuolo
Università di Napoli Federico II
Department of Physics "E. Pancini"
Naples, Italy
stornaiuolo@fisica.unina.it

Giovanni Ausanio
Università di Napoli Federico II
Department of Physics "E. Pancini"
Naples, Italy
ausaanio@fisica.unina.it

Halima Ahmad
Università di Napoli Federico II
Department of Physics "E. Pancini"
Naples, Italy
halimaahmad76@gmail.com

Alessandro Miano
Università di Napoli Federico II
Department of Physics "E. Pancini"
Naples, Italy
amiano@fisica.unina.it

Abstract— **New quantum sensing technologies can open intriguing possibilities for higher sensitivity or resolution of Electro-Optical (EO) devices. The superconducting technologies can contribute in a significant way in several fields of quantum technologies ranging from *transmon devices* employing different types of superconducting junctions and layouts, which are completely controlled through RF pulses thus reducing flux noise, to *single photon counting cameras*, which open new detection possibilities in the infrared wavelength range for their high photon counting rates, superior time resolution and low jitter. In this paper we present our experimental activities in these two different topics which represent two fields of great interest within quantum technologies.**

Keywords—Ferromagnetic Josephson junctions, superconducting qubits, Superconducting Single Photon Detectors

Introduction

Superconducting technologies represent an important basis for the development of many platforms within the Quantum Technologies Roadmap, in particular for quantum computation and communication. A first example is represented by the Josephson Junction (JJ)

which is the building block of the superconducting qubits, where coherent control has been demonstrated for more than 50 qubits. Superconducting Nanowire Single Photon Detector (SNSPD) is a second example. This single photon detector demonstrated a high level of performance in terms of quantum efficiency, very low dark counts rate, <10ps jitter and high time resolution, with a photon number resolution potential, which is useful in quantum communication and for many entanglement-based protocols.

The aim of this work is to discuss some aspects of superconducting technologies in the quantum context starting from some experiments on both devices under development, thus introducing novel materials and configurations, and possible new operating regime in the single photon measurement configuration.

a) Superconducting ferromagnetic-based Josepshon Junctions for novel qubit approaches

The control of a JJ is quite important for the development of novel concepts and layouts of superconducting elements for a wide range of applications, ranging from digital circuits to different types of superconducting qubits. Beside well established Al-based JJ technology and its problem in ensuring a huge number of working junctions for the quantum computer, it is reasonable to expect that hybrid solutions may offer some alternatives in the realization of complex quantum systems. Hybrid means junctions employing different tunnel barriers from oxides such as AlOx or physical systems able to integrate various quantum systems in the same architecture (e.g. integration of a transmon in a cavity and a spin ensemble [1], or the realization of a gatemon [2]).

A possible approach along this *hybrid view* can be represented by tunnel Superconductor Ferromagnet/Superconductor (SFS) based junctions, and their possible use in quantum circuits, more easily connected to a qubit control driven by Single Flux Quantum (SFQ) logic [3]. Recently, SFS-based JJs have been proposed as spin valves [4] or pseudo-spin valves [5] to control the phase or the critical current magnitude switch between two well-defined states, and memory elements [6].

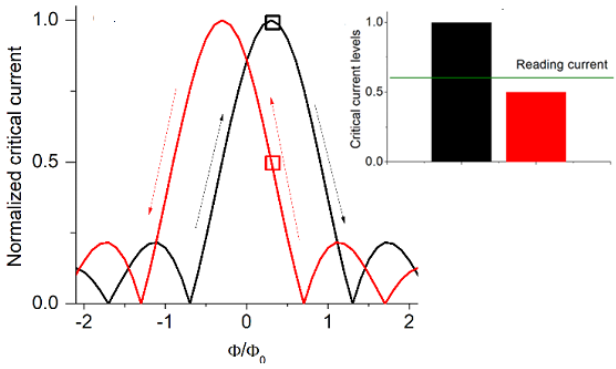

Figure 1. $I_C(H)$ measured on a SIsFS JJ at 3.5 K. Black curve: the external magnetic field is ramped from negative to positive values; red curve from positive to negative values.Inset: Normalized critical current levels corresponding to black and red squares in panel a, respectively. An intermediate reading current is used to read the state of the memory. Figure adapted form Ref. [8]

In these latter Nb-PdFe-Nb trilayers, the two classical logic states correspond to two different critical current levels arising from the behavior of ferromagnetic materials: the multivalued dependence of the magnetization **M** vs the externally applied magnetic field **H** reflects on the Josephson critical current dependence Ic(H) as shown in Figure 1 (a).

By using proper (positive and negative) external magnetic field pulses, the critical current is driven into the two critical states, the lower Ic=I1 [red square in Figure 1] and the higher Ic=Ic2 [black square in Figure 1]. Actually, the readout is performed by applying a reading current Iread between the two levels, and by measuring the voltage across the junction. If the device is in the state with Ic = I1, then the output is a finite voltage, while if it is in the state with Ic = I2 no voltage is detected across the junction. In terms of compatibility with existing superconducting electronics, especially with SFQ circuits, the voltage levels for switching are typically of the order of millivolts, and this suggests the tunnel barrier approach. Recently, dissipation in spin valve JJs with Ho/Co barriers has been fully classified within the existing models to describe a JJ [7].

Recent experiments on tunnel SIsFS JJs, where the barrier is composed by an insulating AlOx, a thin Nb and a ferromagnetic PdFe layer, have demonstrated that

the switching mechanism can be enhanced by using external RF fields [8]. The current level separation enhancement depends on the magnetic field pulse amplitude, on the total energy of the RF train and on the working temperature. The largest effect is observed for intermediate pulse amplitudes where the slope of the M(H) curve allows to appreciate the change in the magnetization induced by the microwave. In particular, the relevant parameter is the total energy associated with the microwaves, rather than the power level or the duration alone: this indicates that the external RF field induces fluctuations in the F layer that are analogous to thermal fluctuations. The effect is larger at temperatures where one of the two mechanisms that cause ferromagnetism in PdFe can be switched off by the fluctuations induced by the microwaves, thus confirming an analogous role played as thermal fluctuations.

The use of RF fields to control the critical current of magnetic Josephson junctions opens the way for the possible use ferromagnetic junctions as active quantum devices [9]. In fact, the tunability of the critical current in different types of tunnel-ferromagnetic junctions leading to their memory capabilities make them possibly useful in the long range not only for the integration in SFQ circuits, but also for the development of specific types of qubits. A transmon could benefit of this degree of freedom since the ratio E_J/E_C between the Josephson energy E_J and the charge energy E_C can be tuned via magnetic pulses or RF trains. In fact, the control input makes possible to obtain different critical current levels and thus different E_J/E_C ratios, which define the transmon energy levels separation.

b) Superconducting Single Photon Nanowire Detectors

A SNSPD consists of a very thin and narrow superconducting wire (typically thickness 4nm, width 100nm and length of tens of micrometers) in which the absorption of a single photon can generate a measurable voltage pulse. Briefly, the superconducting nanowire is biased just below its critical current Icr. When a photon is absorbed, it breaks Cooper pairs and creates a normal region (hotspot) which deviates the supercurrent, producing its spread over the edges of the wire until the critical current density is exceeded. The nanowire locally transits to its resistive state thus generating a voltage pulse. The small thickness and width of the film guarantees a high efficiency in the detection mechanism, while the long shaped meander geometry ensures a high geometrical efficiency.

SNSPDs are wide band detectors since the mechanism of detection is not based on a specific energy. Moreover, they are characterized by low dark count rates. Conventional low-Tc materials such as NbN, NbNTi or WSi[10-13] are employed in the fabrication, and they are commercially available all around the world. Some performances of SNSPDs can be summarized [14] as high quantum efficiency (~94% at λ ~1.31μm, 93% at λ~1.55μm), high operating frequency (~1.2 GHz), low intrinsic dark count rate (~0.1Hz), low jitter (~4.6 ps full-width at half-maximum at λ~1.55μm) and broad spectral range (from visible to mid-infrared).

One of the fundamental questions of SNSPDs is the nature of the intrinsic mechanism responsible for the passage from the superconducting to the resistive state, i.e. hotspot formation. The voltage switching occurs when the current in the strip reaches the maximum critical value Ic related to the maximum velocity of the Cooper pairs. At larger velocities superconductive pairing is no longer possible, and the strip undergoes to a resistive switching. Fluctuation effects of the superconducting order parameter (e.g. phase slips) can influence stochastically the switching. The regime when fluctuations induced switching processes are due to multiple phase slip (MPS) events are observed in 1D wires.

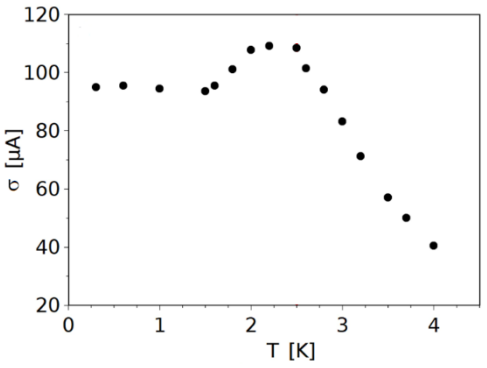

Figure 2. Analysis of the standard deviations of the switching distributions as a function of temperature (from Ref. [14]).

In 2D superconducting strips as the ones used in SNSPDs switching events can be analyzed into the physics of phase slip phenomena. Dark counts, i.e. the false events in a detector, are very low in SNSPDs and constitute one of the most attractive figures-of-merit. We investigate phase slip events in 2D NbTiN strips by measuring the switching current distributions in a wide interval of temperatures from 4.2 K down to 0.3 K. Measurements were performed down to 0.3K: details of both cryogenic and low noise readout electronics are reported elsewhere [15]. The critical temperature Tc of the nanostripe is 6.6 K. The bias current is swept from zero to higher values, and the switching current, I_{SW}, is recorded when the strip exhibits an abrupt transition from the superconducting state (V=0) to a finite voltage state, where it will remain until the current is reduced below the re-trapping value where the superconducting state is achieved again. By repeating the current bias sweeps, we measured the statistical distribution of the switching currents, i.e. $P(I_{SW})$, at different temperatures. Each $P(I_{SW})$ was obtained using a current sweep rate of 845 μA/s and included 10000 switching events [16].

The resistive switching distributions of NbTiN strips have a pronounced region at high temperatures where the switching is caused by MPS events. In this temperature region the width of the switching distribution is reduced down to values below the ones observed at the lowest temperature.

The standard deviations of the switching distributions show an extended region at the higher temperatures where MPS event switching occurs (see Figure 2).

Experiments were performed on NbTiN meandered nanostrips (5 nm thick and 80 nm wide). The superconducting order parameter in our strip is in the 2-dimensional regime, because the coherence length is much lower than the strip width whereas it is similar to the thickness.

The third and fourth moments of the switching distribution confirmed the switching origin to be of multiple phase-slip event type at high temperatures. Beyond the fundamental physics aspects involved in this analysis, it's important to note that a reduction of the switching distribution width as observed at high temperatures reflects that spontaneous switching is consequently small. Accordingly, dark counts are furtherly reduced, and the performances of SNSPDs are enhanced. This is an important aspect within the operation mode of a SNSPD detector.

Conclusions

Superconducting technologies are important in many platforms within the Quantum Technologies Roadmap from computation to communication, and metrology. The search of new JJs configurations with a high degree of tunability of the critical current can be achieved in different types of ferromagnetic junctions, which are interesting both for their memory capabilities in SFQ circuits and developments toward specific types of qubits. We present preliminary data concerning the control of F-based JJs by both external magnetic and RF pulses. Moreover, the fundamental role played by superconducting technologies within quantum platforms is also demonstrated by high performances of SNSPDs. In particular, we discussed dark counts measurements on NbTiN nanowires showing the possibility of a higher temperature operation mode where the role of fluctuations is reduced, and dark counts too.

References

[1] Xiang, Z.L. et al., Rev. Mod. Phys 2013, 85, 623. doi:10.1103/RevModPhys.85.623.

[2] Larsen, T.W. *et al.,* Phys. Rev. Lett. **2015**, p. 127001. doi:10.1103/PhysRevLett.115.127001.

[3] Leonard, E.J.; et al.. arXiv:1806.07930.

[4] Gingrich, E.C. *et al.,* Nat. Phys. **2016**, 12, 564. doi:10.1038/nphys3681.

[5] Baek, B. *et al.,* Nat. Commun. **2014**, 5, 4888. doi:10.1038/ncomms4888.

[6] Bol'ginov, V.V. *et al.*, JETP Lett. **2012**, 95, 366. doi:10.1134/S0021364012070028.

[7] Massarotti, D. *et al.*, Phys. Rev. B **2018**, 98, 144516. doi:10.1103/PhysRevB.98.144516

[8] Caruso, R. *et al.,* Journal of Applied Physics **2018**, 123, 133901. doi:10.1063/1.5018854; Caruso, R. et al., Proceedings MDPI, in press.

[9] Feofanov, A.K. *et al.*. Nature Physics **2010**, 6, 593. doi:10.1038/nphys1700

[10] Murphy, A. *et al*. Sci. Rep. **5**, 10174 (2015).

[11] Dorenbos, S. N. *et al*. Appl. Phys. Lett. **93**, 131101 (2008).

[12] Schuck, C. *et al.,* Sci. Rep. **3**, 1893 (2013).

[13] Bell, M. *et al.*, Phys. Rev. B **76**, 094521 (2007)

[14] Ejrnaes *et al.*, Sci. Rep. in press (2019)

[15] Longobardi, L. *et al*. Appl. Phys. Lett. **99**, 062510 (2011)

[16] Massarotti, D. *et al.*, *Phys. Rev. B* **92**, 054501 (2015).

QUANTUM LIGHT SOURCES FOR ADVANCED SENSORS AND COMMUNICATIONS

Simona Mosca
Consiglio Nazionale delle Ricerche
Istituto Nazionale di Ottica (CNR–INO)
Pozzuoli (Napoli), Italy

Saverio Bartalini
Consiglio Nazionale delle Ricerche
Istituto Nazionale di Ottica (CNR–INO)
Sesto Fiorentino (Firenze), Italy
saverio.bartalini@ino.it

Alessio Montori
ppqSense S.r.l.
Campi Bisenzio (Firenze), Italy
alessio.montori@ino.it

Miriam Serena Vitiello
NEST, CNR – Istituto Nanoscienze and Scuola Normale Superiore
Pisa, Italy
miriam.vitiello@sns.it

Costanza Toninelli
Consiglio Nazionale delle Ricerche
Istituto Nazionale di Ottica (CNR–INO)
Sesto Fiorentino (Firenze), Italy
costanza.toninelli@ino.it

Alessandro Zavatta
Consiglio Nazionale delle Ricerche
Istituto Nazionale di Ottica (CNR–INO)
Sesto Fiorentino (Firenze), Italy
alessandro.zavatta@ino.it

Francesco S. Cataliotti
Dipartimento di Fisica ed Astronomia,
Università degli Studi di Firenze
Sesto Fiorentino (Firenze), Italy
fsc@lens.unifi.it

Marco Bellini
Consiglio Nazionale delle Ricerche
Istituto Nazionale di Ottica (CNR–INO)
Sesto Fiorentino (Firenze), Italy
marco.bellini@ino.it

Paolo De Natale
Consiglio Nazionale delle Ricerche
Istituto Nazionale di Ottica (CNR–INO)
Sesto Fiorentino (Firenze), Italy
paolo.denatale@ino.it

***Abstract* — The advance of quantum communications systems and quantum sensing schemes toward realistic applications relies on efficient sources of quantum light. We are currently studying and developing new sources of quantum light spacing from single-photon to entanglement sources together with the investigation of novel systems able to emit quantum frequency combs. These new systems will enable more efficient free-space communications and quantum state transfer. Finally, we exploited our expertise in quantum technologies to realize a novel quantum key distribution (QKD) system tested in the Florence metropolitan area.**

Keywords—Quantum light state engineering, single-photon sources, quantum frequency combs, quantum cascade lasers, quantum state transfer, quantum key distribution.

Introduction

The National Institute of Optics (Istituto Nazionale di Ottica) of the CNR hosts several activities aiming at the development of new technologies based on the quantum properties of light in collaboration with ppqSense, a CNR's spin-off, focused on development of ultra-sensitive laser systems and ultralow noise electronics.

In particular, our ability to implement single-photon addition and subtraction operations can be used to engineer quantum light states and entanglement in order to design high sensitivity measurements and noiseless light amplification. In this context, we generate single and multiphoton entangled light states that are surprisingly robust against losses and thus well suited to travel over long distances and to be stored in atomic ensembles.

We also develop deterministic sources of single photons, based on single molecules suitable for integration into photonic chips. Particularly, direct coupling of single emitters to optical antennas, waveguides and microcavities has been recently demonstrated. The possibility of coupling quantum emitters to an integrated photonic platform is of primary importance, allowing enhancement and control of the atom-photon interface, hence making realistic the complex manipulation of quantum states of light.

Even though these sources are very promising, they are limited to some specific spectral regions that might be hindered by fog, dust, smoke or turbulent motion. To solve this problem we are also investigating new sources of nonclassical light based on quantum cascade laser frequency combs. These sources are able to emit infrared and THz radiation, which is

optimal to realize free-space communications and air-to-ground links with satellites.

Furthermore, in order to transfer quantum states among different spectral regions, we investigate multipartite entanglement distribution from the optical to the microwave domain. Cascaded second order processes can generate quantum correlation between combs at different spectral regions. Exploiting the unique features of optomechanical systems, which work for any frequency of the electromagnetic spectrum, we combine quantum optical frequency combs with optomechanical transducers in order to integrate distinct quantum technologies.

Finally, Quantum Key Distribution (QKD), the most advanced among all quantum technologies, is almost ready for a large-scale deployment. However, important steps forward are necessary to push this technology toward real-world applications. We are currently working on the development of advanced QKD systems able to work in existing telecom fiber networks.

Entanglement Generation by Light State Engineering

Entanglement is one of the most striking features of quantum mechanics, which allows stronger-than-classical correlations between two parties of the same quantum system. Entanglement is the core of the forthcoming quantum technologies, in particular is crucial for the advance of quantum communications and quantum sensing. However, the development toward real-world applications is strongly connected to the ability of realizing efficient and bright nonclassical light sources. On the other hand, entanglement established between photons remains very fragile and it can be easily lost during propagation. In order to overcome this limitation, it is important to study techniques to generate novel kinds of entangled light states more and more resilient to noise and losses.

It has been widely demonstrated that using single-photon addition and subtraction operations it is possible to engineer the quantum properties of light, generating nonclassicality and entanglement [1]. Moreover, the ability to implement single-photon addition and subtraction operations can be used to obtain quantum devices able to realize several operations such as noiseless light amplification [2] and strong Kerr effect emulation [3].

Using delocalized single-photon addition, we are able to generate multiphoton entangled light states that are surprisingly robust against losses and thus well suited to travel over long distances and to be stored in atomic ensembles [4]. Two distinct field modes, 1 and 2, can be entangled by delocalized addition of a single photon $\hat{a}_1^\dagger \pm \hat{a}_2^\dagger$. In general, the amount of entanglement produced by the balanced superposition of photon creation operations depends on the states of light already present in the modes. If both are originally in a vacuum state, one simply obtains a single-photon mode-entangled state [5]. While if only one mode is populated by a coherent state the scheme generates hybrid entangled states where a discrete-variable qubit is entangled to a continuous-variable one [6]. Instead, here we study the effect of delocalized single-photon addition on two input modes containing identical coherent states (weak laser pulses), as schematically illustrated in Fig.1. Here, a click in the single-photon detector D1, placed after a balanced beam-splitter BS mixing the herald modes of two photon-addition modules, generates entanglement between the two output modes.

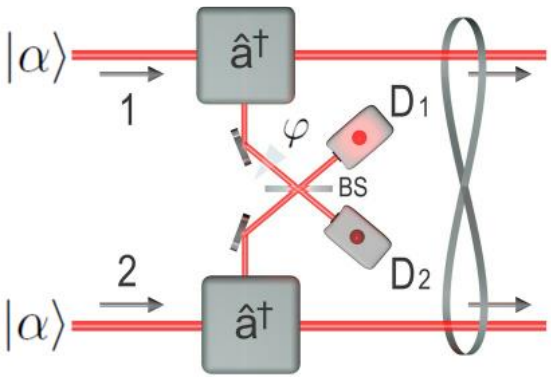

Fig. 1. Delocalized single-photon addition of a single photon between two different spatial modes.

We have observed that entangled states generated with this scheme can contain an arbitrary large number of photons while preserving their non-classical correlations [7]. This kind of entanglement source will be utilized to investigate the possibility to realize new quantum communication protocols and quantum sensing devices.

Single-photon sources

Reliable and bright non-classical light sources are a fundamental ingredient for many quantum technologies, targeting enhanced performance in sensing, imaging and metrology applications [8]. In the last years single quantum emitters under pulsed excitation have been presented as deterministic sources of indistinguishable single photons [9], as opposed to the probabilistic generation of pairs by parametric downconversion. Among them, solid-state emitters such as quantum dots [10], color centres in diamond [11] and single molecules [12, 13] are particularly suitable for integration into photonic chips [14]. In particular, direct coupling of single emitters to optical antennas, waveguides (WGs) and microcavities has been recently demonstrated [15-18] with promising results. The possibility of coupling quantum emitters to an integrated photonic platform is of primary importance, allowing enhancement and control of the atom-photon interface, hence making realistic the complex manipulation of quantum states of light [19]. We particularly focus on the development of scalable platforms, where many quantum emitters can be coupled at once. In this respect we propose 3D patterning of a polymer photoresist around selected single molecules by means of electronic and optical lithography. In Fig. 1 we show two examples for the coupling of single dibenzoterrylene (DBT) molecules embedded in anthracene matrices to a ridge SiN waveguides and to polymeric ones (panel a) and b), respectively).

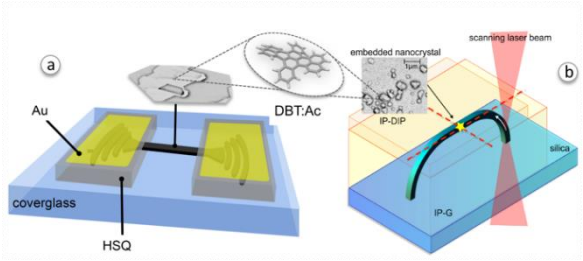

Fig. 2. Coupling of single dibenzoterrylene (DBT) molecules in anthracene matrices.

Novel Infrared Sources for Free-Space Optical Communications

Although very promising, the sources described so far are limited to some specific spectral regions not always compatible with free-space communications. We are currently studying new nonclassical light sources, with squeezing and entanglement capability, based on quantum cascade laser frequency combs [20]. These sources are able to emit infrared radiation which is optimal to heavily reduce scattering losses and are therefore good candidates to realize free-space quantum communications and air-to-ground links with satellites. We are investigating the possibility of transmitting information in free space with sources of coherent radiation in the middle and far infrared (THz) [21], i.e. in the wide wavelength region between 2 and 1,000 microns. Optical communications in free-space require careful optimization of the emitting source, such as wavelength and emitted power; in addition, it turns out that the shape of the emitted beam is an important parameter to be adjusted in order to establish an optimal transmission. This is due to the fact that air transparency window strongly depends on environmental conditions. For example, humidity, fog, dust, aerosols, clouds or strong refractive index gradients can introduce significant energy losses of the radiation being transmitted. Therefore, in order to define the best transparency windows, depending on the environmental conditions, it is necessary to find the best combination of wavelength, power and beam shape conditions. The infrared radiation is optimal to heavily reduce scattering losses, in addition sources emitting in this spectral range are currently subjected to a strong technological improvement. For these reasons, novel sources of infrared radiation such as *quantum cascade (QCL) and interband cascade lasers (ICL)* are good candidates to realize free-space communications and air-to-ground links with satellites.

Quantum devices at Terahertz frequencies

Terahertz (THz) technology has prompted in the last decade a major surge of interdisciplinary researches, inspiring fundamental insights and amazing applications in microscopic and macroscopic systems. Being a transition region between electronics and photonics, between component sizes that are smaller and larger than the radiation wavelength, the THz frequency "gap" offers unusual possibilities in borrowing concepts and technologies from fundamentally different worlds.

Recent technological innovation in photonics and nanotechnology is now enabling Terahertz frequency research to be applied in an increasingly widespread range of applications. In this perspective, the availability of compact THz devices that are conveniently single frequency, high-power, low divergent and narrow linewidth laser sources, is matching increasing demand for quantum and spectroscopy applications encompassing environmental monitoring, security and biomedical

sensing, as well as more fundamental molecular studies and frequency metrology.

Quantum cascade lasers (QCLs) operating at THz frequencies have undergone rapid development since their first demonstration. These laser sources can now be designed with high power, broad tunability, high spectral purity, and ultra-broadband gain.

We have recently developed high spectral purity sources: i) continuous wave compact THz QCL, exploiting novel photonic engineering solutions for achieving high-power, low divergent emission in 1D and 2D resonator architecture; ii) random electrically pumped THz lasers; iii) miniaturized frequency comb synthesizers exploiting record dynamic range; iv) broadly tunable emitters. The combination of the above technologies with quantum nanodetectors exploiting novel 2D material systems and related heterostructures offer a reliable platform for the development of THz sensing systems for high precision metrology and quantum communications

Quantum State Transfer

We investigate multipartite entanglement distribution from optical to microwave domain, providing a route to transfer quantum states between different parts of a quantum network. It was recently demonstrated that a new kind of optical frequency combs, based on cascaded second order processes, generates quantum correlation between combs at different spectral regions, realizing scalable multipartite entangled states [22, 23, 24]. Exploiting the unique feature of optomechanical systems, which work for any frequency of the electromagnetic spectrum, we prospect to combine quantum optical frequency combs with optomechanical transducers in order to integrate distinct quantum technologies.

The process of entanglement transfer between flying modes and localized systems in the case of multipartite systems it has been analyzed [25, 26]. Quantum interfaces, able to store and redistribute quantum information, without introducing decoherence, have been proposed [27, 28]; in such schemes, a mechanical oscillator is physically shared by two cavities, at optical and microwave frequencies, respectively. The mechanical system acts like a nonlinear medium, mixing the two electromagnetic fields. Bidirectional and coherent converters between the microwave and optical regions of the electromagnetic spectrum has been recently realized in the classical regime [29, 30], opening a viable path to the realization of optomechanical interfaces. A great effort has been devoted to preserve the quantum coherence and today the current technology is mature enough to enter the quantum regime. In this contest the prospected entanglement multipartite distribution, based on the coupling of optical frequency comb teeth to different electro-optomechanical systems, is fundamental to integrate a large number of different localized devices in a single hybrid network.

In the conceptual scheme shown in Fig. 3, continuous-variables are sent to *N* nodes of an electro-optomechanical network. The quantum correlations shared by the input noise will link the various electro-optomechanical subsystems to each other and the dynamics of the j_{th} subsystem will depend on the input noise correlators, allowing distributing the entanglement from optical to microwaves variables.

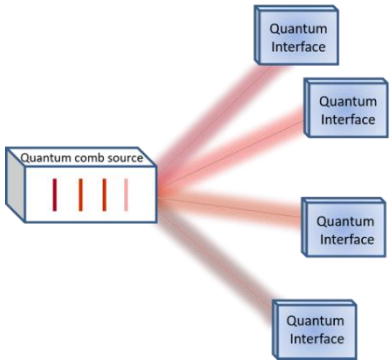

Fig. 3 The transmitter and the receiver are located at the European laboratory for non- linear spectroscopy (LENS). A fiber mirror, located in a telecom datacenter, allows loopback configuration. IM: intensity modulator (for carving pulses and decoy state), PM: phase modulator (phase randomization), BS: beam splitter, APD: avalanche photon detector; DLI: delay line interferometer. SPD: InGaAs single photon detector.

Quantum Key Distribution (QKD) in the metropolitan Florence area

Every second a huge amount of data is transmitted worldwide through internet reaching every corner of the globe. However, increasingly sophisticated cyber-attacks are stressing conventional security techniques. Furthermore, applying newly emerging quantum technologies, such as the quantum computers, will undermine the security of commonly used cryptographic systems. On the other hand, the laws of quantum mechanics can be used to create an

unconditionally secure communications system. Quantum Key Distribution (QKD), when implemented ideally, is guaranteed to be safe by the laws of quantum mechanics, and immune to eavesdropping. Although proposed 35 years ago, this technique is still far to be ready for a large-scale deployment in existing network infrastructures. The low secret-key rate, limited distance between users and high costs are among the main limiting factors. In order to push QKD toward real word deployment, we have realized a low-cost field trial demonstration of a complete QKD system working in the C-band telecom wavelength as shown in Fig. 4. We performed a test over an installed fibre link provided by the Istituto Nazionale di Ricerca Metrologica (INRIM) and located in the metropolitan area of Florence [31].

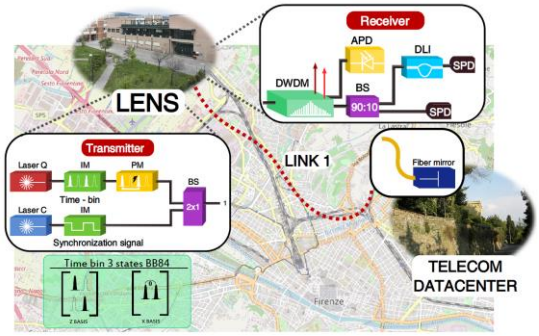

Fig. 4. QKD system in Florence. The transmitter and the receiver are located at the European laboratory for non- linear spectroscopy (LENS). A fiber mirror, located in a telecom datacenter, allows loopback configuration. IM: intensity modulator (for carving pulses and decoy state), PM: phase modulator (phase randomization), BS: beam splitter, APD: avalanche photon detector; DLI: delay line interferometer. SPD: InGaAs single photon detector.

References

[1] M. Bellini, and A. Zavatta, Manipulating light states by single-photon addition and subtraction, Prog. Opt. 55, 41 (2010).

[2] A. Zavatta, J. Fiurasek, and M. Bellini, A high-fidelity noiseless amplifier for quantum light states, Nat. Phot. 5, 52 (2011).

[3] L. S. Costanzo, A. S. Coelho, N. Biagi, J. Fiurášek, M. Bellini, and A. Zavatta, Measurement-Induced Strong Kerr Nonlinearity for Weak Quantum States of Light, Phys. Rev. Lett. 119, 013601 (2017).

[4] P. Sekatski, N. Sangouard, M. Stobi ´ nska, F. Bussières, M. Afzelius, and N. Gisin, Phys. Rev. A 86, 060301(R) (2012).

[5] A. Zavatta, M. D'Angelo, V. Parigi, and M. Bellini, Remote preparation of arbitrary time-encoded single-photon ebits, Phys. Rev. Lett. 96, 020502 (2006).

[6] H. Jeong, A. Zavatta, M. Kang, S. Lee, L.S. Costanzo, S. Grandi, T.C. Ralph, and M. Bellini, Generation of hybrid entanglement of light, Nat. Photon. 8, 564 (2014).

[7] N. Biagi, L. S. Costanzo, M. Bellini and A. Zavatta, Entangling macroscopic light states by delocalized photon addition, arXiv:1811.10466 (2018).

[8] J. P. Dowling and K. P. Seshadreesan, Quantum Optical Technologies for Metrology, Sensing, and Imaging, J. Light. Technol. 33, 2359 (2015).

[9] B. Lounis and W. E. Moerner, Single photons on demand from a single molecule at room temperature, Nature 407, 491 (2000).

[10] S. Buckley, K.Rivoire and J.Vučović, Engineered quantum dot single-photon sources, Rep. Prog. Phys. 75, 126503 (2012).

[11] M. W. Doherty, et al., The nitrogen-vacancy colour centre in diamond, Phys. Rep. 1, 528 (2013).

[12] A. Kiraz, Th. Hellerer, Ö. E. Müstecaplioğlu, C. Bräuchle and A. Zumbusch, Indistinguishable Photons from a Single Molecule, Phys. Rev. Lett. 94, 223602 (2005).

[13] C. Toninelli et al. Near-infrared single-photons from aligned molecules in ultrathin crystalline films at room temperature, Optics Express 18, 6577 (2010).

[14] Zadeh, Elshaari A. W., et al., Deterministic Integration of Single Photon Sources in Silicon Based Photonic Circuits, Nano Lett. 16, 2289 (2016).

[15] S. Checcucci et al., Beaming light from a quantum emitter with a planar optical antenna, Light: Science and Applications 6, e16245 (2017).

[16] Lombardi P. et al., Photostable Molecules on Chip: Integrated Sources of Nonclassical Light, ACS Photonics 5 126 (2017).

[17] C. Toninelli et al, Nanoparticle detection in an open-access silicon microcavity, Appl. Phys. Lett. 97, 021107 (2010).

[18] G. Kewes et al., A realistic fabrication and design concept for quantum gates based on single emitters integrated in plasmonic-dielectric waveguide structures, Scientific Reports 6, 28877 (2016).

[19] Y. Pilnyak et al., Optimal experimental dynamical decoupling of both longitudinal and transverse relaxations, Phys. Rev. A 95, 022304 (2017).

[20] www.qombs-project.eu

[21] M. S. Vitiello, et al., Quantum-limited frequency fluctuations in a terahertz laser, Nature Photonics 6, 525 (2012).

[22] I. Ricciardi, et al., Frequency comb generation in quadratic nonlinear media, Phys. Rev. A91, 063839 (2015).

[23] S. Mosca, et al., Modulation instability induced frequency comb generation in a continuously pumped optical parametric oscillator Phys. Rev. Lett.121,093903 (2018).

[24] G. He, et al., Five-partite entanglement generation between two optical frequency combs in a quasi-periodic χ (2) nonlinear optical crystal, Sci. Rep. 7, 9054 (2017).

[25] F. Casagrande, A. Lulli, and M. G. A. Paris, Tripartite entanglement transfer from flying modes to localized qubit, Phys. Rev. A 79, 022307 (2009).

[26] M. Paternostro, L. Mazzola and J. Li, Driven optomechanical systems for mechanical entanglement distribution, J. Phys. B: At. Mol. Opt. Phys. 45 154010 (2012).

[27] L. Tian and Hailin Wang, Optical wavelength conversion of quantum states with optomechanics, Phys. Rev. A 82, 053806 (2010).

[28] Sh. Barzanjeh, M. Abdi, G. J. Milburn, P. Tombesi, and D. Vitali, Reversible Optical-to-Microwave Quantum Interface, Phys. Rev. Lett. 109, 130503 (2012).

[29] J. Bochmann, A. Vainsencher, D. D. Awschalom, and A. N. Cleland, Nanomechanical coupling between microwave and optical photons, Nature Phys. 9, 712 (2013).

[30] R.W. Andrews, R.W. Peterson, T. P. Purdy, K. Cicak, R. W. Simmonds, C. A. Regal, and K.W. Lehnert, Bidirectional and efficient conversion between microwave and optical light, Nature Phys. 10, 321 (2014).

[31] D. Bacco et al., Field trial of a finite-key quantum key distribution system in the Florence metropolitan area, arXiv:1903.12501 (2019).

SINGLE PHOTON COUNTING IN AUTONOMOUS VEHICLES AND INDUSTRIAL PROCESSES

Sanna Uusitalo
BA1404 Optical measurements
VTT
Oulu, Finland
Sanna.Uusitalo@vtt.fi

Pentti Karioja
BA1501 Photonics integration
VTT
Oulu, Finland
Pentti.Karioja@vtt.fi

Matti Kutila
BA2606 Automated vehicles
VTT
Tampere, Finland
Matti.Kutila@vtt.fi

Dmitry Morits
BA1401 MEMS
VTT
Espoo, Finland
Dmitry.Morits@vtt.fi

Teemu Sipola
BA1404 Optical measurements
VTT
Oulu, Finland
Teemu.Sipola@vtt.fi

Maria Jokela
BA2606 Automated vehicles
VTT
Tampere, Finland
maria.jokela@vtt.fi

***Abstract*— Competitive advantages achieved by photon counting to solve the issues of present three dimensional (3D) sensing technology in autonomous vehicles and process control of industrial high temperature metallurgical processes are presented. Furthermore, the potential of a novel commercial photon counting based Raman instrument to solve the issues rising from the fluorescence background and thermal emission from a sample in process control case of hot industrial processes are discussed.**

Keywords—SPAD, TOF, LIDAR, industrial, autonomous vehicles

Introduction

The demands posed by the needs of emerging business of autonomous vehicles are not yet met with present sensing technologies. Stereo vision cannot provide native 3D data and acoustic sensing cannot reach the desired 50-150 m measurement ranges. Radars can operate in fog and rain, can meet the cost target of few hundred Euros, but they cannot provide the desired angular resolution mainly because of diffraction rising from the combination of wavelength and aperture diameter. LIDAR's (light detection and ranging), utilizing three orders of magnitude shorter near infrared (NIR) wavelengths are not limited by diffraction. Systems based on rotating prisms can meet the specification for maximum range, but are physically too large, cannot operate in adverse conditions because of the high backscatter from fog, rain, snow and their cost is too high, from few thousand Euros to tens of thousands of Euros. The problems of prism based LIDAR's in cost and size are dominated by characteristics of mechanical scanners and the demand for using large emittter apertures to keep the laser emission per unit area within accessible emission limits (AEL) as specified in laser safety Class I. To simultaneously meet laser safety and to minimize the cost, typically several 905 nm lasers are located in a rotating disk. However, besides the size problem, the inherent limitations due to eye safety in spectral region of the silicon detector (< 1000 nm) results in strict limits for the laser power. Limited power in combination with limitations of the linear front-end electronics to resolve temporally sharp echoes from the objects against the strong but temporally even signal from scattering media (eg. fog), results in drastical drop of operational efficiency in adverse weather.

LIDAR's based on MEMS (micro electromechanical system) have been demonstrated to reduce the cost and size of the system, but the inherent limitation of the optical aperture has resulted in limited measurement ranges of few tens of meters.

FLASH LIDAR's, based on 2D focal plane arrays and pulsed lasers can provide native 3D data without moving parts, but since the laser pulse is distributed over a large solid angle, the intensity of the back-reflected radiation decreases below the detection threshold of the detector at distances longer than few 10 meters. Furthermore, since the back-reflected signal is recovered over a large field of view (FOV), the angle of incidence (AOI) at the planar narrow band pass (NBP) filter is varying across the scene. This sets the lower limit for the filter bandwidth (BW) and results in increased amount of ambient illumination entering the receiver, which is a key weakness in FLASH LIDAR's since the ambient illumination is the dominant noise source in LIDAR's in general.

The industrial commodities such as steel, copper, aluminium are produced in high temperature processes, which demand high amounts of energy and inevitably emit substantial amounts of carbon dioxide (CO_2). Substantial reduction in CO_2, demanded energy and high economical advantages could be achieved if the chemistry of the materials in these processes and the physical measures, as level of the liquid metal surface could be sensed more precisely and with shorter time delays for the needs of more precise process control. LIDAR's can be applied for liquid surface sensing and Raman spectroscopy can be used for chemical analysis of the material in the process - even from few meter distance. However, the high density dust of these processes is problematic for present LIDAR's as they are applied for metallurgical processes. The high fluorescence, thermal emission and reflected ambient illumination from the measured object induce high shot noise, ruining the signal to noise ratio (SNR) of the measured Raman spectrum.

Advantages of photon counting in LIDAR applications

a) Ability to discriminate the measured objects from the backscatter of the media

Being able to accumulate the photon echo signal in form of histogram with ultimate (100 ps class) temporal resolution and high dynamic range (single photon sensitivity and low dark current), the rapidly developing photon counting technologies mitigate the problems rising from backscatter (fog, rain) of the present analog front end based LIDAR's. The systems based on photon counting are especially suited for environments with high backscatter since the temporal fidelity of the recorded echo is not degraded by limitations of amplifier stages, since the photons are detected directly, without amplification. This results in enhanced ability to resolve weak but "peak"-like echo of a solid object from continuous echo from fog etc., dispersed evenly in the air.

b) Ability to operate at lower power levels

Whereas traditional linear front end based LIDAR's demand few hundred photoelectrons / pulse to be detected, photon counting based systems can operate at power levels much below 1 photoelectrons / pulse to be generated. This results in relaxed specifications in laser power and/or in optical aperture, which translates in smaller physical size of the system and lower cost. The reduction in demand for the optical aperture allows us to use MEMS as the scanning element, resulting in drastical reduction in cost and physical size of the system.

Advantages of photon counting for raman analysis applied for on-line industrial process control

Novel commercially available [1] Raman system, based on single photon avalanche detector (SPAD) array, and a pulsed laser can reach 100 ps class temporal resolution. Since the time constant of fluorescence is typically between 1000 ps to 100 ns, a substantial, factor 10-1000 reduction in fluorescence background can be achieved in the measured Raman signal [2].

The thermal emission and reflected ambient illumination are evenly distributed over time. Thus, compared to traditional continuous wave (CW) Raman system, the reduction in these two noise sources is equivalent to the duty cycle (typically 10,000) which results in huge increase in SNR allowing us for example to observe objects well above 1500 °C whereas traditional Raman systems are limited to temperatures below 400 °C.

The goals of the 3d-lidar project

a) A Low cost LIDAR for autonomous vehicles operating at adverse weather conditions

The targets are:

- 50 - 100 meter range
- FoV horizontal 40°
- Temperature range -40 … +85°C
- MEMS mirror for laser scanning for low cost
- 1550 nm diode laser source for maximum eye safety
- Low price ~ 1000 €

b) An industrial LIDAR for metallurgical applications

The industrial LIDAR is designed to observe the effect of the height of the steel/slag surface for more precise process control and to follow the wear of argon oxygen decarburator (AOD) converter working lining over time.

Successful on-line measurement would increase the process efficiency, economics and improve sustainability by by reducing the use of gases and reduction materials/chemicals,energy, processing time, reducing CO2 emissions.

c) Piloting time-gated stand-off Raman for fast EAF slag analysis

During processing of stainless steel with electric arc furnace (EAF) valuable chromium can end up in the slag, because fast enough analysis mehtods for the chemical composition of slag do not exist. A stand-off Raman system based on single photon counting is to be built and tested to evaluate it's performance.

References

[1] Time Gate Instruments, Oulu, Finland www.timegate.com

[2] J. Kostamovaara, Fluorescence suppression in Raman spectroscopy using a time-gated CMOS SPAD. 2013 | Vol. 21, No. 25 OPTICS EXPRESS

DOWNSIZING EARTH-OBSERVATION INSTRUMENTS THROUGH KEY TECHNOLOGY ENABLERS: A THEORETICAL STUDY

Tessa Verstrynge
Project Engineer
OIP Sensor Systems
Oudenaarde, Belgium
tve@oip.be

Ludovic Aballea
System Engineer
OIP Sensor Systems
Oudenaarde, Belgium
la@oip.be

***Abstract*—For future developments of high spatial resolution instruments for Earth-Observation missions, there is a demand to reduce the cost of such missions. This can be obtained by downsizing the instrument size. OIP Sensor Systems has performed studies to identify enabling technologies capable of bridging the gap between high-end instruments with large dimensions and smaller instrument design concepts. A key element in the size reduction of the optical systems for earth observation instruments is located in the availability of small pixel size, high-speed, high-response detectors. With such detectors high resolution and an excellent radiometric sensitivity can be obtained, avoiding the need of very complex Time-Delay-Integration (TDI) schemes to compensate for the poor signal-to-noise performances of low F/# optical systems. In this field, the development of large array avalanche photodiodes, operating at temperatures higher than 99K, could provide a substantial advantage as compared to conventional detectors.**

Keywords—Earth observation, remote sensing instruments, APD

Introduction

A few years ago, OIP was given the challenge to ensure the continuity of the Vegetation products by developing the successor of the SPOT VEGETATION instrument. While keeping the performance requirements, the new instrument had to reduce in volume and mass from about 1 m³ and 150 kg to 500 mm³ and 30 kg. OIP has proven the feasibility of this activity, as in 2013, the PROBA-Vegetation instrument has started its land imaging activity after a successful launch. Based on this development, OIP has recently been awarded with a study to define the possible architecture of next generation compact high spatial resolution instruments for Earth-Observation missions integrating a large number of different spectral bands.

As part of this activity, the initial task was to investigate which elements of a given set of requirements are the major contributors to the instrument size. As a second instance the analysis was focused on the possible technical means to enable shrinking the dimensions of such high end multispectral imager below the 500 mm³.

Requirements

As a starting point of the study, a set of requirements was given for the land imager. The intention was to develop a moderate resolution multispectral imager which could cover the globe with a moderate swath. The study included the integration of a list of 7 different VNIR bands, 2 SWIR bands and 2 TIR bands in the instrument volume.

The Ground Sampling Distance (GSD) and the swath were respectively specified to be 30 m for most bands and 185 km for all bands. These requirements define the minimum pixel array necessary to sample the scene and therefore have a direct impact on the focal plane array dimensions. Furthermore, the requirement of the relative edge response and its transfer in the Modulation Transfer Function (MTF) requirement was identified to be quite demanding for each band representing a need for high performances up to a high spatial frequency.

Regarding the radiometric requirements, the Signal to Noise Ratio (SNR) is certainly the most important driver. In this frame, the instrument is required to ensure a high SNR above 100 for most spectral bands while ensuring a high dynamic range of incoming radiance levels. These requirements are not only driving the collected light flux by the optics, but also the way the detection system can cope with a large dynamic range.

GSD, Minimum Edge Slope and Maximum Half Edge Extent Specifications

#	Band	Nominal GSD	Minimum Slope	Maximum Half Edge Extent
1	Coastal Aerosol	30 m	.027 / m	23.0 m
2	Blue	30 m	.027 / m	23.0 m
3	Green	30 m	.027 / m	23.0 m
4	Red	30 m	.027 / m	23.5 m
5	NIR	30 m	.027 / m	24.0 m
6	SWIR 1	30 m	.027 / m	28.0 m
7	SWIR 2	30 m	.027 / m	29.0 m
8	Panchromatic	15 m	.054 / m	14.0 m
9	Cirrus	30 m	.027 / m	27.0 m

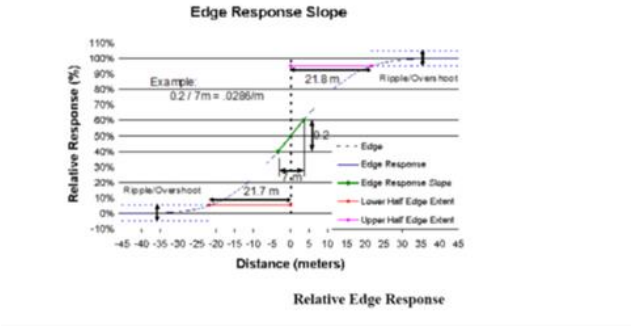

Fig.1 GSD and Image quality requirements specified in terms of RER for each spectral band of interest.

Radiance Levels for Signal-to-Noise Ratio (SNR) Requirements and Saturation Radiances

#	Band	Radiance Level for SNR, L (W/m^2 sr µm)		Saturation Radiances, L_{Max} (W/m^2 sr µm)
		Typical, $L_{Typical}$	High, L_{High}	Requirement
1	Coastal Aerosol	40	190	555
2	Blue	40	190	581
3	Green	30	194	544
4	Red	22	150	462
5	NIR	14	150	281
6	SWIR 1	4.0	32	71.3
7	SWIR 2	1.7	11	24.3
8	Panchromatic	23	156	515
9	Cirrus	6.0	N/A	88.5

Fig.2. Required dynamic range for the multispectral instrument.

Finally, the incentive to downsize the instrument such that mass volume and finally mission cost could be reduced, was defined as the driver of the study.

Instrument size drivers

On the basis of an initial trade-off, the instrument design has been initiated on a pushbroom instrument. In this approach, the instrument sensor is oriented perpendicular to the satellite track and the second dimension of the image is ensured thanks to the S/C motion. All elements contributing to the instrument dimension constrains are considered.

a) GSD & Swath

The instrument design starts considering the ground sampling distance requirement and the swath width, which are defining the pixels footprint on ground and also the minimum number of pixels in the detector array. In order to get an image with a swath of 185 km and a GSD of 30 m, 6167 pixels as a minimum are needed to sample the scene (Swath/GSD = # pixels). Based on a given flight altitude, these parameters define the minimum Focal Length (FL) of the optical design as there is a direct relationship between the detector pixel size, the flight altitude (H) and the GSD:

$$FL = \frac{\text{pixel size}}{\frac{GSD}{H}} \qquad (1)$$

In order to achieve a high resolution for the space instrument, it might appear beneficial to fly at low altitudes as this would imply using smaller sensors with a lower frame rate due to the S/C ground track speed. However, a low altitude usually implies a shorter lifetime for the mission due to atmospheric drag, which is not desirable for high end remote sensing systems planned for long operational time. In this study, a flight altitude about 660 km was assumed.

Once the flight altitude is defined, the focal length is frozen, leaving the only way to make the volume smaller by reducing the pixel size. The main drawback of the pixel size reduction is that the surface available to collect photons is getting reduced while the pixel noise is still present. Therefore, for the same amount of incoming photons, a reduction of the pixel SNR is experienced. This SNR reduction is usually compensated by means of increasing the light throughput of the instrument through an expanded entrance pupil aperture. Hence, the size of the optics is enlarged.

b) MTF

The MTF is the product of the optical MTF and the detector MTF. Considering that the detector MTF at Nyquist is a given, the natural way of optimizing the instrument MTF performances is by optimizing the optical MTF. The optical MTF of an aberration-free image with a circular pupil, is a function of the spatial resolution (ξ):

$$MTF(\xi) = \frac{2}{\pi}(\varphi - \cos\varphi \sin\varphi) \quad (2)$$

$$\varphi = \cos^{-1}\frac{\xi}{\xi_c} \quad (3)$$

$$\xi_c = \frac{D}{\lambda * FL} \quad (4)$$

Where ξ_c is the cut-off frequency which is dependent on the optical system entrance pupil aperture (D). Therefore, achieving high MTF performances at instrument level without ground processing involvement has a direct impact onto the optics entrance pupil diameter and overall optics dimensions.

c) F number

Disregarding the radiometric requirements, it was shown that for a given detector MTF, the optical MTF determines the minimal aperture size by diffraction limit effects. On the other hand, the GSD requirement and volume constraint define the pixel size. In these conditions, the minimal aperture size for the visual to SWIR channels was theoretically calculated to be 73 m. From iterations of the optical design it was confirmed that an entrance pupil of about 100 mm was feasible.

The f number F/#, which is the ratio of the focal length to the aperture diameter, was calculated for different values of the pixel size for an aperture around 100 mm. The results are shown in 0

TABLE I. F NUMBERS

Pixel size	FL [mm]	Aperture diameter [mm]		
		90	*100*	*110*
13	305.5	3.39	3.06	2.78
15	352.5	3.92	3.53	3.20
20	470	5.22	4.70	4.27
25	587.5	6.53	5.88	5.34
30	705	7.83	7.05	6.41
40	940	10.44	9.40	8.55

Based on these focal length values, the ideal depth of focus δ was calculated according to (5) for the different channels, of which the results are shown in TABLE II

$$\Delta = \frac{2\lambda}{\sin\left(\tan^{-1}\left(\frac{1}{F/\#}\right)/2\right)^2} \quad (5)$$

TABLE II. DEPTH OF FOCUS [µM]

Spectral band	F number		
	3	*4*	*5*
Blue	9	16	24
Green	10	18	28
NIR	16	28	44
SWIR1	31	53	82

Going towards f numbers lower than 20 presents several limitations. Firstly, the faster (low f number) an optical system is, the tighter the optical tolerances become, which increases the risk that the high MTF performances which were targeted will not be achieved. Secondly, the presently achievable state of the art minimal sensor flatness is around 20 µm. Consequently, the depth of focus which could be realistically envisioned is constrained and therefore, the f number.

This shows that the pixel size has a lower limit too in combination with a certain maximal aperture size. The requirements are thus tending to pull apart instrument design constraints and design optimization, so technical improvements are needed to reconcile these demands.

Oversampling

- The minimal aperture size to meet the optical MTF requirement, can be reduced by oversampling. By allocating e.g. 3 pixels instead of one for the 30 m required GSD, each pixel samples 10 m. As a consequence, the detector is operating at a frequency lower than its Nyquist so the overall MTF is improved greatly. This improvement gives the opportunity to relax on the optical MTF while still meeting the overall MTF requirement.

- A drawback of such approach is that the focal plane array has to be larger, which tends to increase the overall instrument dimensions. To maintain an equivalent focal plane array dimension, a smaller pixel pitch is needed. However, one has to keep in mind that both the aperture and pixel size reduction have an impact on the SNR. Therefore, the problem had to be considered in two dimensions, geometric and radiometric. An analysis of the trade-off made for each spectral band is illustrated in Fig.3 in case of a TIR band. The red curve gives the GSD that can be achieved while ensuring the MTF performances are met. The blue line gives the minimal GSD for a

«conventional» linear detector achieving the SNR requirements.

- It is quite challenging though feasible, with already available sensors to try bringing these requirements together. Nevertheless, the dimensions which can be achieved are still out of the target dimensions. To reduce the dimensions further than this, it is mandatory that a significant improvement on detector performances is achieved.

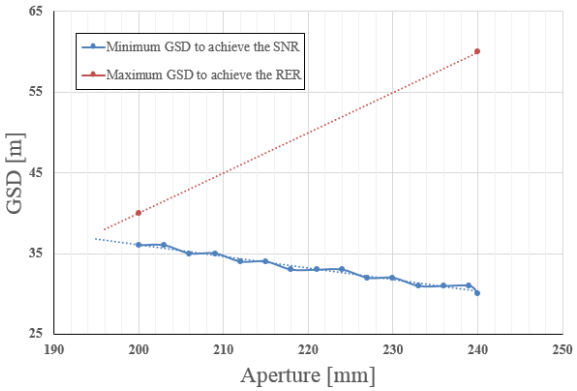

Fig.3. Limitations on the GSD.

Detector

In order to be able to use oversampling while keeping the f number within limits together with keeping the volume of the instrument small, a reduced pixel pitch is necessary. As an outcome, the SNR MTF and dynamic range of the instrument encounter a reduction. A counterbalance of these elements can be found in detector improvements.

First of all, a higher Quantum Efficiency (QE) and photoresponse result in a higher signal. Thus, if keeping the noise as low as possible, this would lead to a high SNR. Furthermore, the detector MTF could be nearly perfect if electron diffusion is limited for smaller pixels. Additionally, by making use of a CMOS detector, small pixels with high anti blooming would keep the dynamic range within requirements.

a) Type of material

Silicon and InGaAs detectors are very common, but their spectral sensitivity is limited to a few channels. This means that a combination of the two would be needed in order to image all the spectral bands. An MCT detector however, has a high sensitivity over a broad range of wavelengths, and the volume that can be reduced by only having to use one detector compensates for the volume that has to be sacrificed to implement a radiator, as an MCT detector needs cooling in order to keep its high performance.

By adding anti-reflective (AR) coatings, the quantum efficiency will be even higher for the different channels.

b) Type of detector

In a way, the quantum efficiency of a conventional linear detector limits the signal output, as the value of the gain cannot exceed unity. Therefore, the option of an Avalanche Photodiode Detector (APD) was considered. This kind of detector has a high photoresponse through the process of impact ionization, resulting in a gain higher than unity.

Some simulations were done for a linear detector in a system with a 100 mm aperture diameter as shown in TABLE III. With a certain optical set-up, the different channels' central wavelengths lead to a given photon flux. When taking the quantum efficiency into account, together with the aperture size and integration time, the received signal in electrons can be calculated. In order to prevent saturation, this signal has to stay below the full well capacity of the detector. Three different noise contributions are shown. The dark current, which is dependent on the operating temperature, the signal shot noise to the signal and the fixed noise to the detector pixel design and readout. With these parameters, the Signal to Noise Ratios fulfil the set of requirements.

The case of an Avalanche Photodiode Detector is shown in TABLE IV. An APD has a high photoresponse, e.g. if 15 electrons are created for each received photon, the signal will be much higher than a conventional detector. As a consequence, the aperture diameter can be reduced to a size of 20 mm without affecting the SNR. However, such approach can only be enabled by further improvement of current state of the art APDs:

- An APD's dark current is dependent of the temperature and most current APDs work only at cryogenic temperatures, which requires complex cooling systems and limits their practical operability in a space environment. A higher temperature range of operability, ideally above 170K with low dark

current is therefore an asset and requires further development of performant readout circuitry insensitive to radiation effects.

- Most APD arrays are still quite "small" pixel arrays (256x320 pixels at most), which requires to develop butting of multiple detectors onto a single focal plane array. This technique presents an additional complexity and risk which would be prevented by larger pixel arrays as the one which could be achieved in conventional CMOS technology going beyond the 4kx4k pixels.

Also, in order to maintain performances over a large dynamic range and prevent possible saturation effects while looking at bright scene as snow or deserts, a real time adaptive integration time mechanisms would be needed to adjust the instrument response to the radiometric inputs. Finally, due to the non-linearity of the APD, the instrument calibration and radiometric validation would have to be thought of in a different manner such that absolute radiometric measurements could be performed.

Despite these new constrains, such design would provide superior opportunities of miniaturization by significant oversampling while allowing a significant reduction of the optics dimensions without impacting the optical nor radiometric performances of the instrument.

Conclusions

Over the scope of the theoretical study performed, multiple elements have been identified, requirements and technologies, as driving a multispectral imager dimensions. The identified elements appeared to be mostly common to any type of mission involving high end remote sensing instrument.

Based on the performed analysis it appears that volume reduction of any remote sensing system lies within the breakthrough made in detection capabilities applied in conjunction with new operation techniques and data processing approaches. Because its high photoresponse, an APD appears to be the most appropriate detector choice for a small instrument combining the possibilities of focal plane size reduction, optical design volume optimization while maintaining geometric, radiometric and optical performances at the same level as conventional large EO instruments.

Based on the presented study, the detector profile which would be looked at would preferably have small pixels with a pitch around 10 µm and present a large dimension above 1kx1k pixels. Finally, to enhance its radiometric performances, it would be composed of an MCT photosensitive layer with an efficient AR coating readout by a low noise high speed readout circuitry. It would operate at high temperatures, preferably above 170K, to prevent the need of a considerable cooling system.

Based on the presented study, if future detector developments would enable such performances, downsizing 1m³ instrument into a 500m³ volume appears to be realistic with as a consequence, a significant cost improvement for high end earth observation missions.

TABLE III. LINEAR DETECTOR WITH 100 MM APERTURE

Spectral band	Wvl [nm]	Photon Flux [ph/m²/sr/s]	QE	Signal in electrons	Full Well	Dark current shot noise [e⁻]	Signal shot noise [e⁻]	Fixed noise [e⁻]	SNR	Requirement
Blue	482	$1.4337*10^{19}$	0.65	304826	530000	150	553	208	500.07	360
Green	562	$1.3612*10^{19}$	0.65	289405	530000	150	538	208	485.58	390
NIR	865	$2.0204*10^{19}$	0.65	429568	530000	150	656	208	609.88	460
SWIR1	1610	$2.1596*10^{19}$	0.65	459165	530000	150	678	170	642.28	540

TABLE IV. AVALANCHE PHOTODIODE DETECTOR WITH 20 MM APERTURE

Spectral band	Wvl [nm]	Photon Flux [ph/m²/sr/s]	Photo-response	Signal in electrons	Full Well	Dark current shot noise [e⁻]	Signal shot noise [e⁻]	Fixed noise [e⁻]	SNR	Requirement
Blue	482	$1.4337*10^{19}$	15	300136	530000	150 (?)	548	208 (?)	496.06	360

EUROPEAN DEFENCE AGENCY

PART II

COMMUNICATIONS & SENSORS QUANTUM TECHNOLOGIES

THE QUANTUM INTERNET: UNDERSTANDING AND LEVERAGING QUANTUM NETWORKS FOR THE DEFENSE DOMAIN

Marcello Caleffi
FLY: Future communications laboratorY
University of Naples Federico II
80125 Naples, Italy
National Laboratory of Multimedia Communications, CNIT
80126 Naples, Italy
marcello.caleffi@unina.it

Angela Sara Cacciapuoti
FLY: Future communications laboratorY
University of Naples Federico II
80125 Naples, Italy National Laboratory of Multimedia Communications, CNIT
80126 Naples, Italy
angelasara.cacciapuoti@unina.it

***Abstract* — The interconnection of quantum devices via the Quantum Internet – i.e., through a network enabling quantum communications among remote quantum nodes – represents a disruptive technology. In fact, the Quantum Internet can provide functionalities with no counterpart in the classical world, such as secure communications, blind computing, exponential speed-up of the quantum computing power and advanced quantum sensing techniques. And the Defense Domain is at the forefront of the markets and industries that could benefit from the Quantum Internet leap.**

Keywords — Quantum Internet, Quantum Networks, Entanglement, Quantum Teleportation.

Introduction

After decades of pure science phase, the research on quantum technologies is finally reaching the engineering phase, getting out of the labs into business reality. Almost all the tech giants are actively engaged in the quantum race. In November 2017 IBM released a 50-qubits processor [1], whereas in March 2018 Google announced a 72-qubits processor [2]. Meanwhile, other big players – like Intel and Alibaba – as well as start-ups – like Rigetti – are actively working on double-digit-qubits proof-of-concepts. In terms of funding, in April 2017 the European Commission launched a ten-years 1€-billion flagship project to boost European quantum technologies research [3], followed by the similar 1.2$-billion U.S. *National Quantum Initiative* program approved in December 2018 [4].

In this exciting context, the design of the Quantum Internet [5], i.e., a network enabling quantum communications among remote quantum nodes, is widely considered mandatory to fully unleash the ultimate vision of the quantum revolution.

In fact, the Quantum Internet can provide functionalities with no counterpart in the classical world [6]. With reference to the Defense Domain, its killer applications range from secure communications through quantum sensor & radar networks to blind quantum computing. In a nutshell, the Defense Domain is at the forefront of the markets and industries that could benefit from the Quantum Internet leap.

The idea is to interconnect multiple quantum devices via a quantum network to transmit quantum bits (qubits) or to create distributed entangled quantum states. This network will have no counterpart in classical networks.

Basic Quantum Background

The power of quantum computation/information lies in its foundation on quantum mechanics, the deepest explanation of the reality surrounding us.

Quantum bits (qubits) are the building blocks of quantum computation. Qubits can be realized with different technologies – ion trap, quantum dots, super-conducting circuits etc.– but the principles of quantum mechanics hold independently of the underlying technology.

While a classical bit can be in one state – either 0 or 1 at any time – a qubit can be in a *superposition* of two basis states - 0 and 1. Two qubits can exist in a superposition of 4 states. With 3 qubits, the states become 8 and, with 4 qubits, the states become 16. Thanks to the superposition principle, the computational power of a

quantum device grows exponentially with the number of embedded qubits.

Quantum states are fragile. Any interaction with the environment irreversibly affects any quantum state, causing a loss of its quantum properties in a process called *decoherence*. The classical strategy – storing redundant copies of the fragile data – is not a solution. The *no-cloning theorem*, in fact, prohibits to clone an arbitrary quantum state, and it turns out to be a valuable property for securing communications.

By measuring a qubit, the quantum state is irreversible changed: any superposition probabilistically collapses into a single state. The measuring principle deeply affects computing: clever ways to manipulate quantum states without measuring them are essential for quantum algorithm design.

As an example, the Quantum Internet may provide an exponential scale-up of the quantum computing power through the *distributed computing* paradigm. Specifically, by interconnecting isolated quantum devices via a communication network and by adopting a distributed approach, a virtual quantum processor is built up and it is constituted by a number of qubits that scales exponentially with just a linear amount of physical resources, i.e., the number of interconnected devices. Hence, if we consider two isolated 10-qubit devices, they can represent 2^{10} states each, thanks to the superposition principle, for a total of $2 \cdot 2^{10}$ states at once. But if we interconnect these two devices with a quantum network, the resulting cluster can represent up to 2^{18} states[1] [7], with an exponential increase of the associated state space dimensionality.

Quantum Internet Design

At a first look, the design of the Quantum Internet may sound like an easy task. After all, the number of devices interconnected by the current Internet exceeds 17 billion, so it should not be a big deal wiring quantum computer as well. However, fundamental and unconventional features of the Quantum Internet impose terrific constraints for its design and deployment [8].

The quantum internet is governed by the laws of quantum mechanics. Hence, weird phenomena with no counterpart in the classic reality, such as no-cloning, quantum measurement, entanglement and teleporting, imposes terrific constraints for the network design

Entanglement: the core of the Quantum Internet

Entanglement, defined as a *spooky action at distance* by Einstein, is a property of two quantum particles. The particles exist in a shared state, such that any action on a particle affects instantaneously the other particle as well. This sort of *quantum correlation*, with no counterpart in the classical world, holds even when the particles are far away each other.

Entanglement provides an invaluable tool to transmit qubits without violating the no-copying theorem and the measuring principle. With just local operations and an entangled pair of qubits shared between source and destination, it is possible to "transmit" an unknown quantum state between two remotes quantum devices.

This process is known as quantum teleportation. It implies the destruction of the original qubit and the entanglement pair member at the source due to the measurement process performed at the source. The original qubit is reconstructed at the destination once the output of the source measurement – 2 classical bits – is received via classical channel.

Indeed, the Quantum Internet lies its foundations on the marvels of entanglement – a sort of fragile quantum correlation with no counterpart in the classical world.

Nowadays, there is a global consensus toward the use of photons as carries – i.e., as flying qubits – to distribute the entanglement among remote quantum devices. The rationale for this choice lies in the advantages provided by photons for entanglement distribution: weak interaction with the environment (e.g., good coherence), easy control with optical components as well as high-rate long-range

[1] Depending on the number of qubits devoted to inter-connecting functionalities.

transmissions. But several challenges and open problems arise for interfacing the flying qubits with the matter qubits – i.e., with the qubits devoted to store/process the quantum information within the quantum devices [8].

References

[1] IBM. 2017. IBM Announces Advances to IBM Quantum Systems & Ecosystem. (Nov. 2017

[2] J. Kelly. 2018. Engineering superconducting qubit arrays for Quantum Supremacy. In APS March Meeting. Bulletin of the American Physical Society.

[3] E. Gibney. 2017. Europe's billion-euro quantum project takes shape. Nature 545, 7652 (May 2017), 16.

[4] E. P. DeBenedictis and M. P. Frank, "The National Quantum Initiative Will Also Benefit Classical Computers [Rebooting Computing]," in *Computer*, vol. 51, no. 12, pp. 69-73, Dec. 2018.

[5] H. J Kimble, "The quantum internet," *Nature*, vol. 453, no. 7198, pp. 1023–1030, June 2008.

[6] S Wehner, D Elkouss, and R Hanson, "Quantum internet: A vision for the road ahead," *Science*, vol. 362, no. 6412, 2018.

[7] M. Caleffi, A.S. Cacciapuoti, G. Bianchi, "Quantum internet: from communication to distributed computing!," Invited Paper, Proc. of ACM NANOCOM, 2018.

[8] A. S Cacciapuoti, M Caleffi, F Tafuri, F. S Cataliotti, S Gherardini, and G Bianchi, "The Quantum Internet: Communications and Networking Challenges," *ArXiv e-prints*, Oct. 2018.

MINIATURE ATOMIC VAPOR CELLS QUANTUM DEVICES FOR SENSING AND METROLOGY APPLICATIONS

Markku Lahti
VTT Technical Research Centre of Finland
Oulu, Finland
markku.lahti@vtt.fi

Mika Prunnila
VTT Technical Research Centre of Finland
Espoo, Finland
mika.prunnila@vtt.fi

Pentti Karioja
VTT Technical Research Centre of Finland
Oulu, Finland
pentti.karioja@vtt.fi

Kari Kautio
VTT Technical Research Centre of Finland
Oulu, Finland
kari.kautio@vtt.fi

Sanna Uusitalo
VTT Technical Research Centre of Finland
Oulu, Finland
sanna.uusitalo@vtt.fi

***Abstract*—Essential features of packaging of miniature atomic clocks in vacuum are presented. The package contains several temperature-sensitive optical components, which limit the maximum allowed temperature in packaging processes. The most promising sealing method was identified to be laser-welding. The package consisted of low temperature co-fired ceramics technology.**

Keywords—packaging, LTCC, vacuum, atomic clock

Introduction

European Commission launched a large-scale initiative called The Quantum Flagship in the end of 2018. It is a billion euros program for 10 years timescale. In the first call 20 projects were funded. One of these projects was MACQSIMAL (Miniature atomic vapor cells quantum devices for sensing and metrology applications) coordinated by CSEM. The project aims to develop technologies for timing, medical sensing and positioning systems. Miniature atomic clocks (MAC) have been identified as one of the key components in the project. VTT has been collaborating with CSEM in this topic for a long time.

Packaging of components is an essential task in the development of MACs. It is complicated by some restrictions. Typical sealing temperatures used in soldering cannot be used due to some temperature-sensitive optical components. Also, magnetic materials should be eliminated as well as possible. This paper reviews some of the most essential topics of low-temperature vacuum-level packaging.

Low temperature co-fired ceramic (LTCC) technology

The LTCC technology is a multi-layer process based on a glass-ceramic substrate. The technology permits the co-firing with highly conductive materials (silver, copper and gold). LTCC also features the ability to embed passive elements, such as resistors, capacitors and inductors into the ceramic package, minimising the size of the completed module. Other advantages of LTCC include mechanical rigidity and hermeticity, both of which being very important in high-reliability and environmentally stressful applications.

The flow chart of the LTCC process is shown in Fig. 1. Each layer is processed individually. The process starts by making electrical and thermal via holes onto individual tape sheets. The most common way to make these holes is using the mechanical punching method. Via holes are filled with a conductor paste by stencil-printing, and solvents of the paste are removed by drying in an oven. The conductor layers are then screen-printed onto tape sheets and the paste solvent is again dried. The layers are then stacked over each other and aligned by utilising the registration holes in the tapes. The stacked sheets are laminated in an isostatic chamber. Co-firing is typically carried out at temperatures of 850-900 °C. The size of the fired panel varies from LTCC suppliers to another. For example, VTT has the panel size of ~100x100 mm^2. The panel contains several circuits, which can be separated by

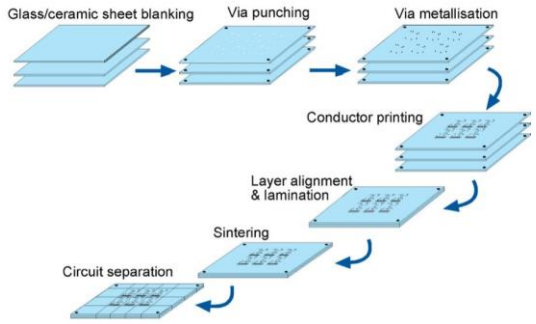

dicing. The key process parameters of VTT's process is shown in Table 1.

Fig. 1 LTCC process flow.

TABLE 1. Key process parameters of VTT's LTCC process.

Parameters	Production State-of-the-art	Special applications
Min. printed linewidth [µm]	50	40
Tolerance of linewidths [µm]	±5	±5
Layer-to-layer positioning accuracy [µm]	±15	±10
Min. diameter of vias [µm]	80	50
Min. via pitch [µm]	160	125
No. of layers	<20	<30

Miniature atomic clocks

LTCC packaging has been utilized in the manufacturing of miniature atomic clocks (MAC) [1]. The package contains several optical components, such as atomic vapor cell, laser unit, photodiodes, waveguides and getter. The challenge from the packaging point of view is maximum allowed temperature (<150 °C) restricted by e.g. the laser and photodiodes. The vacuum level inside the package was planned to be $<10^{-3}$ mbar. The size of the package was 15x21 mm. A concept view of the package is shown in Fig. 2.

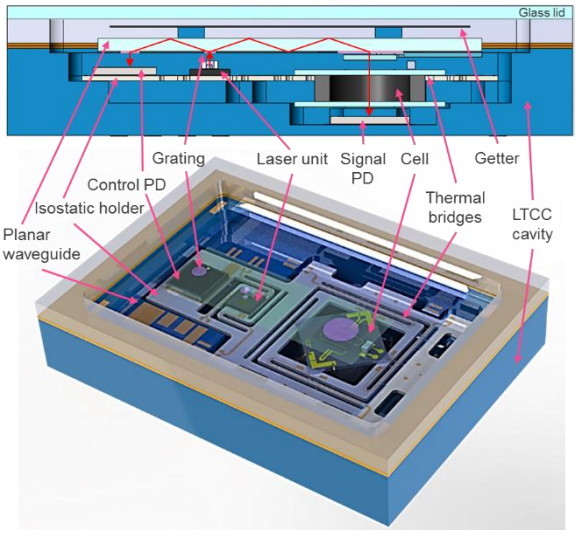

Fig. 2 Overview of the LTCC package.

Vacuum-level packaging can be realized by different methods. Soldering would be the most straightforward methods. The melting temperature of solder is, however, too high for this case. Therefore, other options have been looked for.

One of the developed vacuum-sealing methods is based on the use of glass-to-glass direct laser welding. The process requires two flat glass surfaces which are spot-welded together using a picosecond-type laser. Glass frame was first sealed to the LTCC package using sealing glass. The process looked promising although the vacuum level degraded as a function of time due to defects in the sealing glass. Development work is to be continued in MACQSIMAL project.

Conclusions

LTCC technology has been utilized in vacuum-level packaging. Low-temperature sealing methods have been developed using direct laser-welding approaches. The designed vacuum-level was achieved.

References

[1] J. Haesler, K. Kautio, L. Balet, S. Karlen, T. Overstolz, B. Gallinet, S. Lecomte, F. Droz, P. Karioja and M. Lahti, "Ceramic based flat form factor miniature atomic clock physics package," Workshop on Microwave Technology and Techniques, ESA/ESTEC Noordwijk, The Netherlands, April 3-5, 2017.

QUANTUM RADAR: STATE OF THE ART AND POTENTIAL OF A NEWLY-BORN REMOTE SENSING TECHNOLOGY

Giovanni Serafino
Consorzio Nazionale Interuniversitario per le Telecomunicazioni (CNIT)
Pisa, Italy
g.serafino@santannapisa.it

Antonella Bogoni
Sant'Anna School of Advanced Studies
Pisa, Italy
antonella.bogoni@cnit.it

***Abstract*— Quantum technology has already been introduced in many fields, like information processing and communications, and it can potentially change our approach to remote sensing in the microwave and millimeter-wave domain, leading to systems known as Quantum Radars. This new generation of systems does not leverage directly on quantum entanglement, since the latter is too "fragile" to preserve in a noisy and lossy environment, as a radar scenario, but rather on the high level of coherence derived from quantum entanglement. Quantum Illumination is a process that exploits quantum coherence of non-classical states of light for remote sensing. It allows for the generation and reception of highly correlated signals in the form of optical or microwave photons. By correlating the received signal photons with photons entangled with the transmitted ones, it is possible to clearly distinguish, among all the received photons, the echoes from background noise and interferences, boosting to an unprecedented level the sensitivity of remote sensing. Therefore, in principle, it is possible to detect very low cross-radar section objets, such as stealth targets. Nowadays, very few experiments on Quantum Radar transceivers have been reported. This work aims at summarizing the state of the art of Quantum Radar, introducing its basic working principles, though raising the possible issues of such a technology; secondly, it will point out the possibilities of photonics-assisted Quantum Radars, proposing photonics as the ideal field where quantum science and remote sensing can meet for an effective cross-fertilization.**

Keywords—Quantum Technologies, Photonics, Radar, Quantum Radar

Introduction

Although the roots of quantum mechanics can be traced back to the first half of the 19th century, it still represents a branch of physics that questions the way we observe and interpret reality since some centuries. Despite not being a very young discipline, beyond its help in understanding matter and interactions between particles, only recently it started having a technological usefulness. Indeed, in the last decades, the possibility of demonstrating many of the peculiar properties of quantum mechanics with real experiments has gradually opened the way to new technological applications. In particular, although theoretically pointed out as a paradox by Einstein, Podolsky, and Rosen in their famous paper [1], violations of locality and realism have been recently irrefutably demonstrated [2] by the Bell's inequality violations [3].

Nowadays, quantum technologies are the object of an intense research that led to the development of quantum cryptography [4], quantum computing [5] and, most recently, quantum sensing [6] - [10]. Nowadays, many different approaches have been employed to realize quantum-based systems for any of the above mentioned applications. In particular, both electronics- and photonics-based solutions have been proposed, although no winner did emerge yet. In particular, in this domain, photonics can be very attractive [9], since the generation of light beams with the needed quantum features can be easier than working only in the electrical domain [11] - [13]. Moreover, it has been demonstrated that signals with quantum features can be generated at microwave frequencies starting from light sources [8], [14], [15]. This makes quantum technologies particularly appealing for remote sensing applications, such as radars. A Quantum Radar (QR) is a remote sensing system leveraging on quantum mechanics properties of the electromagnetic fields to enhance detection capabilities with respect to classical radars. Overlooking possible military classified activities, it seems that, today, we are just at the dawn of research and development in the field of QRs. A demonstration of a complete system field trial has not been reported yet, not considering claims with no supporting evidence [16].

In this paper, we outline an updated state of the art of technology for the newly-born application of QR,

considering both electronics-based and photonics-assisted technologies, particularly focusing on possible photonics solutions. Indeed, photonics already offers the possibility of enhancing radar systems capabilities with frequency and waveform agility, higher stability and resolution, and efficient signal distribution [17]. Moreover, since photonics allows for an efficient generation of quantum-entangled signals [11] - [15], it can be considered as a promising candidate to provide sources and detectors for quantum systems. The paper is structured as follows: after the Introduction, in section "Quantum entanglement and quantum radar" we briefly expose the fundamentals of quantum-based technologies, starting from the concept of *quantum entanglement* (QE); then, we focus on one of the most interesting strategies for quantum-assisted remote sensing, namely Quantum Illumination (QI), and report on the first laboratory demonstrator of a QR. In section "Photonics and quantum radar", we show some photonics-based subsystems for the development of a QR transceiver, before outlining conclusions and perspectives a the end of the paper.

Quantum Entanglement and Quantum Radar

a) The Concept of Quantum Entanglement

In 1935, Einstein *et al*. attacked quantum mechanics [1] arguing that its description of physical reality, although correct, was "not complete". Indeed, they raised a crucial issue consisting in quantum mechanics violation of two principles: reality and localism, that had never before been seriously questioned. Nevertheless, quantum mechanics assumptions lead to the concept of QE, which was previously unknown, and considered by Einstein some sort of inexplicable "spooky action at a distance". Two entangled systems are deeply related, in the sense that any change (or measurement) applied to one of them, instantly affects the other, no matter how far in space they are. There are two possible explanations to this seemingly bizarre behaviour: either local realism can be violated by this category of systems, or "information" between the systems can travel even faster than light in vacuum, which is a violation of general relativity. Einstein *et al.* rejected both explanations, indirectly suggesting the presence of "hidden variables", later analyzed by Bell [3], that should be added to quantum-based assumptions and interpretations, to give a satisfactorily complete description of the physical reality.

Many years later, however, the former of the two possible above-mentioned explanations has been demonstrated to be true [2], [3]. Bell's theorem proves that no hidden variable-based model can complete quantum mechanics without violating local realism anyway, and experiments supported this theoretical result [2]. Thus, entanglement between particles has become a common phenomenon, even in small macroscopic systems [18], and its features have been demonstrated to be useful in many applications. If a pair, or a group, of entangled photons is generated, the perturbations experienced by one or more of them is instantly transferred to all the others, even though they did not undergo the same perturbations, no matter where they are located. These unique features of entangled particles can be employed in remote sensing, as exposed in the following.

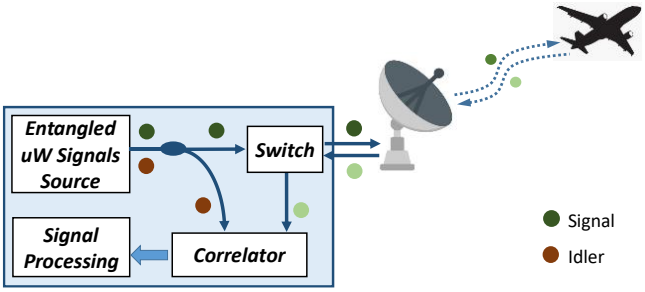

Fig. 1. Basic scheme of a Quantum Radar.

b) The Technique of Quantum Illumination and the Quantum Radar.

Any electromagnetic field, regardless its frequency, is "carried" by photons. As a fact, any pair or group of photons, at any wavelength (or frequency), from radiofrequency (RF) to light, can be generated as entangled. Throughout this paper, we will commonly refer to RF photons or optical photons, depending whether we are talking about an electrical or an optical signal. Let's consider a system generating entangled photons, and assume a part of them is launched toward a target, whereas the remaining ones are stored in the system. Ideally, when the launched photons interact with the target, somehow changing their properties, the remaining local ones, due to QE, would show the same changes, even

though they did not hit the target. This does not really happen, and it is not QE itself being directly employed for sensing. Indeed, QE is very "fragile", and it does not survive to losses and noise typical of the radar environment: when the sensing photons reach the target, QE with the local photons is already lost and the above-described approach does not apply. However, even though in this scenario the QE is broken, all the photons still maintain an extremely strong coherence, that can be exploited in QRs similarly as in classical radars. The technique relying on this non-classical coherence for remote sensing is Quantum Illumination.

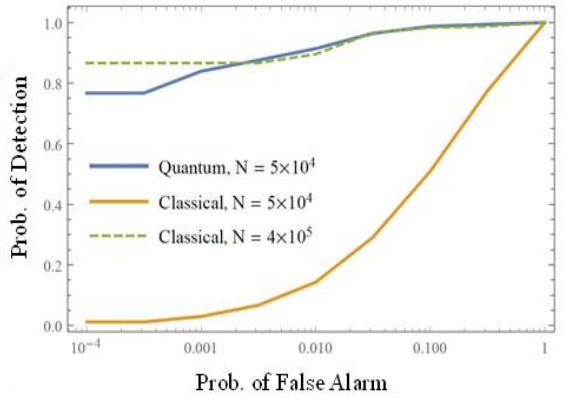

Fig. 2. Comparison between the ROC curves of the QR (blue line) and of an equivalent classical radar (orange and dashed green lines) [10].

The scheme of principle of a QR exploiting QI is depicted in Fig. 1. The entangled photons generated by a source at microwave frequency are separated as signal (deep green circles in Fig.1) and idler (deep red circles). The signal photons are sent to an antenna, whereas the idler photons remain in the system. Once the signal hits a target, it is backscattered to the antenna (light green circles), being received and fed back into the system, where it is correlated with the idler. This way, the preserved coherence deriving from QE allows distinguishing the photons composing the backscattered echoes from any other photon that is part of noise or other transmissions.

c) The First Laboratory Demonstrator of a Quantum Radar

Very recently, Luong *et al*. reported the first example of a complete prototype of a lab-operated QR [10]. The presented system is completely based on electronic technology and is inspired by, but does not directly leverage on QI, since it does not need joint measurements on signal and idler, but it needs just independent measurements. The entangled employed signals are generated by a Josephson Parametric Amplifier (JPA), amplifying vacuum quantum fluctuations, producing a double sideband RF signal. The two sidebands, at 6.1445 and 7.5376 GHz, are entangled. The former is employed as the idler, whereas the latter is the signal transmitted by an antenna. In [10], the signal is received directly by another nearby antenna, thus performing a sort of back-to-back measurement of the system characteristics. The transmitted power is -82dBm, and the correlation between the idler and the received signals are exploited to extract the transmitted signal from the background noise, without any particular effort to attenuate multipath effects and clutter. To better assess the performance of the proposed QR, it is compared with a similar classical radar. The receiver operating characteristic (ROC) curves of both systems have been measured, as reported in Fig. 2. Apparently, the classical system, to have comparable performance, needs a much higher number of integrated echoes, corresponding to an eight-time longer integration time. It is also proven that the correlation between the QE-generated signal and idler is up to 2.5 times stronger than in the case of the classical coherent radar.

However, a big limitation of this proposed QR is that the JPA is a microwave resonator based on superconductivity, meaning that it requires cryogenic temperatures to operate. In [10], a bulky dilution refrigerator is necessary, to make the JPA operate at a temperature as low as 7 mK. This feature does not really meet the needs for a future cheap, small-size, and low-power hungry solution.

d) The Photonics-Assisted Quantum Radar

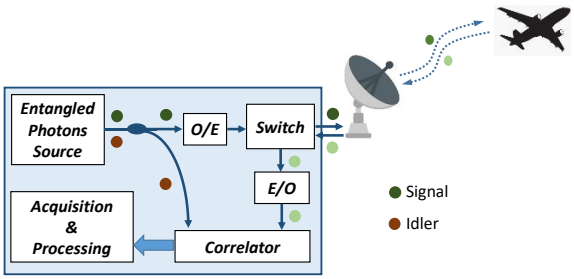

Fig. 3. Basic scheme of a photonics-assisted Quantum Radar. The Entangled photons source produces photons with QE starting from low-frequency electrical domain signals.

At first, QI for remote sensing has been proposed in the optical domain [6], [7], applied to photodetection. By exploiting the strong correlation persisting between formerly entangled particles or fields, it showed a remarkable enhancement of the signal-to-noise ratio (SNR), thus improving the detection of low-reflectivity targets. Later, it has been demonstrated that QI can be operated also in the microwave domain, but the signal generation is still performed optically [8], showing that photonics sources and detectors can greatly be of help in developing a QR.

The scheme of a photonics-assisted QR is depicted in Fig. 3. It is very similar to the scheme in Fig. 1, with the fundamental difference that the generation and the acquisition of signals is operated in the optical domain, exploiting the advantages offered to microwave systems by photonics. The generation can consist in the photonic up-conversion to RF frequency of one, or more, low-frequency electrical signals composed by entangled photons, operated by an electro-optical (E/O) conversion stage. Conversely, reception may exploit photonic down-conversion in an opto-electronic (O/E) conversion stage. E/O and O/E operations can be performed with techniques described in [17], provided that photonics-assisted up- and down-conversions do not alter the quantum features of the original signal.

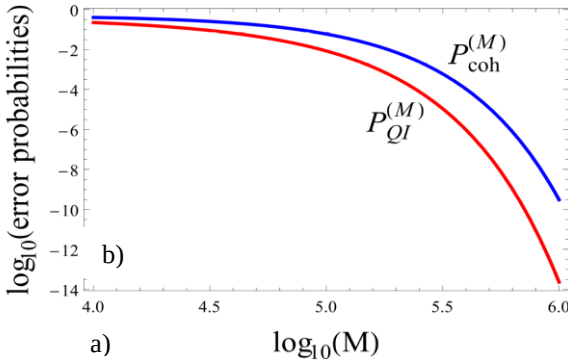

Fig. 4. Performance comparison between the error probability of a QI receiver (red curve) and a classical coherent receiver (blue line) [8].

Fig. 4 shows the performance comparison between a microwave QI system (red line) and an equivalent classical coherent radar (blue line), as reported in [8]. The plot traces the detection error probability as a function of a parameter *M*, equivalent to the system time-bandwidth product, for *M* >>1, witnessing the better performance achieved by QI. This is possible because the error probability depends on the SNR, and QI guarantees a much higher SNR for faint returning echoes. The main drawback of QI, as it has been proposed, is that it needs joint measurements of the signal and idler, meaning that the backscattered signal should be correlated with its idler, that should be stored in the system by quantum memories or optical fiber loops [8].

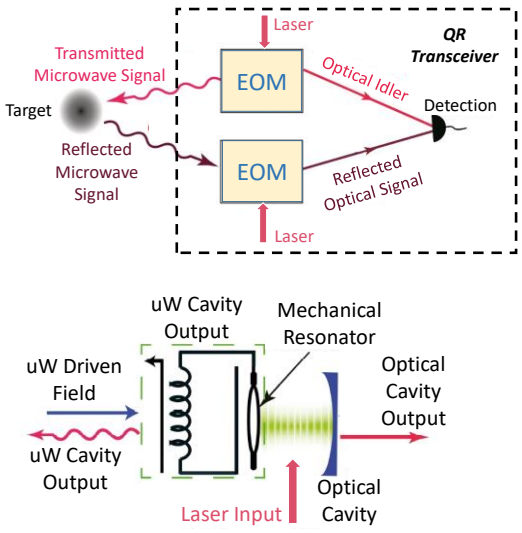

Fig. 5. a) Scheme of a photonics-assisted QR transceiver; b) Scheme of the electro-optical modulators (EOMs) performing E/O or O/E conversions for quantum radar applications [8].

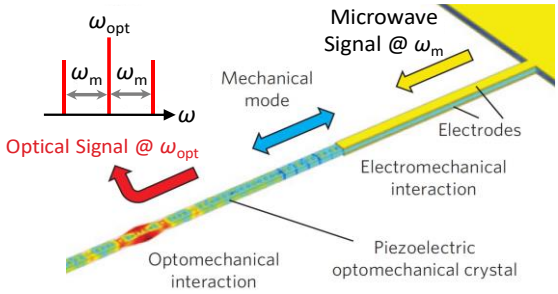

Fig. 6. Scheme of the photonics-integrated modulator for coupling microwave quantum-entangled signals with optical signals [14].

The translation of the quantum properties of an entangled microwave signal to the optical domain (O/E) and viceversa (E/O) is possible thanks to E/O modulators (EOM) as reported in Fig. 5. Fig. 5 a) schematically shows how they can be employed to operate sensing in the microwave domain but generate and acquire the signals with photonic techniques. These EOMs can exploit, for instance, opto-mechanical effects by coupling, thanks to a mechanical resonator, an optical cavity fed by a laser input, with a microwave cavity driven by a RF signal, as depicted in Fig. 5 b).

A very interesting solution to modulate optical signals with entangled RF signals is reported in [14]. This EOM has been realized in Aluminum Nitride, monolithically integrated on a single photonic chip. An optical waveguide, contacted with metal electrodes, is injected with a continuous wave laser at an optical telecom frequency $\omega_{opt} = 2\pi\times196$ THz, by means of a Bragg grating (BG). As sketched in Fig. 6, a microwave signal made by entangled RF photons, oscillating at frequency $\omega_m = 2\pi\times4.2$ GHz, is applied to the electrodes, thus exciting a mechanical mode inside the waveguide crystal. This mechanical mode is carried by phonons, that can oscillate at the frequency of the applied electrical signal. This way, they modulate the injected laser, creating two entangled sidebands at $\omega_{opt} \pm \omega_m$. Therefore, this device acts as a quantum transducer, allowing the transfer of the quantum state of a microwave signal to the optical domain. Such an EOM can be employed to exploit the advantages brought about by microwave photonics in the radar domain, as extensively explained in [17].

Conclusions and Perspectives

Quantum properties of electromagnetic fields disclose the possibility of breaking classical limits in many domains, in particular in that of remote sensing. It gives, in principle, an impressive enhancement of sensitivity, especially when detecting targets with very small radar cross-sections and weak returning echoes. This can be achieved because, among all the photons received by a QR, it is possible to extract only the photons related to the transmitted signal, thanks to the strong correlations created by QE. This is true, in principle, no matter how faint is the received echo. Therefore, quantum technologies can boost the sensitivity of remote sensing to an unprecedented level, potentially excluding the possibility of having stealth targets and overcoming jamming techniques.

Recently, it has been demonstrated that QR is feasible, albeit a lot of research is still to be carried on to take this kind of systems to an acceptable technological readiness level. On the other hand, in the last decade, microwave photonics has shown its capabilities of enhancing the performance of RF systems leveraging on the unique features of optical and electro-optical technology. Nowadays, photonics can be a key enabling technology also for QRs, considering that it already allows efficiently generating and detecting quantum entangled photons, and quantum transducers between optical and RF domain are already available. Photonic sources of optical entangled photons have been reported in [11] - [13], but research has still to be brought on to ascertain if it is possible to exploit these sources to obtain RF entangled signals and idlers, e.g. thanks to classical direct or external modulation by non-entangled electrical signals.

Finally, it is important for EU to foster research activities to fill the technological gap between actually existing photonic technology and the requirements of QR systems. Indeed, some non-EU countries are massively investing in quantum technologies, including QR, and EU should keep the pace of these developments.

References

[1] A. Einstein, B. Podolsky, N. Rosen, “Can Quantum Mechanical Description of Physical Reality be Considered Complete?”, Physical Review47, 777-780 (1935).

[2] The BIG Bell Test Collaboration, “Challenging local realism with human choices”, Nature 557, 212–216 (2018).

[3] J. S. Bell, “On the Einstein Podolsky Rosen paradox”, Physics 1, 195-200 (1964).

[4] S.K. Liao *et al.*, “Satellite-to-Ground Quantum Key Distribution”, Nature 549, 43–47 (2017).

[5] J.L. O’Brien, “Optical Quantum Computing”, Science 318 (5856), 1567-1570 (2007).

[6] S. Lloyd, “Enhanced Sensitivity of Photodetection via Quantum Illumination”, Science 321 (5895), 1463-1465 (2008)

[7] E. D. Lopaeva *et al.*, “Experimental Realization of Quantum Illumination”, Phys. Rev. Lett. 110, 153603 (2013).

[8] Sh. Barzanjeh *et al.*, “Microwave Quantum Illumination”, Phys. Rev. Lett. 114 (8) (2015).

[9] S Pirandola *et al.*, “Advances in Photonic Quantum Sensing”, Nature Photonics 12, 724–733 (2018).

[10] D. Luong *et al.*, “Receiver Operating Characteristics for a Prototype Quantum Two-Mode Squeezing Radar”, arXiv:1903.00101 [quant-ph] (2019).

[11] O. Alibart *et al.*, “Quantum photonics at telecom wavelengths based on lithium niobate waveguides”, Journal of Optics 18 (10) (2016).

[12] P. Kultavewuti *et al.*, “Polarization-entangled photon pair sources based on spontaneous four wave mixing assisted by polarization mode dispersion”, Scientific Reports 7, 5785 (2017).

[13] Kim Fook Lee *et al.*, “Generation of high-purity telecom-band entangled photon pairs in dispersion-shifted fiber”, Opt. Lett. 31, 1905-1907 (2006).

[14] J. Bochmann, A. Vainsencher, D.D. Awschalom, A.N. Cleland, “Nanomechanical coupling between microwave and optical photons”, Nature Physics 9, 712–716 (2013).

[15] R.W. Andrews *et al.*, “Bidirectional and efficient conversion between microwave and optical light”, Nature Physics 10, 321–326 (2014).

[16] https://www.scmp.com/news/china/article/2021235/end-stealth-new-chinese-radar-capable-detecting-invisible-targets-100km.

[17] G. Serafino *et al.*, “Towards a New Generation of Radar Systems Based on Microwave Photonic Technologies”, *J. Lightw. Technol.* 37 (2), 643-650 (2019).

[18] C. F. Ockeloen-Korppi *et al.*, Nature 556, 478–482 (2018).

QUANTUM-BASED METROLOGY FOR TIMING, NAVIGATION AND RF SPECTRUM ANALYSIS

G. Baili, P. Berger, A. Brignon, T. Debuisschert, M. Dupont-Nivet, G. Feugnet, F. Gutty, C. Larat, L. Mayer, L. Morvan, P. Nouchi, D. Dolfi
Thales Research & Technology – France, 1 Av. Augustin Fresnel, 91767 Palaiseau, France

Abstract — **Quantum technologies have been identified as breakthrough technologies with a potential high impact on future navigation, timing and communication systems since the end of the 90's. We will review how these technologies can contribute to electromagnetic spectrum dominance through the use of SHB (spectral hole burning) based spectral holography and of NV (nitrogen vacancy) centers in diamond. Quantum technologies, with integration techniques, will also improve the performances of navigation systems thanks to ultra-precise clocks, accelerometers and gyroscopes.**

Keywords—NV centers, spectral hole burning, CPT clock, atom chip

Introduction

The increasingly complex signals emitted by modern RF sensing and communication systems make the availability of broadband and real-time microwave spectrum monitoring tools crucial. Indeed, from few tens of megahertz to few tens of gigahertz, the microwave spectrum is now occupied by frequency-hopping and bursting signals whose time-frequency characteristics are almost impossible to analyze with standard swept spectrum analyzers. To ensure a large coverage of the spectrum with 100 % probability of intercept (POI), the most stringent applications need an instantaneous analysis bandwidth of at least several GHz, along with a high sensibility and dynamic range, which is far from the capabilities of the most recent digital real-time spectrum analyzers. Therefore, we propose two original techniques, based on quantum technologies, which can provide simultaneously analysis of RF signal over frequency bandwidths of typically 20 GHz, with a MHz resolution and 100% POI. The first one is the so called "rainbow analyzer". *This approach is detailed in Section "SHB based rainbow analyzer".* The second one, operating at room temperature, is based on ensembles of nitrogen vacancy (NV) centers in diamond. *This approach is detailed in section "NV centers based RF spectrum analysis"*

In order to address the challenges of future information and communication technology (ICT) but also the challenges related to defense systems such as strategic communication networks, multi-static radars and navigation in GNSS denied environment, there is an increasing need of compact frequency and time standards, i.e. accurate clocks. Atomic frequency references are now the best commercially available time and frequency references for timescales longer than few seconds. Therefore we propose the original approach of a pulsed coherent population trapping (CPT) Cs clock, based on the use of a dual frequency laser, with the targeted objective of frequency stabilities, below 5.10-13 at 1 s and 2.10-14 at 1 h, in a volume smaller than 2 liters. *This approach is detailed in section "CPT Cs Clocks, based on the use of a dual frequency laser"*

Cold atoms based sensors will strongly impact inertial navigation systems, replacing global navigation satellite systems or enabling driver-free vehicles with precise navigation systems. Demonstrations of free falling cold atom sensors in laboratories have been quite successful with ultra-precise measurements of accelerations and rotations. To move these high-precision cold atom sensors from the lab into a wide range of applications, within civilian and defense domains, several important barriers need to be overcome: portability, sensitivity/speed, robustness and cost. One very promising approach to overcome these barriers and to allow onboard applications is based on the use of atom chips, i.e. chips in the vicinity of which ultra-cold atoms can be trapped and used to measure time, acceleration and rotation. *This approach is detailed in section " "Atom chip based sensors".*

SHB based rainbow analyzer

The principle of the rainbow architecture is depicted in Fig.1. The investigated microwave signals are transposed on a cw optical carrier with a Mach-Zehnder electro-optics modulator. The sidebands of this polychromatic beam (#1) are then composed of the spectral components of the RF signals (see Fig.1.ii).

The spectral components of the microwave signal are then diffracted and simultaneously retrieved in different directions. An array of photo-detectors finally detects the diffracted beams (#2) and records the spectrum of the microwave signals.

The physical principle [1] relies on the engraving of several monochromatic gratings through spectral hole burning in a rare-earth ion doped crystal cooled at low temperature (~5 K). The crystal is illuminated by two programming beams (#3 and #4) coming from the same laser whose frequency is scanned over the required bandwidth of analysis Δf. In addition, beam #3 is angularly scanned in synchrony with the frequency scanning. Consequently, the beams #3 and #4 engrave a continuum of monochromatic Bragg gratings, and burn the corresponding spectral holes in the absorption profile of the crystal: each diffraction angle is then associated with a specific spectral component. A large number of gratings can coexist within the inhomogeneous absorption line of the crystal, which may reach 10s of GHz. The spectro-spatial pattern must be refreshed at a rate corresponding to the population lifetime. The Fig.1.iii shows the implemented geometry for simultaneous programming and detection allowing a continuous spectral analysis.

The SHB based "rainbow" architecture enables to monitor and record the spectrum of complex microwave signals over an instantaneous bandwidth up to 20 GHz, with a time resolution down to 10 µs, 400 resolvable frequency components (limited by the resolution of the camera) and a POI of 100 %. The rainbow RF spectrum analyzer has the potential to offer high time-resolved RF spectrum analysis, with unequaled frequency resolution and RF sensitivity for pulsed signals. It provides an ideal trade-off for the spectrum control of pulsed signals [2]. An example of recorded spectrograms is shown below.

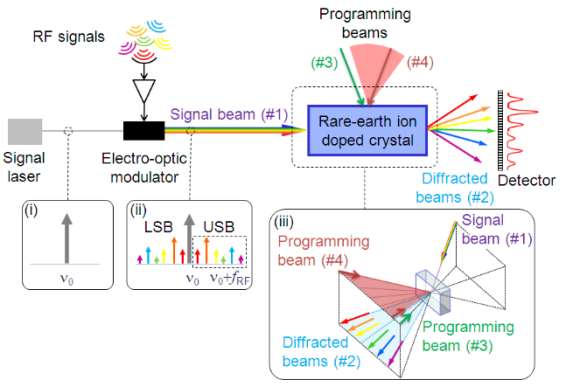

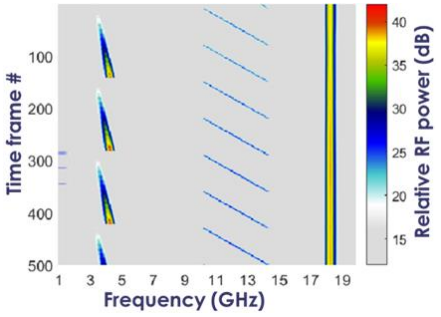

Fig. 1. (Upper) Operating principle of the rainbow architecture. The crystal diffracts the spectral components of the microwave signals in different directions. The programmed processing function, a spectro-spatial pattern, is stored in the crystal. The inserts (i) and (ii) respectively depict the spectra of the cw laser and the modulated laser with the lower sideband (LSD) and upper sideband (USB). (iii) shows the counter propagating box geometry of the four beams which enables to simultaneously program the crystal and diffract a third polychromatic beam. (Lower) Spectrogram over 20 GHz with a frame rate of 25 kHz. Three generators are used to create (i) a signal around 4 GHz swept in frequency and amplitude, (ii) a cw signal at 10 GHz swept over 4 GHz and, (iii) a cw signal at 18.5 GHz.

NV centers based RF spectrum analysis

The NV center is a point defect of diamond constituted of a nitrogen atom (N) and a vacancy (V) in two adjacent crystallographic sites. Its main axis joins the N to the V and follows one of the four crystallographic directions of the diamond lattice. When pumped with green light (532 nm), it emits a red photoluminescence signal (from 600 to 800 nm). This system possesses an internal degree of freedom linked to its electronic spin that can be both initialized and readout through optical excitations. Two electronic spin resonances, induced by an oscillating magnetic field in the microwave range can be detected by a decrease of the NV center photoluminescence. Applying an external magnetic field induces a Zeeman shift that lifts the degeneracy of those resonances. When the transverse part of the magnetic field is negligible with respect to the longitudinal part, the Zeeman shift is linear and proportional to B// the projection of the field along the N-V axis. The frequencies ν_- and ν_+ of the resonances are given by: $\nu_\pm = \nu_0 \pm \gamma_{NV} \cdot B_\parallel$. $B_\parallel$, where $\nu_0 = 2.87\ GHz$ is the resonance frequency without external magnetic field and $\gamma_{NV} = 28\ MHz/mT$ is the electron spin gyromagnetic ratio. Using those properties, the NV

center has been intensively studied as a quantitative magnetic field sensor, the frequencies of the magnetic resonances ν_- and ν_+ being used to measure $B_{\parallel}$.

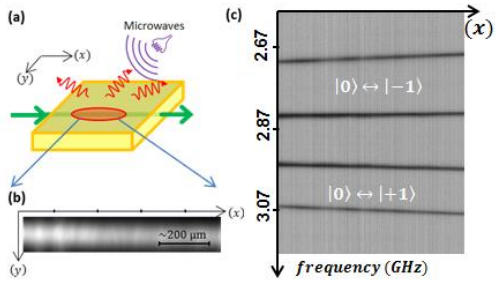

Fig. 2. (a) A CVD diamond plate (yellow) holds NV centers in its volume. It is pumped by a laser beam at 532 nm (green arrow). The induced red photoluminescence is collected through an optical microscope and monitored by a camera. (b) Typical image of the photoluminescence. (c) The normalized photoluminescence is plotted as a function of the position along the (x) axis and of the microwave frequency. Resonance lines are detected by a drop of the photoluminescence. Their frequencies are linked to $\boldsymbol{B}_{\parallel}$.

An ensemble of NV centers in a bulk diamond is used to directly sense the microwave signal. A static magnetic field, with controlled spatial distribution, associates a Zeeman shift, and thus a resonance frequency, to each position in the sample. Then, when a microwave signal with an unknown frequency is applied, a resonance appears at the position corresponding to that frequency. It is thus possible to reconstruct the whole frequency spectrum of a complex signal in one exposure of the camera. The acquisition is instantaneous for the entire bandwidth, which makes possible the real-time spectral survey of quickly changing signals with a nearly 100 % POI.

Detection of monochromatic RF signals of a few 100 µW is easily obtained. In addition, the contrast of the resonance has been measured to be proportional to RF signal intensity. Therefore the proposed approach can give quantitative data on the spectral components of the incoming signal.

A first demonstration is performed measuring the frequency spectrum of amplitude modulated (AM) signal with a carrier at 2.2 GHz with a modulation at 40 MHz. This signal is then sent to the antenna to induce the magnetic resonance signal of the NV centers. The photoluminescence is plotted in Fig.3.a as a function of the spatial axes (x) and (y). The carrier and the two side-bands induce three resonances that are detected by a decrease of luminescence. Their frequencies are linked to the position along the (x) axis. A frequency resolution of 7 MHz is extrapolated. To show the ability to monitor instantaneous frequency variations, the AM signal is now time-dependent. Carrier and modulating signal frequencies are swept while the photoluminescence is monitored. The acquisitions are repeated in time to monitor the temporal frequency evolution of the signal. The spectrogram is plotted in Fig.3.b showing the versatility of the device as an instantaneous spectrum analyzer.

Improvement of this device will allow a 30 GHz instantaneous bandwidth with a resolution of few MHz. This covers a large number of applications in the domains of tactical communications and electronic warfare.

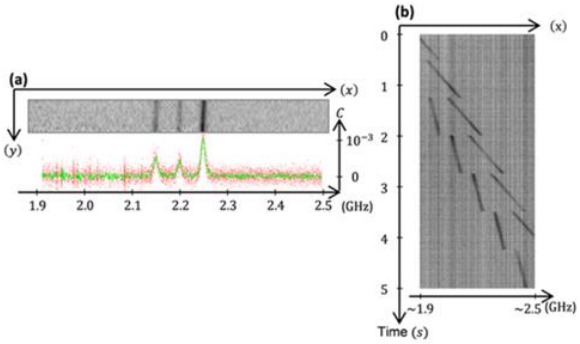

Fig. 3. (a) The relative photoluminescence image of the NV centers submitted to an AM signal is plotted in grey levels along (x) and (y) directions. The carrier at 2.2 GHz and the two side-bands at 2.16 and 2.24 GHz are visible. The spectrum (red dots) is obtained plotting the relative photoluminescence of each pixel and exploiting the correspondence between position and frequency. The green line corresponds to a resampling with a 5 MHz resolution that allows eliminating the high frequency noise of the raw data. (b) Spectrogram: The average relative photoluminescence is displayed in a 2D plot with one axis representing the frequency ν, and the other one representing the time. The carrier is swept from 1.8 to 2.6 GHz in 5s. The modulated signal is swept from 40 to 80 MHz in 0,7s.

CPT Cs clock, based on the use of a dual frequency laser

Accurate clocks are needed for authentication and time stamping of financial transactions. Wireless telecommunication networks need ultra-precise time

references for network management, for time tagging and for synchronization of frequency references. Satellite navigation systems are also relying on high precision time references. Fast recovery of GNSS signals in dense or conflict situations, synchronization of electronic warfare/intelligence and radar systems are also of high interest. Each current technologies of atomic clock have its own performance and volume, determining its field of application. Hydrogen masers and Cesium (Cs) clocks are two technologies often used as primary references clocks (PRC) in applications where frequency accuracy and stability requirements are the most stringent, such as GNSS.

The main advantage of a Hydrogen maser is its short term stability. However, Cs clock exhibits better long term stability, complying with PRC's frequency stability specification (better than 10-13 over one week). The wide scale deployment of these two technologies is limited by their cost, large power consumption and volume. For embedded and portable applications, less demanding in terms of performances, considerable research and development efforts have been carried out and have conducted to the realization of commercial clocks on a chip such as the CSAC from Symmetricon with a relative frequency stability of 10-10 at 1 second with a volume < 10 cm3.

Better performances, 10-13 at 1 s, while keeping a volume of a few liters, are required in several fields such as telecommunications and satellite radio-navigation. For these applications, the Cs clock based on Coherent Population Trapping (CPT) is a promising approach. In a CPT-based atomic clock, the microwave interrogation delivering the atomic reference signal is induced by two phase-coherent laser fields at resonance with a common excited state. When the frequency difference between the two laser fields corresponds exactly to the ground-state hyperfine splitting (equal to 9.19 GHz with 133Cs atoms), the atoms are trapped in a dark state and stop interacting with the laser light. The resulting narrow transmission line in the atomic absorption spectrum is used as a frequency reference. In order to guarantee the stability of the clock frequency, CPT atomic clocks require a high purity, optically-carried, microwave signal as well as low-noise properties for the laser source (intensity and frequency fluctuations).

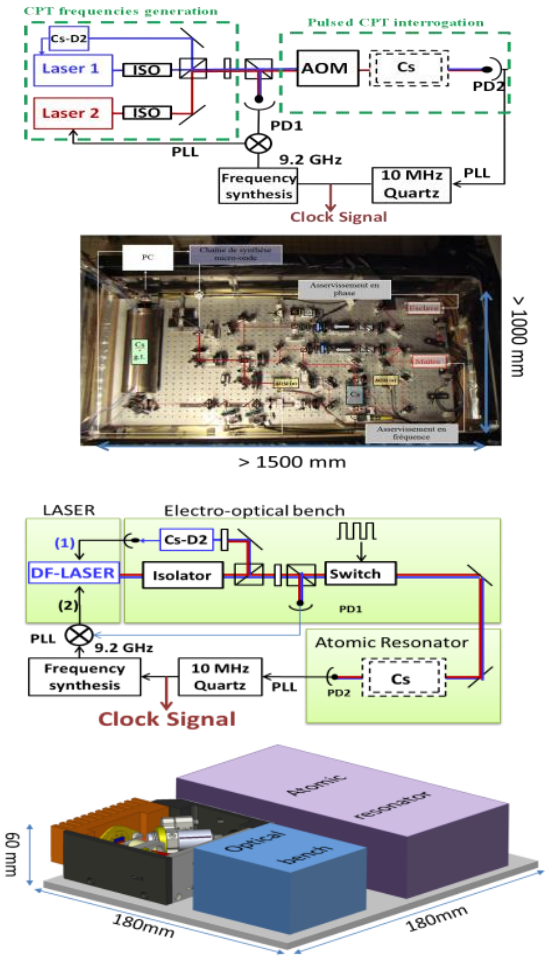

Fig. 4. (Upper) A schematic and a picture of one of the first CPT Cs optical clock developed at SYRTE, based on two phase-locked external cavities lasers. ISO: optical isolator, AOM: acousto-optic modulator, PD: photodetector, PLL: Phase-locked Loop. Cs-D2: D2 transition of Caesium atoms for optical frequency locking. (Lower) So called CHOCOLA CPT Cs Clock whose development is in progress. It uses a dual frequency ultra-low noise VECSEL and a compact electro-optic bench to reach at the same time the targets in terms of performances and compactness.

SYRTE demonstrated, in a pulsed interrogation scheme a short-term frequency stability of 2x10-13 at 1s [4]. A schematic representation, based on two phase-locked lasers, is given on Fig.4.a.

In order to reduce size and complexity within this CPT approach, we propose to use metrological lasers. Dual-frequency and dual-polarization version of such lasers would be particularly well suited to optically drive the so-called "lambda scheme". Dual-frequency

(DF) Vertical External Cavity Surface Emitting Lasers (VECSELs) are good candidates. Indeed, as emphasized above, they allow the replacement of two independent lasers by a unique laser source, thus reducing significantly the size and complexity of the system. Furthermore DF-VECSELs inherently present a low noise operation: at frequencies above few kHz, the intensity and phase noise are shot-noise limited [5], thus pushing at their lowest possible level the clock frequency instabilities, and maximizing the signal-to-noise ratio of the clock signal detection. The availability of new emerging technologies for optical functions as optical isolation and optical switching has to be considered for the implementation of a compact atomic clock, compatible with the required frequency stability. The so called CHOCOLA CPT Cs clock under study combining a DF-VECSEL with a largely fibered compact electro-optic bench is presented in Fig.4.b.

A DF-VECSEL prototype operating at 852 nm has then been realized, including the simultaneous control of optical frequency via intra-cavity etalon and cavity length adjustments, and of the frequency difference (9.2 GHz) via electro-optic element in order to properly address Cs transitions [6]. The laser setup is compact (9x9x4 cm3), and provides excellent mechanical and thermal stability.

Atom chip based sensors

Atom interferometers have proven very successful in precision measurements such as sensing of gravity, gravity gradients and rotation. They also show great promise to perform general relativity tests.

In parallel, atom chips provide a robust and versatile tool to trap and manipulate ultra-cold atoms, and are now routinely used in a variety of setups, including compact atomic clocks. In this context, they are very promising candidates for next-generation compact atomic acceleration and rotation sensors, including onboard applications. However, while a variety of integrated beam splitters and coherent manipulation techniques have been demonstrated, none of the chip-based atom interferometers developed so far has reached metrological performance.

One of the initial problems encountered by atom-chip interferometers, namely the difficulty to maintain stable trapping and a reasonable trap-surface distance during the coherent splitting process, has been overcome by the use of dressed state adiabatic potentials. However, another issue remains unresolved: trapped-atom interferometers using Bose-Einstein condensates are especially sensitive to atom-atom interactions which induce phase diffusion, limiting their coherence time and putting a serious constraint on the achievable precision in the measurement of the relative phase between the two arms of the interferometer. One possible way to reduce the interaction strength is the use of a trapped but thermal (i.e. non-degenerate) atomic cloud whose density is sufficiently low that the effect of interactions is negligible.

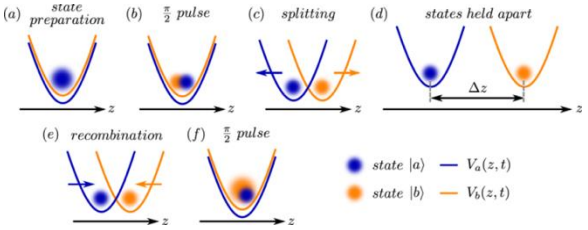

Fig. 5. Schematic of a Ramsey interferometer protocol using internal state labelling. Time increases from (a) to (f). The size of the blue (respectively orange) shaded-disc, represents the population in state |a> (respectively |b>). The blue (respectively orange) arrows indicate the direction of the displacement of the trap V|a>(r) (respectively V|b>(r)). Adapted from [7].

This choice is somewhat analogous to using incoherent light in an optical interferometer. As in a "white light interferometer", the short coherence length of a thermal cloud (typically the de Broglie wavelength) requires that the interferometer arms be kept sufficiently symmetric (in a sense that the shape difference between the two traps realizing the interferometer arms must as close as possible to zero [7]) in order to observe any interference. Theoretical model linking the symmetry of the interferometer arms and the coherence length has been derived and checked experimentally [8].In [9] we proposed a protocol for a symmetric atom interferometer suitable for thermal atoms, using internal state labeling and adiabatic microwave dressed potentials. We proposed the use of two microwave (MW) frequencies on two separate planar waveguides, each one interacting with one (and only one) of the two internal states involved in the interferometer (namely |a>=|F=1,mF=-1> and |b>=|F=2,mF=1> of 87 rubidium). In combination with a DC trap the first MW frequency creates a dressed potential only seen by the internal state |a>. The same DC trap and the second MW frequency create a dressed potential only seen by the internal state |b>. This protocol allows to control individually each

interferometer path and to control their relative shape difference. An atom chip implementation of this protocol is described in reference [9]. This interferometer works as a Ramsay atomic clock except that the two internal states of the Ramsey interferometer are spatially split just after the first pi/2 pulse and merge just before the second pi/2 pulse (Fig.5). For example, to measure acceleration the two states |a> and |b> are split along a straight line [7]. The typical sequence is as follows: (Fig.5.a) the atomic cloud is prepared in internal state |a> and (Fig.5.b) a first pi/2-pulse puts the atoms in a coherent superposition of the two internal states |a> and |b>. (Fig.5.c) The two trapping potentials V|a>(r) (created by the first MW frequency) and V|b>(r) (created by the second MW frequency) are moved to spatially separate the two internal states, (Fig.5.d) then the two internal states are held apart allowing the Ramsey interferometer to be sensitive to differences of potential acceleration energy. (Fig.5.e) after the two trapping potentials V|a>(r) and V|b>(r) are moved to spatially recombine the two internal states. (Fig.5.f) A second pi/2-pulse closes the interferometer. This protocol could be adapted to measure rotation.

Acknowledgment

These developments are funded by the Direction Générale de l'Armement (DGA). Support from European Commission (DIADEMS project) is also acknowledged.

References

[1] Lorgeré, I., et al., Journal of Modern Optics, vol. 49, no. 14-15, 2459 - 2475 (2002).

[2] Berger, P., et al., J. Lightwave Technol., 34, 4658 - 4663 (2016).

[3] Chipaux, M., el al., Appl. Phys. Lett. 107, 233502 (2015).

[4] Tricot, F., et al., 2016 European Frequency and Time Forum 2016 (EFTF 2016), York, 1-3, 10.1109/EFTF.2016.7477813, (2016).

[5] Baili, G., et al., J. Lightwave Technol., 32, 3489 - 3494 (2014).

[6] Dumont, P., et al., "Low-noise dual-frequency laser for compact Cs atomic clocks", J. Lightwave Technol., 32, 3817-3823 (2014).

[7] M. Dupont-Nivet, et al., New J. Phys., 18, 113012 (2016).

[8] M. Dupont-Nivet, et al., New J. Phys., 20, 043051 (2018).

[9] M. Ammar, et al., Phys. Rev. A, 91, 053623 (2015).

CONCLUSIONS

Several different research topics and applications of quantum technologies related to Optronics were presented at the workshop and most of the related papers are published in these proceedings.

As regards defence applications, the following conclusions can be drawn.

1) The Technological Readiness Level (TRL) of quantum technologies still remains quite low when it comes to defence applications, and most of today's research activities are carried out by scientific research centres.
2) Several devices that were presented at the workshop make use of quantum principles, but they are not strictly quantum technologies-based devices (for instance they don't use photon pair entanglement).
3) Most quantum-based devices/technologies are interferometers, gravitometer (cold atoms), magnetometer, photon counting cameras, gyroscope, superconducting etc.
4) Applications span from metrology, ghost imaging, beyond the wall detection, autonomous navigation, time synchronization, quantum internet, secure communication, quantum radar, quantum computing, quantum cryptography, quantum illumination, to innovative detectors.
5) The advantages for OPTRONICS are improved sensitivity, reduction of noise and background, hidden target detection, system compactness.

The use of quantum technologies in defence is not straightforward and it still seems far away from the actual defence capabilities needs. Even if the civilian market can push these technologies, massive investments from the defence side will be needed in the future, especially in key driving technologies (e.g. detectors, single photon camera etc.).

PDF ISBN: 978-92-95075-41-2 doi:10.2836/848731 QU-02-19-876-EN-N